K. Jeyapalan, M.A. Stein, R. Awuah-Baffour,
Jijong Wang, B. Luzem, and Yan Wang

Final Report

Use of GPS for Photogrammetry

January 1993

Sponsored by the Iowa Department of Transportation
and the Iowa Highway Research Board

Iowa DOT Project HR-342
ISU-ERI-Ames-93096

Department of Civil and Construction Engineering
Engineering Research Institute
Iowa State University, Ames

Iowa Department
of Transportation

report

College of
Engineering
Iowa State University

K. Jeyapalan, M.A. Stein, R. Awuah-Baffour,
Jijong Wang, B. Luzem, and Yan Wang

Use of GPS for Photogrammetry

Sponsored by the Iowa Department of Transportation
and the Iowa Highway Research Board

Iowa DOT Project HR-342
ISU-ERI-Ames-93096

engineering
research institute
iowa state university

TABLE OF CONTENTS

	page
List of Figures	vii
List of Tables	ix
Executive Summary	xiii
Chapter 1. Introduction	1
Chapter 2. The Global Positioning System	5
2.1 Satellite Orbit and Signal Characteristics	5
2.2 Receiver System Operation	10
2.3 General Operating Theory	11
2.3.1 Stand Alone Mode	11
2.3.2 Differential GPS	13
2.3.3 Static Mode	17
2.3.4 Kinematic Mode	17
2.4 Post-Processing Software	17
Chapter 3. Photogrammetry	19
3.1 Introduction	19
3.2 Theory of Photogrammetry	19
3.2.1 Single Photo Geometry	19
3.2.2 Stereophotogrammetry	25
3.2.3 Analytical Photogrammetry	27
3.2.4 Analogue Photogrammetry	27
3.2.5 Digital Photogrammetry	32
3.3 Photogrammetric Instruments	32
3.3.1 Aerial Camera	32
3.3.2 Scanners	35
3.3.3 Stereoplotters	37
3.3.4 Analytical Plotters	42
Chapter 4. Aerial Triangulation	42
4.1 Independent Model Aerial Triangulation	42
4.2 Simultaneous Adjustment Method	46
4.3 Strip Triangulation	48
4.4 Block Triangulation	48
4.5 Flight Planning	50
4.6 Control Planning	50
4.7 Location of Control	51
4.8 Determination of Photo Coordinates	51
4.9 Determination of Pass and Tie Point Coordinates	51
Chapter 5. Airborne GPS	54
5.1 Camera Offset From Antenna	54
5.2 Base Station Coordinate	54
5.3 Camera Location	54
Chapter 6. Test Flights and Results	58
6.1 Mustang 90 Flight	58
6.2 NOAA 91 Flight	62
6.3 St. Louis 92 Flight	77
6.4 California Project	86
6.5 Texas Project	89
6.6 Study of Multi-Antenna Airborne GPS	93

page

Chapter 7. Conclusions and Recommendations 96
Acknowledgments 97
Bibliography 98
Appendix
Summary of MAPP/PAL/ALBANY 102
Observation Procedures Using the STK-1 Wild Stereocomparator 108
Determination of Camera Locations 122

List of Figures

page

Chapter 2
Figure 2.1 GPS System 6
Figure 2.2 Satellite Orbit 7
Figure 2.3 Satellite in the Elliptical Plane 8
Figure 2.4 Interferometric Method 14

Chapter 3
Figure 3.1 Aerial and Terrestrial Photogrammetry 20
Figure 3.2 Map Projection 22
Figure 3.3 Height Distortion 24
Figure 3.4 Coordinate System 26
Figure 3.5 Stereoscopy 28
Figure 3.6 Photo Coordinates 29
Figure 3.7 Stereoplotter 31
Figure 3.8 Measuring System 33
Figure 3.9 Aerial Camera 34
Figure 3.10 Scanner 36
Figure 3.11 Analogue Stereoplotter 38
Figure 3.12 Digital Photogrammetry 39
Figure 3.13 Analytical Plotter 41

Chapter 4
Figure 4.1 Independent Model 43
Figure 4.2 Tie for Block 45
Figure 4.3 Control for Block 47
Figure 4.4 Collinearity 47
Figure 4.5 Strip 49
Figure 4.6 Block 49
Figure 4.7 Target 52
Figure 4.8 Control Network 52
Figure 4.9 Fiducial Point 52

Chapter 5
Figure 5.1 Control and Base Station 55
Figure 5.2 Taxi Point 55
Figure 5.3 Control Network 56
Figure 5.4 GPS Camera Location 56

Chapter 6
Figure 6.1 90 Strip and Control 60
Figure 6.2 Flight Plan for 91 61
Figure 6.3 91 Control 63
Figure 6.4 Aircraft with GPS Antenna 64
Figure 6.5 Offset of Camera 65
Figure 6.6 Ames Airport Station 66
Figure 6.7 Location of Camera from Taxi Station 67

page

Figure 6.8 Elevation vs Time by GPS Tracking of Aircraft 68
Figure 6.9 Northing vs Easting from GPS Tracking of Aircraft 69
Figure 6.10 High 91 - Difference in Camera Location . . 72
Figure 6.11 1992 Flight 78
Figure 6.12 Low 92 - Difference in Camera Location . . 79
Figure 6.13 California Flight Layout Diagram 87
Figure 6.14 California Difference in Camera Location . 88
Figure 6.15 Texas Flight Layout Diagram 90
Figure 6.16 Texas Difference in Camera Location 92
Figure 6.17 Multi-Antenna Concept 94

List of Tables

		page
Chapter 6		
Table 6.1	Standard Deviation of Differences of Coordinates Comparing Various Adjustments. .	59
Table 6.2	Camera Data from Strip	70
Table 6.3	Camera Data from Albany	70
Table 6.4	Block Adjustment Using Different Control . .	71
Table 6.5	AGPS vs. Albany in NOAA Flight	73
Table 6.6	Standard Errors of Control	73
Table 6.7	Standard Error of Unit Weight by AGPS . . .	74
Table 6.8	Standard Error of Unit Weight by FORBLK . .	75
Table 6.9	The SAS System	76
Table 6.10	Standard Error by Albany	77
Table 6.11a	Standard Deviation of Difference in x Coordinates by Ground Control and Camera Location	80
Table 6.11b	Standard Deviation of Difference in y Coordinates by Ground Control and Camera Location	81
Table 6.11c	Standard Deviation of Diffference in z Coordinates by Ground Control and Camera Location	82
Table 6.11d	Standard Deviation of Difference in x Photo Coordinate Residuals by Ground Control and Camera Location	83
Table 6.11e	Standard Deviation of Difference in y Photo Coordinate Residuals by Ground Control and Camera Location	84
Table 6.11	92 Flight by AGPS	85
Table 6.12	Weight Used in FORBLK	85
Table 6.13	Difference Between Kinematic Camera Control and Ground Control Bundle Adjustment	86
Table 6.14	Difference Between Pseudorange Camera Control and Ground Control Bundle Adjustment	86
Table 6.15	Residuals in Control and Image	89
Table 6.16	Standard Error in Control by Albany	91
Table 6.17	Weight for AGPS	91
Table 6.18	Exterior Orientation Elements	93

EXECUTIVE SUMMARY

Five test flights were conducted to study the use of GPS in Photogrammetry, three in Iowa, one each in California and Texas. These tests show that GPS can be used to establish ground control by the static method and to determine camera location by the kinematic method.

In block triangulation, six GPS controls are required and additional elevation control along the centerline is also required in strip triangulation.

The camera location determined by aerial triangulation depends on the scale of the photography. The 1:3000 scale photography showed that the absolute accuracy of the camera location by GPS is better than five centimeters. The 1:40000 scale photography showed that the relative accuracy of the camera location by GPS is about one ~~mill~~meter.

In a strip triangulation elevation control is required in addition to the camera location by GPS. However, for block triangulation camera location by GPS is sufficient . Pre-targeting of pass and tie points gives the best results in both block and strip triangulation.

In normal mapping for earth work computations the use of 1:6000 scale photography with GPS control instead of 1:3000 scale is recommended.

It is recommended that research be done in the use of GPS for navigation in aerial photographic missions. It is highly recommended that research be done in the use of GPS to determine tip and tilt of the aerial camera, that is required in stereoplotting.

Use of GPS for Photogrammetry

Introduction

A typical engineering project involves planning, reconnaissance, preliminary survey, design layout survey, construction and maintenance. Global Positioning System (GPS) can be used in preliminary survey, layout survey, and maintenance, while photogrammetry is invaluable in reconnaissance, design, and maintenance. The advantage of GPS is its ability to determine precisely the location of points at any time, anywhere in the world, on a local state or global coordinate system; and photogrammetric techniques can identify and locate objects, produce topographic maps, and three dimensional data fairly rapidly and cost effectively. When using photogrammetry for location or mapping purposes, three dimensional coordinates of some points, obtained by other methods, are required. Thus, GPS and photogrammetry can complement each other in the implementation of engineering projects. During the era of World War II, topographic maps were produced by analogue stereo plotting instruments, using aerial photographs and ground control established by conventional survey methods. With the advent of computer technology, digital imaging and analytical plotters, aerial and terrestrial triangulation softwares now produce the digital topographic information used in earth work computation, highway design and other analysis within Geographic Information Systems (GIS).

During the last decade, GPS technology has improved considerably. At present, we have in orbit the complete constellation of satellites needed to determine three dimensional coordinates (location) of points anywhere in the world, at any time. Using static mode of processing, locations can be determined with a relative accuracy of about ± 2 cms. Using kinematic mode, locations of moving vehicles, such as aircraft, can be determined at every second with a relative accuracy of ± 5 cms or better.

A prerequisite for producing digital data or topographic maps from aerial photographs is either ground locations of three or more points per stereo pair or six exterior orientation elements (camera location, heading,tip and tilt) of each photograph. In the past, the locations of three or more points per stereo pair are determined by conventional survey methods or by a combination of conventional survey and aerial triangulation methods. The aerial triangulation methods currently used need at least three to nine control points to process a block of photographs. Also, most modern softwares such as Albany can process about 4000 photographs simultaneously.

This research project shows, that not only can conventional survey methods for establishing ground control be replaced by GPS, but that the conventional aerial triangulation methods can also be modified so that the location of camera obtained by GPS, known as airborne GPS, can be used to eliminate the need for ground control points. This important finding will result in considerable time and cost saving to the Ia DOT.

Aerial triangulation without any ground control requires a

block of photos with 60% forward and 60% side overlap . In addition, at least one strip with different flying height and targeted pass and tie points will help to eliminate any systematic error. It appears that further research in Airborne GPS may yield results that eliminate the need for aerial triangulation to determine the exterior orientation elements of photos; a prerequisite for topographic mapping or collecting digital three dimensional data in earth work computation.

These findings were the results of five projects Mustang, NOAA, St. Louis, California, and Texas. The Mustang project was conducted to evaluate the use of GPS for establishing ground control in aerial triangulation. In this project a strip of 33 aerial photos were taken at 1500 ft flying height over Highway 30 between Nevada and Colo, covering an area of about 6 miles. Aerial triangulation using GPS control indicated

- an accuracy of better than 10 cms,
- that 6 GPS points together with elevations along the center line, provides the best result for strip aerial triangulation.

In 1991, a flight using National Oceanic and Atmospheric Agency's (NOAA) aircraft, Cessna Jet, equipped with GPS antenna, Trimble GPS receiver, and Wild RC 20 camera, was done over the Mustang project area at 1500 ft and 3000 ft flying heights. Three strips of photos at the lower flying height and one strip at the higher flying height were taken with 60% forward overlap. The lateral overlap of the lower strips were 30%. The GPS control, PIs along the center line and a number of pass and tie points were targeted prior to flying. A number of softwares, DOT, Albany, FORBLK and AGPS, were used to adjust the aerial triangulation data. The high altitude photos were observed both by IaDOT and ISU. The agreements between softwares and data collection were found to be satisfactory. The analysis of the data indicates that camera locations by GPS is better than 10 cms using the aerial triangulation as the standard. The analysis also showed that aerial triangulation using a block of photos with 60% forward and 30% lateral overlaps can be adjusted with only camera location and without any ground control. A strip of photos with 60% forward overlap can be adjusted with camera locations and, at least, one elevation control. There exists a systematic error between camera location and ground control. The AGPS, the software that compensates for the systematic error, appears to give satisfactory results. A combination of high and low flights eliminates most of the systematic error between ground control and camera locations.

In 1992, a flight using twin engine aircraft owned by Maps Inc. of St Louis and equipped with LMK 2000 camera and Ashtech's GPS receivers, was done over the Mustang area. Unlike 1991 flight, a 60% lateral overlap was used for the lower strip and all pass and control points were targeted. The Ashtech receiver collected data every half second as opposed to the every second collection by the Trimble receivers in the '91 flight. The photo coordinates were observed by ISU using Wild Stereocomparators. Even though all pass points were targeted, some natural points had to be used because the photographs were not taken at the location planned. If GPS can

be used to navigate the aircraft, then pin-point photography over the flight line can be achieved, eliminating the use of pug or natural points .

The '92 flight of photos were adjusted using Albany, AGPS and FORBLk softwares. The results show that 3000 ft flying height photography with GPS control can be used for earthwork computation, in place of the 1500 ft flying height photography now being used. This substitution will result in a saving of 25 to 50% in control and plotting time.

These results show that using high and low flight photography with camera locations by GPS can yield satisfactory aerial triangulation adjustments; and that camera orientation parameters determined using ground control may have systematic errors. The results shows that the camera location determined by GPS and the photo coordinates determined by stereocomparator are comparable, indicating that it is important to target pass and tie points. Further indications are that the relative accuracy of camera locations are better than 1 cms. These results also show that lower order ground control combined with camera location by GPS, yield excellent results while eliminating any systematic errors between ground control and camera locations. Thus, PIS established during preliminary survey can be combined with camera location to do the aerial triangulation, eliminating the need for additional ground control survey.

The California project was done by the U.S. Forestry. This consists of 4 strips in the North-South direction with 60% forward and 40% side overlap at 20,000 flying height using Zeiss Top camera. The Trimble GPS receivers capable of collecting pseudorange and kinematic phase data were used. The data were processed using Albany, AGPS, and GAPP (used by NOAA) softwares. The results indicate that kinematic data are superior to pseudorange for camera location. The accuracy of aerial triangulation using ground control is about one meter, which is satisfactory for the scale of photography used. The error is partly because of the pugging tie and pass points and of the 40% lateral overlap. When compared to aerial triangulation using ground control, the accuracy of camera location by kinematic processing is better than 1 m. The AGPS software indicates that the systematic error between camera location and ground control can be eliminated using heavy weights on camera location and photo coordinates and light weights on ground control. Doing so results in standard error of unit weight of one. It can be concluded that camera location is as good or better than the photo coordinates, indicating a relative accuracy of 2-3 cms in the camera locations determined by GPS.

The Texas project was conducted by the Texas DOT. This consists of three strips in the North Easterly direction at 1500 ft flying height with 60% forward overlap and 24 to 48% side overlap. Using the Albany software and the middle strip, the camera location as determined by GPS is better than 10 cms. The Albany results show that the standard error on control is less than 5 cms for the middle strip and is less than 1 meter for the block, indicating that tie and pass points have errors resulting from pugging or geometry of the location due to low side overlap. The side overlap

of 50 to 60 can be maintained as planned if the navigation of the flights was done using GPS or other external devices other than visual navigation. Adjustments using AGPS software indicates that the best results are obtained by constraining the photo coordinates and camera location heavily, and lightly constraining the ground coordinates. AGPS software also shows that there is systematic error between ground control and camera location, which can be eliminated by the AGPS software.

At present IaDOT uses photogrammetry in collecting three dimensional data for highway design and earthwork computation. In this process IaDOT spends annually about $100,000 for aerial photography; $20,000 on about 20 aerial triangulation projects and about $70,000 on 125 miles of conventional surveying for ground control. IaDOT already possesses 3 GPS receivers that are being used in preliminary survey. By using GPS for ground control, the costs (of establishing control) can be cut by 25% and the accuracy of the survey can also be improved. By using airborne GPS the cost of ground control can be further reduced by 25%, and the cost of aerial triangulation reduced by 25%. If multi antenna airborne GPS can be developed the cost of aerial triangulation and ground control survey can be further reduced by another 25 to 50%. Also, aerial photographs and the exterior orientation elements from multi-antenna GPS can be used on a real time basis to update GIS, so that the data can be analyzed for highway maintenance and for studying natural disasters caused by hurricanes, floods, earthquake, etc. Thus, research on airborne GPS using multiantenna is highly recommended.

The work done in the research project and its conclusion and recommendation are presented in the following chapters.

Chapter 2 describes the GPS system
Chapter 3 describes the photogrammetric system
Chapter 4 describes the Aerial Triangulation
Chapter 5 describes airborne GPS
Chapter 6 describes test flight and results of five projects and Chapter 7 gives the conclusion and recommendation

2.0 THE GLOBAL POSITIONING SATELLITE (GPS) SYSTEM

For the past decade, the U. S. Department of Defense has been developing the GPS system. When this system is fully operational, perhaps by 1993, approximately 18 to 24 satellites will orbit at about 20000 km above the earth in three to six orbit planes. The objective is to provide visibility to four to six satellites about 5° above the horizon, at any time anywhere in the world, so as to provide sufficient geometry (see fig. 2.1). These satellites will emit two coded signals that can be used by a receiver to determine the receiver's position, velocity and time. Presently, there are about 19 operational satellites. Of the nine original Block I satellites, only six are operational; the Block II satellites are being continuously deployed. The present configuration gives a window of about 18 hours for three-dimensional observations and about 24 hours for two-dimensional observations. In the near future,we will have the full constellation of satellites enabling GPS location at any time.

2.1 Satellite Orbit and Signal Characteristics

The satellite, m, of the GPS, orbits the earth along an elliptical (nearly circular) path (see fig. 2.2). The satellite operates in a 12-hr orbit at an altitude of 20,183 km with an inclination of 55° to the equator. A constellation of 18 to 24 satellites in three to six orbital planes, 30° to 60° apart, is proposed. At the time of this writing, it appears there will be 24 satellites in six orbital planes. Two systems of nomenclature exist. One system is the NAVSTAR (Navigation Satellite Timing and Ranging), which is launch dependent. The other is the SV (space vehicle) system, which is related to its designated p-code.

The satellite coordinates [x,y,z] on an earth centered WGS-72/84 geocentric coordinate system (see Figs. 2.2 & 2.3) are determined by using these orbital parameters:

$(A)^{1/2}$ = square root of semi-major axis of the satellite orbit.
e = eccentricity of the elliptical orbit
Ω_o = longitude (right ascension) of the ascending node or reference time
i_o = inclination angle at reference time
ω = argument of perigee
M_o = mean anomaly at reference time, corresponding to time anomaly V and eccentric anomaly E
t_{oe} = ephemeris reference time or epoch of perigee

Their corrections are

i = rate of inclination
Δn = mean motion difference from computed value
Ω = rate of right ascension
C_{us} = amplitude of the sine harmonic connection to the argument of latitude
C_{uc} = amplitude of the cosine harmonic correction

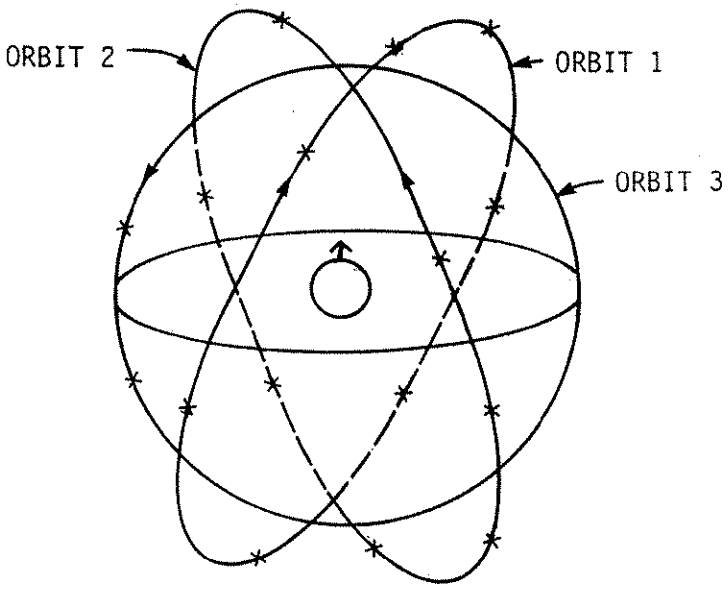

Figure 2.1 GPS System

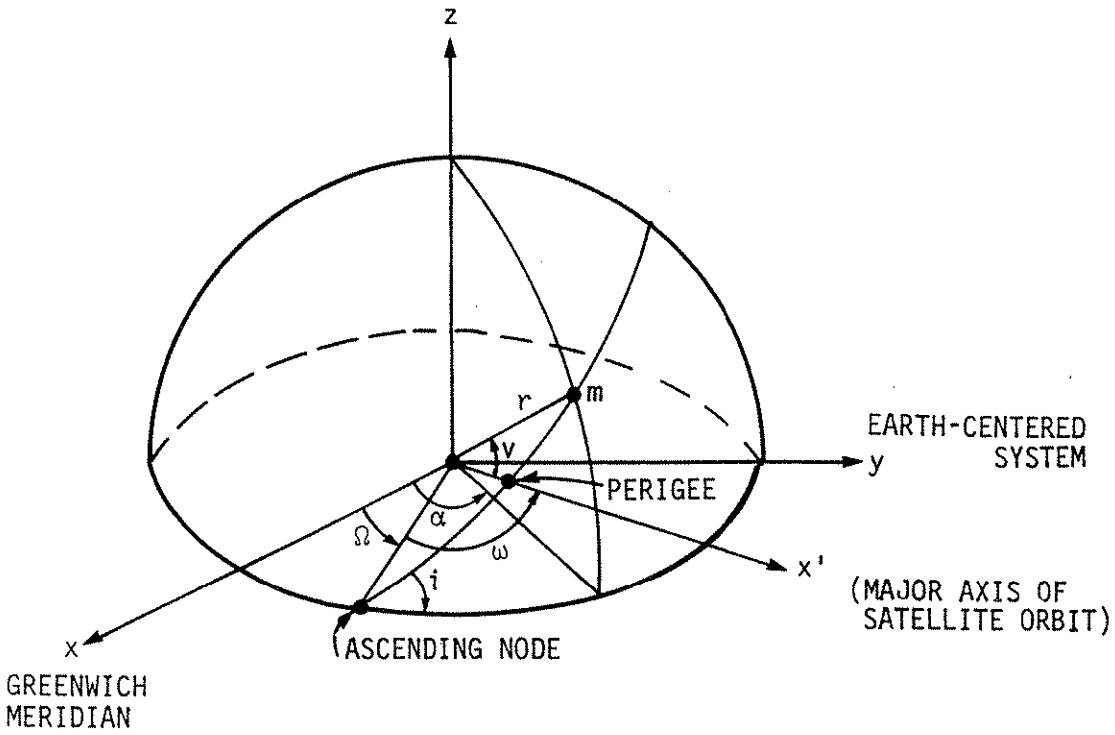

Figure 2.2 Satellite Orbit

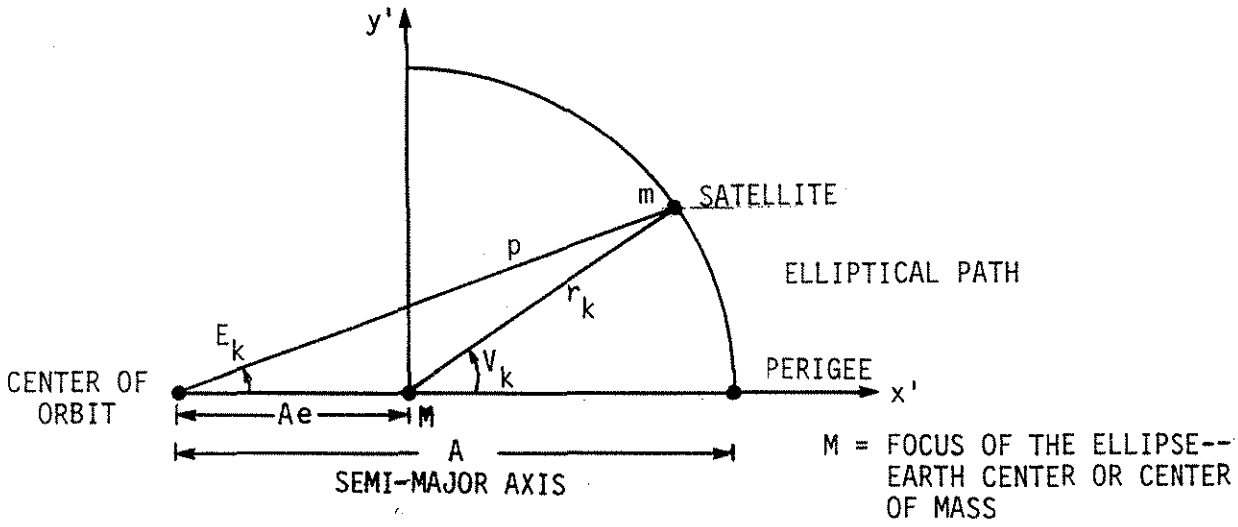

Figure 2.3 Satellite in the Elliptical Plane

C_{rs} = amplitude of the sine harmonic correction term to the orbit radius
C_{rc} = amplitude of the cosine harmonic correction to the orbit radius
C_{ic} = amplitude of the cosine harmonic correction term to the angle of inclination
C_{is} = amplitude of the sine harmonic correction term to the angle of inclination.

These parameters and corrections are provided by a control segment that consists of four monitor stations (MS): an upload station (ULS), and a master control station (MCS). The monitor stations are located at Hawaii; Elmendorf AFB, Alaska; Guam; and Vandenberg AFB, California. Using the data collected at the Mss, the MCS, located at Vandenberg AFB, computes the satellite's orbital parameters and their correction terms. The ULS, also located at Vandenberg AFB, updates the navigation message (containing the orbital parameters) of each satellite at 6-hour and 24-hour intervals. The message also includes AODE (age of data):

$$\text{AODE} = t_{oe} - t_l$$

where t_l = the time of last data

The satellite transmits signals L_1 at center frequency of 1575.42 MHz and L_2 at center frequency of 1227.6 MHz. Each of the two signals is modulated by a 10.23 MHz clock-rate precision, P signal, and/or a 1.023 MHz clear/acquisition (C/A) signal. The C/A code is short, repeating every millisecond. Each satellite broadcasts a different C/A code from the family of 1023 specified codes. The selection of codes minimizes interference between C/A signals and permits positive satellite identification. The p-code is a long sequence, repeating every 280 days, and each satellite is assigned a week - long portion of this sequence. The high-rate, long-duration p-code appears as random noise to an observer and hence is described as pseudo-random noise.

Each of these two modulation binary signals has been formed by a p-code or C/A code, which is module 2 added to 50 bps (bits per second) data to form P + D and C/A + D, respectively. The modulation D contains information regarding the satellite ephemeris, satellite clock correction terms (af_o, af_1,af_2), ionospheric delay term (TGD), and the like.

The L_1 in the phase component of the carrier is modulated by the P signal; P + D and the quadrature carrier are modulated by C/A + D. Thus, the L_1 signal transmitted by the satellite is given by

$$S_{L_1}(t) = A_p P_i(t) + D_i(t)\cos(\omega_1 + \phi) + A_c C_i(t) D_i(t)\sin(\omega_1 t + \phi)$$

The L_2 is biphase modulated by the p-code; thus the L_2 signal transmitted is given by

$$S_{L_2}(t) = B_p P_i(t) D_i(t)\cos(\omega_2 + \alpha)$$

2.2 Receiver system operation

After the antenna of a GPS receiver is positioned over the point, the antenna cable and external battery pack (if used) are connected with receiver. When the receiver is switched on, the system initiates a self test procedure to verify system integrity. If a problem is located, an error message will remain on the display and operation will stop. After the self-test, the receiver begins an automatic search for all satellites. The status of each satellite being searched is displayed on the "Skysearch" information displayed on the front panel of the receiver . Channel numbers and their associated satellites, SV, are listed across the display. As the receiver scans the frequencies, the status (STAT) number of the search changes from frequency number, to SN ("sniffed") and finally to "LK" as the system "locks" on the frequency of the particular satellite. As the satellites are located, the total number found is displayed as SV. Before a satellite is located, the display shows the time elapsed since the receiver was turned on. After the first satellite is found, the receiver time is set and GPS time is displayed. After the "GPS-UTC" parameters are collected from any satellite, which takes about 12 minutes, the Greenwich mean time (GMT) is displayed.

The receiver collects and displays orbit parameters from each satellite found and computes elevation, azimuth and other information. Tracking information, displayed on the front panel by pressing a specified key, shows the satellites (SV) being tracked, the number of continuous (CNT) data collected from the satellites since last lock or cycle slip, the elevation (Elev) to each satellite, the azimuth (AZM) to each satellite, the range accuracy (URA) to each satellite, the health (HEL) of each satellite, and the age of satellite, also indicating the time elapsed since the lock with the satellite was lost From the information received from the constellation of satellites, the receiver computes and displays the latitude (Lat), longitude (Long), altitude (ALT), the course over ground and speed over the ground of the receiver. In addition it computes and displays information on destination points (known as "way points") the distance to destination (DTD), the course to destination (CTD), and time to destination (TTD). The position and navigation, displayed, seen on the front panel by pressing a specified key, shows LAT, LON, ALT, COG, SOG, DTD, CTD, TTD, and also the quality of geometry The quality of the geometry is measured by GDOP, which has several components: PDOP ($\sigma_x^2+\sigma_y^2+\sigma_z^2$), HDOP ($\sigma_x^2+\sigma_y^2$), VDOP ($\sigma_v^2$), and TDOT ($\sigma_t^2$).

The satellites tracked and data collected can be controlled by the control parameters menu,that can be changed by the operator Initially, before tracking of satellites, the operator can enter the estimated ϕ,λ parameter of the position (POS) using the "data" entry mode. The operator can control the data recording interval, the minimum number of satellites to be used, the minimum elevation of satellites to be used, the use of elevation control in static mode, and the use of unhealthy satellites. The satellite selection menu enables the specific satellite data to be collected. The site

information menu is used to enter site name, session ID, receiver number, antenna number, month/day operations interval, the instrument height, wet and dry bulb temperatures, and barometric pressure. It can also be used to control the recording of data as well as the number of epochs to be recorded in the kinematic survey.

The history of recorded display show the amount of data collected from each satellite. The record & delete file directory menu shows the names of files in the internal memory and can also delete any files or close any file during observation. The differential GPS display are used in special real time differential GPS applications. The way points for navigation are used in the application of GPS in navigation.

2.3 General Operating Theory

2.3.1 Stand-Alone Mode

The receiver performs a cross-correlation operation to extract the signal and recover the data from the satellite. The receiver initially generates an appropriate C/A code, compensating for both Doppler shift and the estimated time difference, and performs a cross-correlation with the received signal. The correlation function between the received signal and the generated C/A code is given by

$$C_i'(t-t')\,S_{L_1}(t) = A_p C_i'(t-t')\,P_i(t)\,D_i(t)\cos(\omega_i t+\phi)$$

$$+A_c C'_i(t-t')\,C_i(t)\,D_i(t)\,(\sin\omega_1 t+\phi)$$

where C'(t-t') is the C/A code generated by the receiver shifted in time t' with respect to C/A code generated by the satellite. The correlation in maximum C'(t-t'). C(t) is one. Thus, a value of t' can be determined when the maximum correlation occurs. Because the period (T_o) of C/A code is set at 1 m sec, the transit time is $\tau' = t'+n$ where n is an integer. The pseudo range, R', between the satellite and the receiver is given by $R' = C\tau'$ where C is the velocity of the electromagnetic wave.

The cross-correlation of the C/A code also enables access to the data code D(t), which contains satellite orbital parameters, satellite clock error, ionospheric delay, and so on. Using these data, the receiver computes the satellite coordinates (U_s,V_s,W_s) and the error in transit time. The corrected pseudo range, R, is given by

$$R = C(\tau'+\Delta\tau_s) = C\tau = [(U_s-U)^2+(V_s-V)^2+(W_s-W)^2)]^{1/2}-C\Delta\tau$$

where U,V,W are the receivers coordinates and

$\Delta\tau_s$ = satellite clock, ionospheric and atmospheric error

$\Delta\tau$ = the synchronization error between satellite and receiver clock
τ = corrected transit time.

Thus, by using pseudo-range measurements to four or more satellites, the four unknowns, U,V,W, and $\Delta\tau$ are computed (see Fig. 2.12). The computations are performed every epoch. Since there are 12 channels, data from 12 satellites are collected every epoch. The (U,V,W) coordinates are converted to latitude ϕ, longitude λ, and elevation H and displayed on the display screen of the receiver. If only those satellites are visible, then the receiver can compute the three unknowns. In practice, if the elevation is constrained, the receiver can use three satellites and compute the ϕ, λ, and $\Delta\tau$.

Because of the relative motion of the satellite with respect to the receiver, the signal is subject to varying Doppler shift. The electronic correlation process must time-shift the receiver codes at rates proportional to the Doppler shift. Since

$$t = \frac{1}{\lambda} T_o$$

where
λ = wave of signal
1 = portion of the distance < λ and
t = portion of the time < T_o
we have

$$t = \frac{1}{c} T_o f$$

(where f=frequency)

therefore

$$dt = \frac{1}{c} T_o df = T_o \frac{f}{C} dl$$

However, the phase angle ϕ is given by

$$\phi = \omega t$$

where

that is,

$$\omega = \frac{2\pi}{T_o}$$

$$d\phi = \omega dt$$

therefore

$$dl = \frac{C}{2\pi f} d\phi$$

also

$$R_2 - R_1 = (c/2\pi f)(\phi_2 - \phi_1) = \text{dl (delta range)}$$

and because

$$(U_s - U)^2 + (V_s - V)^2 + (W_s - W)^2 = R^2$$

we have

$$(U_s - U)(dU_s - dU) + (V_s - V)(dV_s - dV) + (W_s - W)(dW_s - dW) = RdR = Rdl = \frac{RC}{2\pi f} d\phi$$

where (dU_s, dV_s, dW_s) and (dU, dV, dW) are the velocity components of the satellite and receiver, respectively. Using the delta range and velocity of the satellite, the velocity of the receiver, $(dU^2+dV^2+dW^2)^{1/2}$, was computed by the receiver every epoch. The delta range is derived by tracking the carrier phase and computing the change in the carrier phase to the satellite over every subsequent epoch. By knowing the velocity of the satellite from the satellite orbital parameters, the velocity of the receiver is computed and displayed using the delta range or Doppler shift of three or more satellites. The computed positions ϕ, λ, h, and the receiver's velocity, dU, dV, dW, as well as pseudo range, doppler shift and the like are stored in the central memory's every epoch for future references.

2.3.2 Differential GPS

If receiver 1 and 2 (see Fig. 2.4) are located at two stations, then the phase difference, $\Delta\phi$, between the signals received by the two receivers corresponds to the difference in distance traveled by the signal to the two receivers. Thus, $\Delta\phi = \Delta D\cos\theta$ (see Fig. 2.13) where θ is the direction of the signal with respect to base line and ΔD is the component of the difference in distances to the satellite in the direction of the baseline. Since the wavelength of the carrier wave is 19 cm, only portions of phase difference less than 19 cm can be measured initially. In practice,

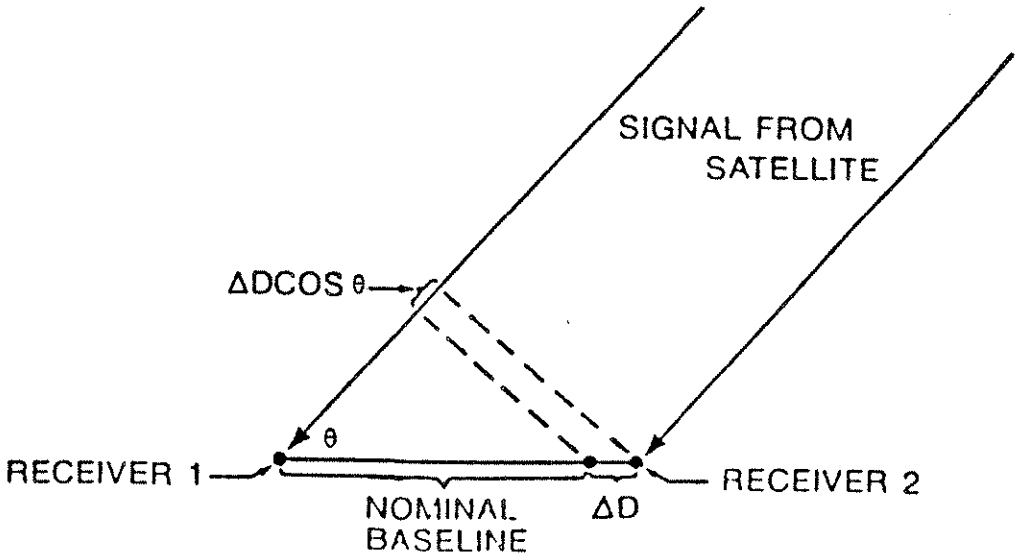

Figure 2.4 Interferometric Method

the distance between the receiver can be estimated by using the stand alone mode to with in ± 5 m. Thus we have

$$\Delta\phi = U_o + U + \Delta D\cos\theta + \nu + t$$

where

U_o = predicted phase difference between stations
U = unknown integer
$\Delta\phi$ = measured phase difference
ν = measured noise
t = clock synchronization error

Now, if we observe the phase difference to four or more satellites then the clock synchronization error will be the same. Since

$$\Delta D = \frac{\Delta X}{D}\delta x + \frac{\Delta Y}{D}\delta y + \frac{\Delta Z}{D}\delta z$$

where D = estimated distance between two stations,

$\Delta X, \Delta Y, \Delta Z$ = estimated difference in X,Y,Z coordinates between two stations, and
$\delta x, \delta y, \delta z$ = corrections for estimate of difference, so we have

$$\Delta\phi = U_o + \left[\frac{\Delta X}{D}\cos\theta, \frac{\Delta Y}{D}\cos\theta, \frac{\Delta Z}{D}\cos\theta\right]\begin{bmatrix}\delta x\\ \delta y\\ \delta z\end{bmatrix} + U + t + V$$

If $\Delta\phi_1$, $\Delta\phi_2$, $\Delta\phi_3$, and $\Delta\phi_4$ are observations to four satellites, then

$$\begin{bmatrix}Z_1\\ Z_2\\ Z_3\\ Z_4\end{bmatrix} = \begin{bmatrix}\Delta\phi_1 - U_{o_1} - U_1\\ \Delta\phi_2 - U_{o_2} - U_2\\ \Delta\phi_3 - U_{o_3} - U_3\\ \Delta\phi_4 - U_{o_4} - U_4\end{bmatrix} + \begin{bmatrix}-V_1\\ -V_2\\ -V_3\\ -V_4\end{bmatrix} = \begin{bmatrix}\frac{\Delta X}{D}\cos\theta_1 & \frac{\Delta Y}{D}\cos\theta_1 & \frac{\Delta Z}{D}\cos\theta_1 & 1\\ \frac{\Delta X}{D}\cos\theta_2 & \frac{\Delta Y}{D}\cos\theta_2 & \frac{\Delta Z}{D}\cos\theta_2 & 1\\ \frac{\Delta Z}{D}\cos\theta_3 & \frac{\Delta Y}{D}\cos\theta_3 & \frac{\Delta Z}{D}\cos\theta_3 & 1\end{bmatrix}\begin{bmatrix}\delta z\\ \delta y\\ \delta z\\ t\end{bmatrix}$$

If the measured noise, ν, is random and the integer U is determined, $\delta x, \delta y, \delta z$, and t can be determined by the principle of least squares using a number of observations of four or more satellites. In practice this is done by post-processing the data collected. The unknown integers, U, are determined by single, double, float double, and triple-differences method.

Suppose $S(k_1,j,i)$ is the signal carrier phase received by receiver K_1 from satellite j at epoch i and $S(k_2,j,i)$ is the carrier phase at receiver K_2 from satellite j at epoch i; then

$$S(K_1, j, i) = C_j + n_1\pi - \phi_{K_1}$$

$$S(K_2, j, i) = C_j + n_2\pi - \phi_{K_2}$$

where, C_j is the initial phase of the signal from satellite j, n_1 & n_2 are integers, and ϕ_{K1} and ϕ_{K2} are phases measured by receivers K_1 and K_2.
A single difference, SD(j,i) is formed by differencing the carrier phase observable from two receivers k_1 and k_2 at the same epoch i from the satellite j. Thus

$$SD(j,i) = S(K_2,j,i) - S(K_1,j,i)$$

$$= (n_2 - n_1)\pi - \phi_{K_2} + \phi_{K_1}$$

$$= U_j + \Delta\phi_j + t$$

where U_j is the integer for satellite j, t is the receiver clock error, and $\Delta\phi_j$, is the true phase difference. SD(j,i) is independent of the satellite clock error.

A double difference DD (j_1, j_2, i) is formed by differencing a single difference between a reference satellite j and another satellite j_2 at the same epoch i. This results in

$$DO(j_1, j_2, i) = SD(j_2, i) - SD(j_1, i)$$

$$= U_{j_2} + \Delta\phi_{j_1} - \Delta\phi_{j_1}$$

$$= (U_{j_2} - U_{j_1}) \left[\frac{\Delta X}{D}(\cos\theta_1 - \cos\theta_2) \quad \frac{\Delta Y}{D}(\cos\theta_1 - \cos\theta_2) \quad \frac{\Delta Z}{D}(\cos\theta_1 - \cos\theta_2) \right] \begin{bmatrix} \delta x \\ \delta y \\ \delta z \end{bmatrix}$$

The double difference DD(j_1, j_2, i) is independent of $(\delta x, \delta y, \delta z)$, the receiver clock error. By keeping track of the complete cycles in the phase measurement, the integer ambiguities can be determined. If the ambiguity $(U_{j2} - U_{j1})$ is solved as a variable, then the solution is known as float double difference.

A triple difference TD (j_1, j_2, i) is formed by differencing the double difference for the same satellite pair at some integer of

succeeding epochs i and i + 1. Thus

$$TD(J_1, J_2, i) = DD(J_1, J_2, i+1) - DD(J_1, J_2, i)$$

$$= \frac{\Delta X}{D}(\cos\theta_{i1} - \cos\theta_{(i+1)} - \cos\theta_{(i+1)2})\,\delta x + \frac{\Delta Y}{D}(\cos\theta_{i1} - \cos\theta_{(i+1)} - \cos\theta_{(1+1)2})$$

$$+ \frac{\Delta Y}{D}(\cos\theta_{i1} - \cos\theta_{(i+1)} - \cos\theta_{i2} + \cos\theta_{(i+1)2})\,\delta z$$

The triple difference is independent of the integer ambiguities and clock error. The triple difference solution needs a number of observations and since the coefficients of $\delta x, \delta y$, and δz are small compared to double difference, it may not be reliable.

2.3.3 Static Mode

In a static mode the receivers collects data in differential mode for 45 minutes to about 2 hours, depending on the distance between the two stations and the accuracy required.

2.3.4 Kinematic Mode

The kinematic mode consists of one receiver remaining primarily static over a known station while a rover receiver collects data at unknown points as it travels. To initiate the kinematic survey, the exact position of two points must be known very accurately. The master receiver occupies a known point; and the rover, the other point known point. The master remains on its known point and the rover move sequentially to the other unknowns points throughout the survey. After the final unknown point, the rover is returned to its first known point location for few minutes of data collection

2.4 Post Processing Software

Post-Processing Software, which includes post-processing of data in static, kinematic, and as well as a variety of coordinate conversions,are provided by the GPS manufacturers.

The receiver is connected with the post processing computer with the appropriate cable with RS 232 connector on the back panel. The software presents the following main menu:

a) auto processing
b) down load receiver
c) editing Planning
d) manual processing
e) post mission
f) select directory

The "auto processing" option will allow the user to automatically process the data in static or pseudo-kinematic modes. The "download receiver" option enables the user to download the data from the receiver to the PC using a program "HOSE," which also allows the direct download of an almanac file for use in a

satellite visibility program. HOSE program bendata, navigation, and site files in the PC. The "editing/planning" option enables the user to convert files to print and edit various data files by using the program called "file t001" in order to produce a satellite visibility chart using the "GPSMAP" program and the almanac-data file. "Manual Processing" allows the user to run the "ANTSWAP" used in kinematic surveys and create both common navigation files using "COMNAV" program and create log files used in the kinematic survey by using "Gem log" program, run "KINSRVY," the program for computing the rover position using data collected for kinematic survey, run the "Line Comp" program for computing the baseline vector from static or pseudo-kinematic data, run the "Make U file," which creates the U file consisting of difference phase data files from the bendata and navigation files from each of the base stations, and run the "Make Inp" program to create and edit Baseline.Inp files required in "line comp." The "post mission" menu enables the user to create data for adjusting networks, and "select directory" permits the user to choose different directories in the PC.

The common procedure used in this project , is to download the data from the receiver and create the Bendata, navigation, and site data files. Then, by using the manual processing, the U files and Baseline.Inp files are created and the Linecomp/kinsurvey is executed. The programs will compute and print the baseline vector, baseline distance, base line azimuth, latitude, longitude, and elevation as well as the X,Y,Z coordinates of the base stations using double difference, float double difference, and triple difference. They also provide statistical data for analyzing the results.

3.0 PHOTOGRAMMETRIC SYSTEM

3.1. Introduction

Photogrammetry is defined as the "science or art of obtaining reliable information by means of photography". Ever since the invention of the pin-hole camera, man's quest for discovery has led him to find many uses for photography: storing information, documenting evidence, identifying objects, locating places, determining shapes and sizes of objects, determining land and property boundaries and plotting contours. Photogrammetry uses photography to do all these and more. The scope of photogrammetry is changing rapidly as new fields of scientific knowledge are opened by fresh discoveries. With the advent of space and computer technologies, photogrammetry is able to map earth systems and record global changes in real time and to do all these with efficiency and accuracy hitherto considered to be impossible.

3.2. Theory of Photogrammetry

The theoretical developments in photogrammetry have advanced very rapidly from single photo-geometry to multi-photo adjustment using constraints in exterior orientation from kinematic satellite tracking, and in interior orientation from dynamic calibration. These developments can be described under the following headings: single photo-geometry, analogue stereo photogrammetry, analytical photogrammetry, close-range photogrammetry, terrestrial photogrammetry and digital photogrammetry.

3.2.1. Single photo-geometry

A single photo can be treated as a projection of objects in space through a single point O, the center of the lens. The simplest case is a perspective projection where a point (X,Y) on an object plane is projected as an image point (x,y) through the perspective center onto an image plane (see figure 3.1). The (x,y) coordinates are related to (X,Y) thus:

$$x = \frac{a_{11}X + a_{12}Y + a_{13}}{a_{31}X + a_{32}Y + a_{33}}$$

$$y = \frac{a_{21}X + a_{22}Y + a_{23}}{a_{31}X + a_{32}Y + a_{33}} \qquad \text{(1)}$$

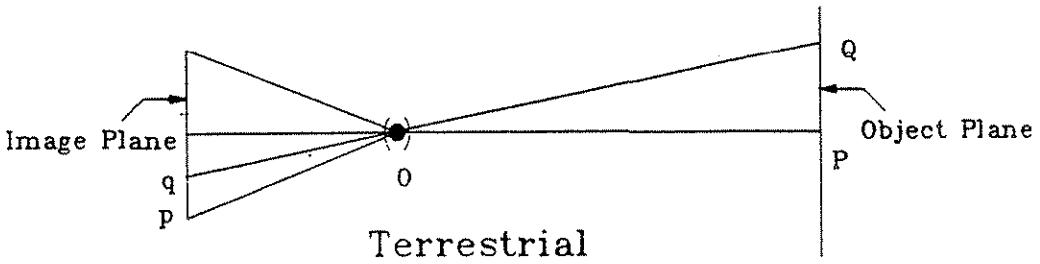

Terrestrial

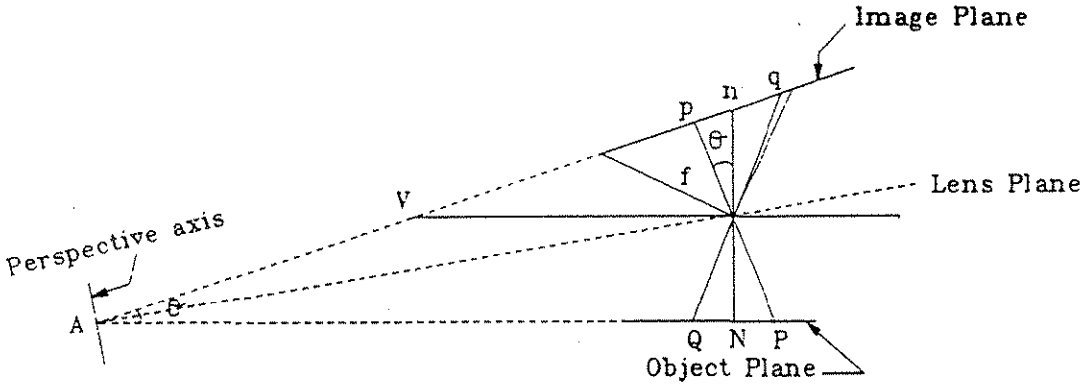

Aerial

Fig. 3.1 Aerial and terrestrial photogrammetry.

(Note: All figures in Chapter 3 are from the following reference. K.Jeyapalan, "Photogrammetry" in Encyclopedia of Earth Science, Academic Press, New York, 1991.)

where,

$a_{11}.....a_{33}$ are constants which depend on o, f and H

O = the angle between the planes

f = op = the perpendicular distance from center of the lens to the image plane

H = ON = the perpendicular distance from the center of the lens to the object plane

O = the center of the lens or perspective center

P = the principal point

N = the nadir point

Line POp is defined as the principal axis of the lens. If the line POp is horizontal, the projection is described as a horizontal or terrestrial photograph; if it is vertical, it is called a vertical or aerial photograph. If it is neither, but the image of the horizon appears, the projection is known as a high oblique; if the image of the horizon does not appear, it is known as a low oblique.

When mapping the earth, points on its surface are projected onto a number of planes (see figure 3.2). Typically, a map has a scale distortion, meaning that the distance on the ground is not exactly equal to the scaled distance on the map, and an azimuth distortion meaning that the direction on the ground is not exactly equal to the direction on the map. In mapping, these distortions, especially the azimuth distortion, must be minimized because projections with no azimuth distortion, known as conformal projections, are popular in navigation and cadastral surveys.

At a first glance, an aerial photograph would appear to be a suitable projection for mapping the earth. However, an aerial photograph has three distortions; namely, lens, tilt and height. If q is the image of object Q, then according to the perspective projection the points q, O, Q must lie on a straight line (see figure 1). However, this is not so in practice. The deviation of these points from a straight line is due to lens distortion and refraction in the atmosphere. Modern cameras use lenses designed by computers, to reduce the distortion to about + 2 seconds equaling about 0.005 mm on the photograph.

The tilt distortion is due to the fact that the photograph is not truly vertical. However, with modern technology it is possible to take vertical photographs with a tilt of about + 1 to 2 degrees. This photograph can be made into a equivalent vertical photograph by having about four or more control points for which

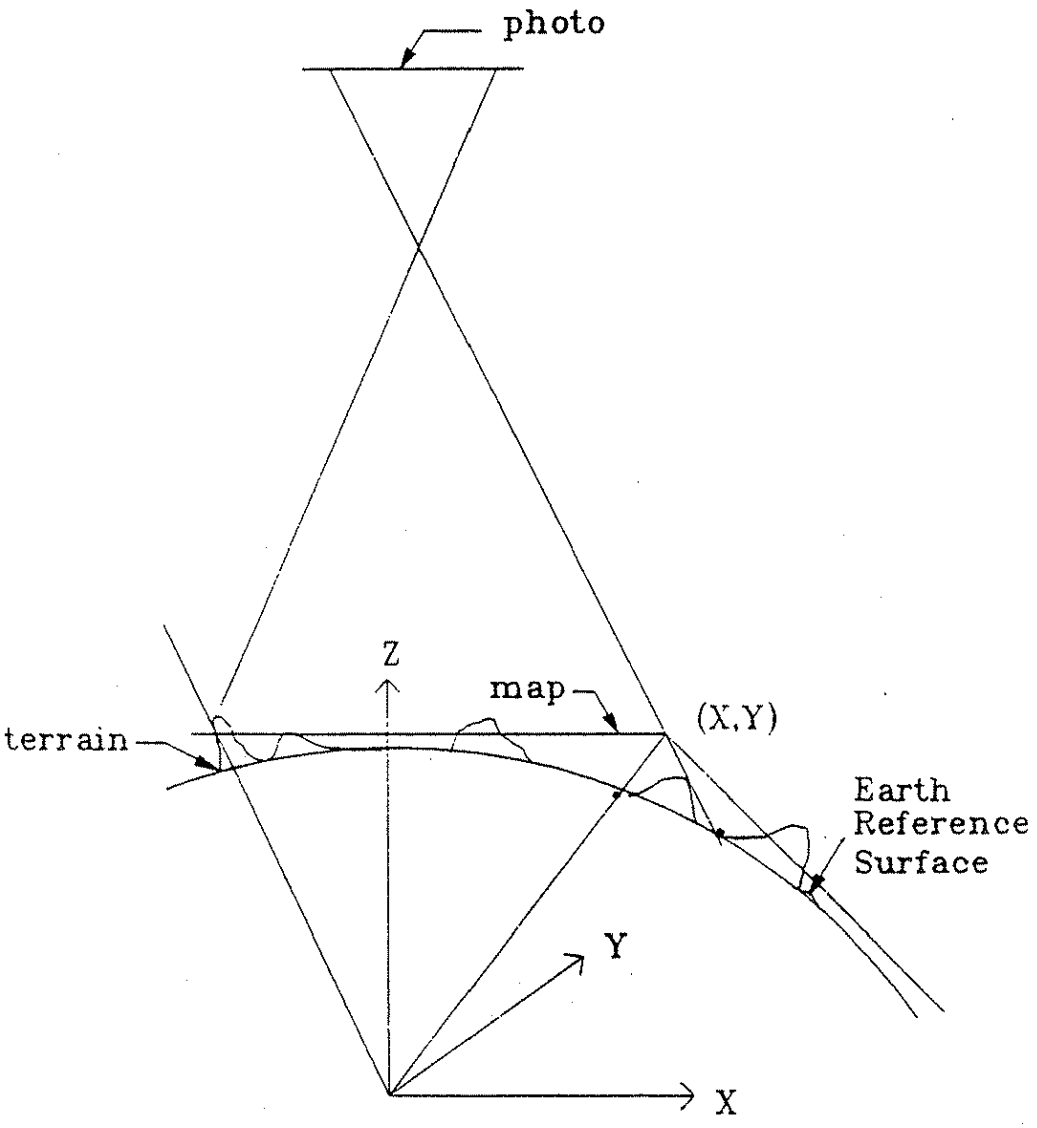

Fig. 3.2 Map projection.

the coordinates (X,Y) on the map are known. The process of producing the equivalent vertical photograph from the near vertical photograph is known as rectification. The analogue instrument capable of producing the rectified print is known as a rectifier. It should have five degrees of freedom to determine scale, tilt in Y direction, tip in X direction, and the translations in X and Y directions. A scanner developed by using modern computer technology scans the photograph and produces a digital point by point (pixel by pixel) image which can be displayed on the screen of a computer. The point by point image can be corrected for tilt distortion, displayed as a map and a hard copy obtained, if necessary. In practice, a number of aerial photographs are taken over an area. If these photographs are assembled after rectification to form a continuous photo image, it is known as a controlled mosaic. The controlled mosaic is equivalent to a map except for its height distortion. Aerial photographs assembled without rectification are known as uncontrolled mosaics.

The vertical distance of a point from a mean level surface is known as the elevation. Height distortion is due to the fact that the points on the surface of the earth are not of the same elevation. Points of the same elevation will be on a plane parallel to the reference surface. The map point of a surface point Q is Q_1. If q, q_1 are the image points of Q and Q_1, then q q_1 are referred to as the height distortion (see figure 3.3). From figure (3.3) we have

$$\frac{pq}{NQ_1} = \frac{f}{H}$$

$$\frac{pq_1}{NQ_1} = \frac{f}{H-h}$$

$$\frac{qq_1}{NQ_1} = \frac{f}{H} - \frac{f}{H-h} = \frac{fh}{H^2}$$

$$dr = qq_1 = \frac{pq_1 h}{H} = \frac{rh}{H}$$

$$dr = \textit{height distortion}, \quad r = pq_1$$

Thus, if the elevation of the points are known, then the height distortion can be corrected for point images. The elevation of points are obtained from (a) Digital Terrain Model (DTM) data, (b) interpolated from contours of existing maps, and (c)

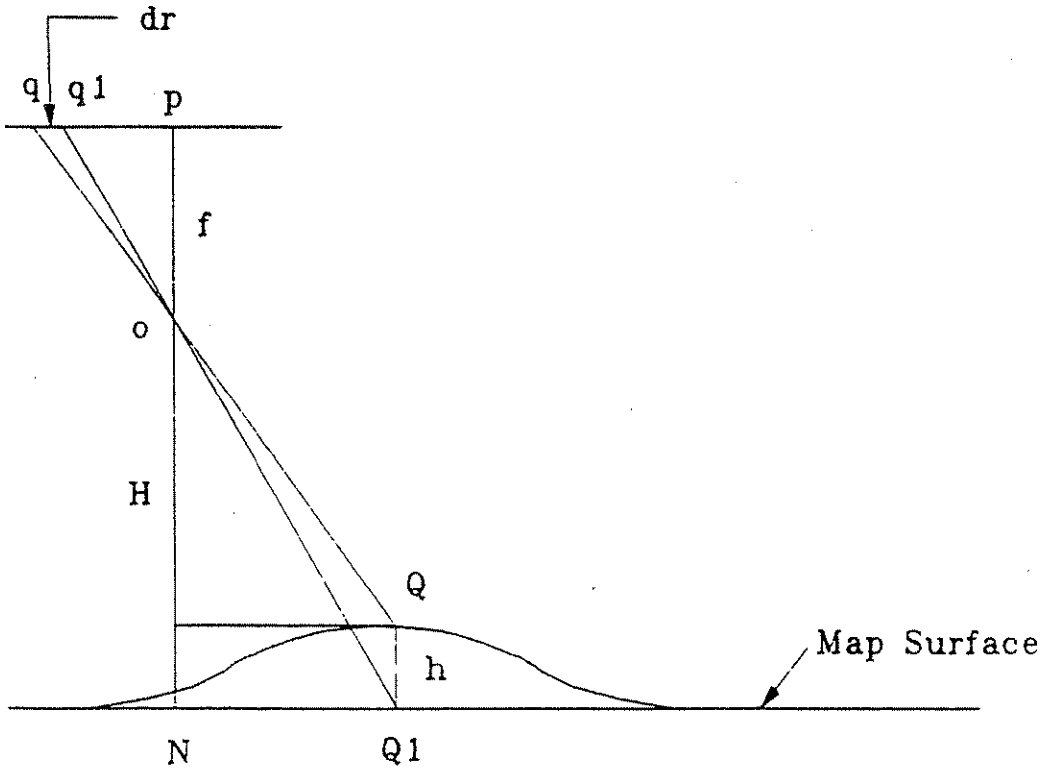

Fig. 3.3 Height distortion.

determined from stereo images either manually or using autocorrelation techniques. A photograph in which height distortion is eliminated is called an orthophotograph. An orthophoto is equivalent to a topographic map except that it does not show contours. Furthermore, in an orthophotograph all information recorded by the camera or sensor are shown without interpretation, whereas in a map selected features are shown with interpretations.

3.2.2. Stereo-photogrammetry

Equation (3.1) gives the perspective transformation of points on an object plane to points on an image plane. However, if the objects are three dimensional, the image points are central projections of the object points (see figure 3.4) and are given by

$$x = \frac{a_{11}X + a_{12}Y + a_{13}Z + a_{14}}{a_{31}X + a_{32}Y + a_{33}Z + a_{34}}$$

$$y = \frac{a_{21}X + a_{22}Y + a_{23}Z + a_{24}}{a_{31}X + a_{32}Y + a_{33}Z + a_{34}} \qquad \text{(3.2)}$$

where (X, Y, Z) are three dimensional coordinates. a_{11}, a_{12} ..... a_{34} are the constants depending on the exterior orientation elements (X_0, Y_0, Z_0, κ, Φ, ω). The principal distance f, and (x,y) are image point coordinates with respect to the photo coordinate system (x,y,z), whose origin is at the center of the lens and the z axis is perpendicular to the image plane. The coordinates (x_0, y_0, z_0) of the principal point in the (x, y, z) system are known as the interior orientation elements.

(X_0, Y_0, Z_0) are the coordinates of the center of the lens in the object coordinate, and κ, Φ, ω are the rotation angles about (x,y,z) axes of the photo system required to make the photo system parallel to the object coordinate system. Thus,

$$a_{14} = -(a_{11}X_0 + a_{12}Y_0 + a_{13}Z_0)$$

$$a_{24} = -(a_{21}X_0 + a_{22}Y_0 + a_{23}Z_0)$$

$$a_{34} = -(a_{31}X_0 + a_{32}Y_0 + a_{33}Z_0)$$

Unlike the set of equations (3.1), the set of equations (3.2)

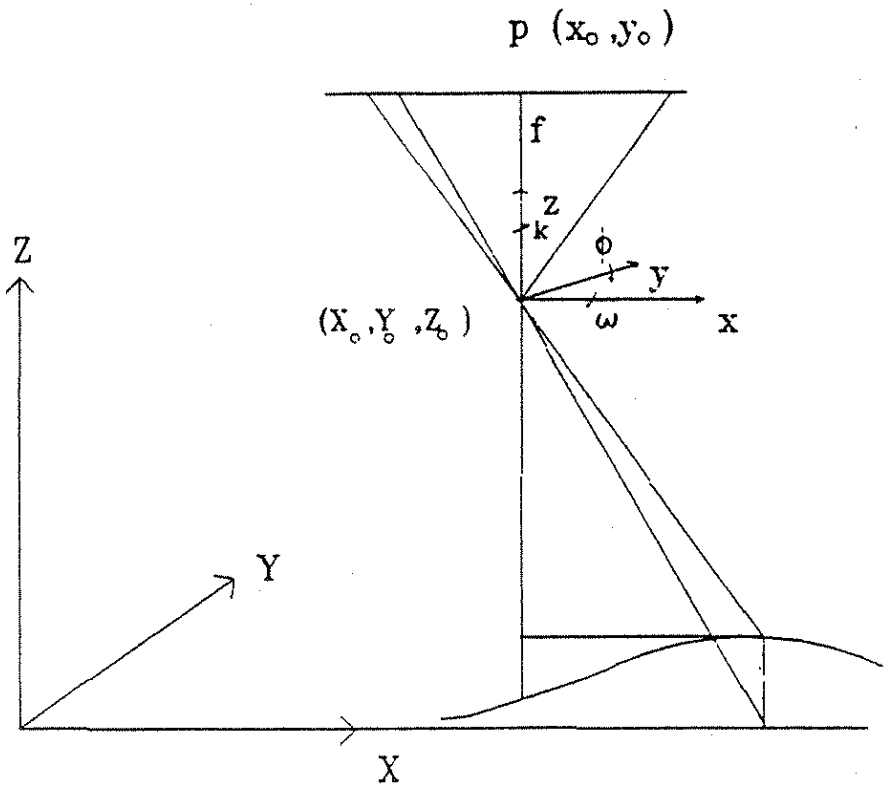

Fig. 3.4 Coordinate system.

suggests that for a single image point there are a number of object points that could satisfy them. In other words, given (x,y) of an image point, we cannot solve uniquely for (X,Y,Z) of the object point from a single photo. However, if the images are formed on two different photographs, then from four equations it is possible to solve for the three unknowns. A pair of human eyes uses this principle to see objects in three dimension. This physiological phenomenon is known as stereo-vision. The depth of perception depends on the paralytic angle, Φ (see figure 3.5). A pair of photographs known as stereo pairs are used to obtain the three dimensional coordinates of an object. This methodology is known as stereo-photogrammetry. The distance between the two photographs, $O_1 O_2 = B$, known as "air base" is comparable to the distance between two human eyes, known as "eye base". In an ideal vertical photograph the difference in x coordinates, known as px or X-parallax, can be used to calculate the elevation h of a point from the equation

$$px = x_2 - x_1 = \frac{Bf}{H-h}$$

3.2.3. Analytical Photogrammetry

In analytical photogrammetry the interior orientation elements of the camera are precisely determined by camera calibration methods. The photo (x,y) system and the principal point is defined by fiducial marks at 4 or 8 points along the border of the photograph (see figure 3.6). The image coordinates (x,y) are measured by comparators to an accuracy of about + 0.001 mm and the exterior orientation elements $(X_0, Y_0, Z_0, \kappa, \Phi, \omega)$ are calculated by using three or more control points for which (X,Y,Z) are known and the set of equations (3.2). This procedure is known as resection. Knowing the exterior and interior orientation elements of the stereo pair, the object coordinates of any point A whose images a_1, a_2 appear on the stereo pair can be computed using the two sets of equations similar to (3.2) and the image coordinates of a_1 (x_1, y_1) and a_2 (x_2, y_2). The pair of points (a_1, a_2) are known as conjugate points and the procedure of determining the object coordinates using the conjugate points is known as intersection. The entire procedure of resection and intersection is known as analytical photogrammetry and is done simultaneously for a number of points or a single point by software which can be run on a personal computer, workstation or mainframe. The software uses the method of least squares with constraints where more equations than unknowns are used in the solution. The equations with more reliability are given higher weights to determine a weighted average solution. This method is known as simultaneous adjustment by constraint.

3.2.3. Analogue Photogrammetry

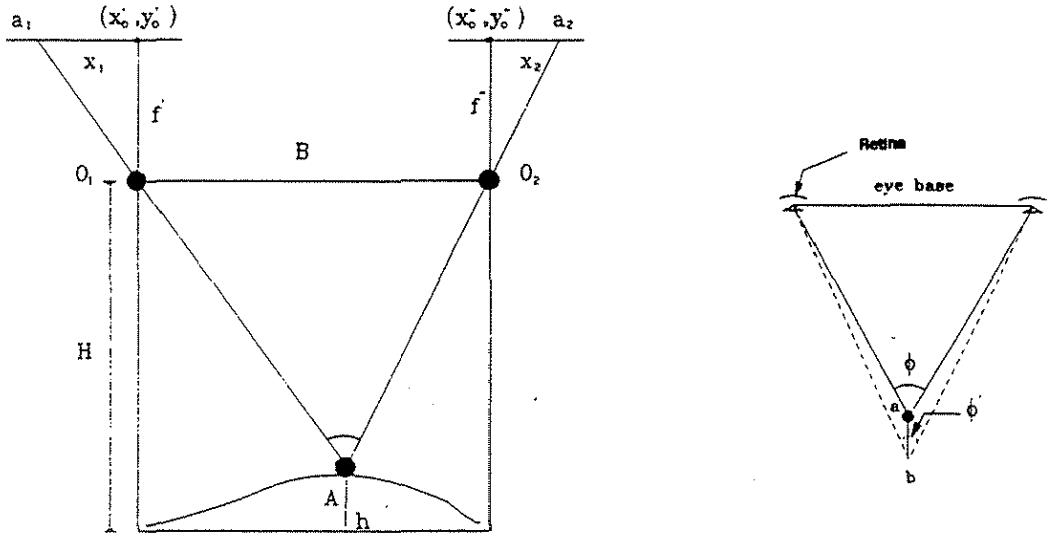

Fig. 3.5 Stereoscopy.

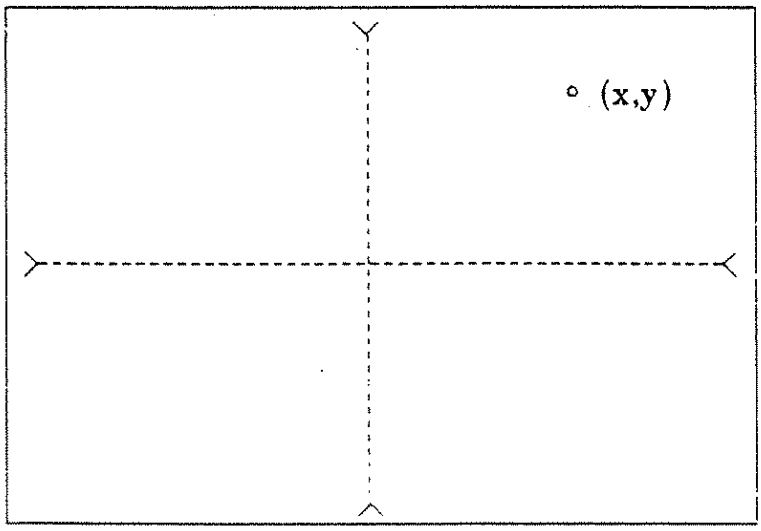

Fig. 3.6 Photo coordinates.

In analogue photogrammetry the object coordinates are determined by mechanical or optical mechanical methods. In this method the diapositives, the positive print of the negative film, are placed on a projector, which has the same interior orientation elements as the camera, and the rays corresponding to the original rays which produce the image are projected back (see figure 3.7). The exterior orientation elements (X_0, Y_0, Z_0, κ, Φ, ω), (X_0',Y_0',Z_0',κ',Φ',ω') of the stereo pair are determined in two steps:

- relative orientation in which five of the twelve elements are determined
- absolute orientation in which the other seven elements are determined.

When rays are projected from the stereo projectors, the corresponding rays from the conjugate points will intersect in space provided the projectors are in the same relative position as of the original cameras. However, if they are not, then the rays at a distance Z from the projectors will have X and Y separation known as X parallax and Y parallax, py. The Y parallax at a object coordinate X, Y, Z is given by

$$py = (Y_0 - Y_0') - \frac{Y}{Z}(Z_0 - Z_0') + X\kappa - (X - B)\kappa' - \frac{(Y^2 + Z^2)}{Z}(\omega-\omega') + \frac{XY}{Z}\Phi + \frac{-(X-B)Y}{Z}\Phi'$$

Due to linear dependency, only 5 of the 12 exterior orientation elements can be determined by measuring the py at 5 or more points. Typically, Y parallaxes are eliminated iteratively at the standard six points. This can be done mechanically or analytically, in a sequence, by elements which do not affect the Y parallax at the previous point.

If the Y parallaxes are eliminated at 5 or more points, then the corresponding rays will intersect in space creating a model of the true earth surface or object. The model so created can be scaled and leveled so that the object coordinates (X,Y,Z) can be determined by measuring the model coordinates (X,Y,Z). Two or more planimetric control points for which (X,Y) and X,Y) are known are required to do the scaling and 3 or more height control points for which Z and Z are known are required to do the leveling. The scaling and leveling procedures determine the seven exterior orientation elements which are not determined by relative orientation. The scaling and leveling are done by mechanical translation and rotation of the stereo projectors.

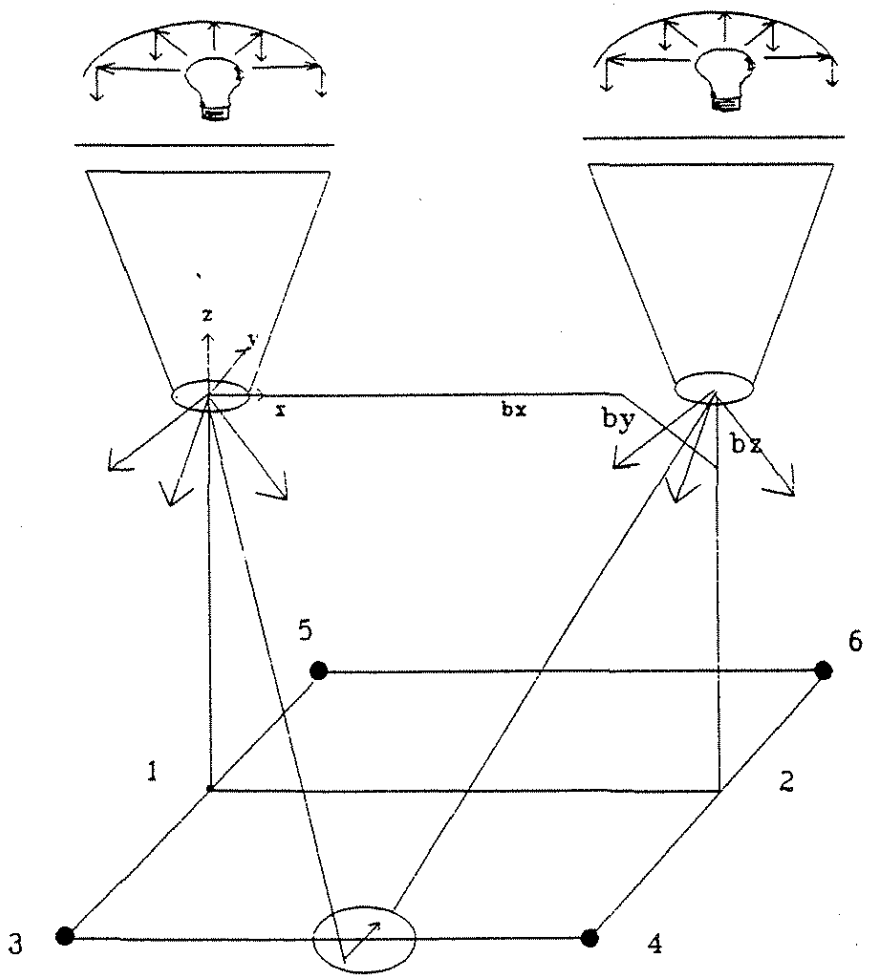

Fig. 3.7 Stereo plotter.

The stereo projectors are also known as stereo plotters.

Once this model is created it can be used to plot both planimetric and contour maps at specified scales depending on the flying height of the aircraft and capability of the stereo-plotters. A reference mark known as the floating mark, made either on a tracing table or created by optical illusion from a pair of marks on the viewing system, is used to trace the features as well as the contours. The position of the mark is plotted directly under it or on a coordinatograph connected by mechanical linkages to produce the maps (see figure 3.8).

3.2.5 Digital Photogrammetry

The object coordinates created by analytical or analogue methods can be transformed either directly or via encoders to a computer. The spatial coordinates can be used by computer algorithms to display points, lines, squares, rectangles, circles, ellipses, and other shapes. The attributes to points, lines and polygons can also be entered into the data base. The data base can then be used to plot maps in different perspective such as planimetric, contour, three dimensional view etc. Data can be saved in different layers, each layer containing different features such as roads, buildings, etc. This information, now known as a Geographic Information System (GIS) can be displayed separately or in combination and plotted in a map form.

Digital photogrammetry can also rasterize the photograph into point images or pixels with radiometric values. Different objects have different radiometric values which depends on the energy emitted and reflected. By assigning different colors to each range of radiometric values, a color image of the photograph can be displayed on the computer screen. Each pixel has a position vector (x,y) which can be transformed into the photo coordinates. Thus, by having small pixel sizes, the resolution of the images as well as the accuracy of the (x,y) can be improved. The (x,y) coordinates can be used in analytical photogrammetry or corrected for tilt, height and other distortions to produce orthophotos. This methodology is called digital orthophotography.

3.3 Photogrammetric Instruments

3.2.1. Aerial Camera

Figure (3.9) shows the sketch of an aerial camera. It consists of a number of lens elements to minimize lens distortion. It also has an internal shutter which can be used to control the aperture size and exposure interval. All electromagnetic energy entering the lens system at the front nodal point leaves the lens system in a parallel direction from the rear nodal point. The film roll is contained in a magazine enabling it to take a number of
exposures without changing the magazine. At the time of exposure

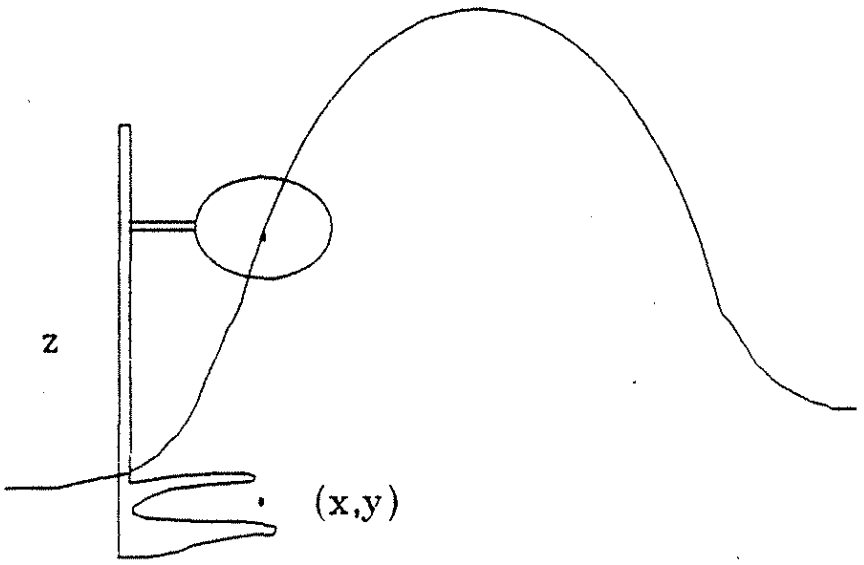

Fig. 3.8 Measuring system.

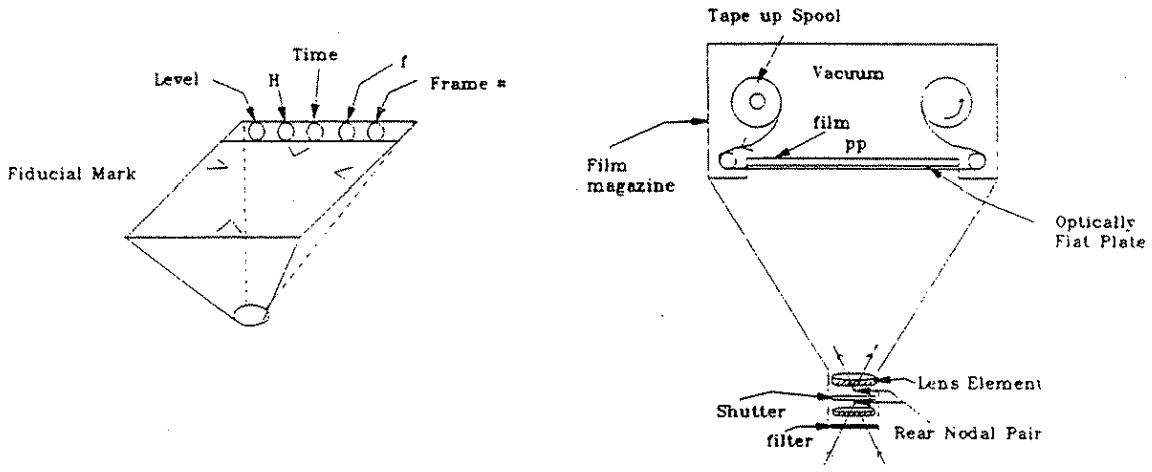

Fig. 3.9 Aerial camera.

the film is kept flat against the optically flat glass plate. The openings in the film frame exposes the fiducial marks, time and date of flight, exposure number, principal distance, altitude and the position of the level bubble indicating the verticality of the principal axis. The intersection of the fiducial mark defines the principal point. The distance from the rear nodal point to the principal point defines the principal distance. The film is coated with emulsion which is sensitive to certain bands of the electromagnetic spectrum. Three types of film are commonly used: orthochromatic, panchromatic, and infra red. Orthocromatic film is sensitive to energy from blue, .4 μm, to green, .6 μm band. Panchromatic is sensitive to energy from blue, 0.4 μm to red, .8 μm. Infra red is sensitive to all visible light with a range from 0.3 μm to 0.9 μm. Though black and white film are generally used, color film and false color film are sometimes used. Color film shows images in true natural color, while false color does not show their true natural color. Positive prints on paper, film base and glass plates are made from the negative. The negatives are developed under ideal conditions in order to retain the geometrical quality.

3.3.2: Scanners

With the development of digital photogrammetry the scanners or vidicon camera may replace the traditional camera. In the scanner the emulsion coated film is replaced by electronic detectors placed at specific locations. The detectors respond to certain wave bands and its responsivity is proportional to the amount of energy in the spectral band. The responsivity for each detector can be stored on magnetic disk or displayed on CRT (see figure 11). The display is a grey level varying from 0 to 250 or a specific color depending on the responsivity. The resolution on the image depends on the size of the detector known as pixel size. The geometric quality of the scanner for photogrammetric application depends on the exact location of the detectors in the image plane, as well as the size of the detectors. The scanners are useful in unmanned space missions in which the radiometric values corresponding to the responsivity of each pixel can be transmitted to ground station. The values can then be analyzed using a computer to identify the objects. This process of identifying objects is known as image analysis. The location of the pixel gives the image coordinates (X,Y) which can be used for photogrammetric applications.

3.3.3. Stereo Plotters

Stereoplotters are classified into two main groups: optical and optical-mechanical. In the optical type the camera is replaced by projectors whose interior orientation elements can be adjusted to be the same as that of the camera. The diapositives are placed in the image plane and the rays are projected through the lens of the projector. The projector must have at least five

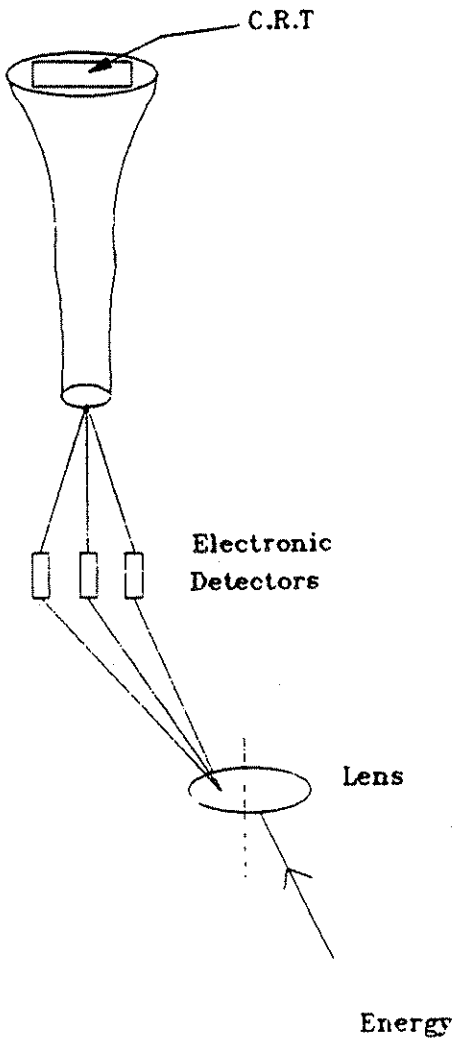

Fig. 3.10 Scanner.

degrees of freedom to do the relative orientation for creating the stereo model and at least one additional freedom of movement for scaling. The rays from the stereo plotters are projected onto a plane of the measuring system (see figure 3.11). The measuring system consists of a reference mark known as the floating mark. It has the capability of measuring the x-parallax, separation of the projection rays in X, and the Y-parallax, the separation of rays in Y. The relative orientation is achieved by eliminating the Y parallaxes. After the Y parallaxes are cleared, the stereo model can be viewed. There are a number of devices to view the stereo model. One of the oldest methods is the anaglyphic method in which the rays from the left projectors are viewed by the left eye and the rays from the right projector, by the right eye. In the modern equipment the rays from the left projector are brought to the left eye by a series of lens and prism arrangements; similarly, the rays from the right projector are brought separately to the right eye. The latter method has the advantage of adjusting the system to suit the individual observer and provides a comfortable seating arrangement for the viewer.

The measurement of the X-parallax after relative orientation gives the differences of height. At any point in the model, if the X-parallax is cleared, then the location of the reference point or floating mark gives the model coordinates (X_m, Y_m, Z_m). The model can be brought to a predetermined scale by changing the distance between the projectors. The planimetric position of (X_m, Y_m) can be plotted on the plotting board and the points of the constants Z_m, a contour, can also be plotted. The model Z_m coordinate system can be made parallel to the ground Z system by either rotating the projectors or the plotting system about the X-axis (ω-tilt) and the Y axis (Φ-tip). In some systems a combination of rotating the projector and the plotting system is used. The rotation ensures that the model height distance is the same as the ground height difference. This system can produce maps of the earth system and also maps showing global changes.

In digital photogrammetry the model coordinates are fed into the computer by using encoders. The coordinates are used as vectors in plotting and displaying ground features and contours (see figure 3.12).

3.3.4. Analytical Plotters

In analytical plotters the dispositive plates are placed on flat holders and viewed or scanned normally. The plate coordinates (x,y) and (x,y) of the conjugate points are measured by the combination movements of the plate holders and scanner. These plate coordinates and ground coordinates of three or more points are fed into a work station where the software computes the exterior orientation elements (see figure 3.13). Using the exterior orientation elements, the computer calculates the Y parallax for points viewed by the scanner and moves the scanner

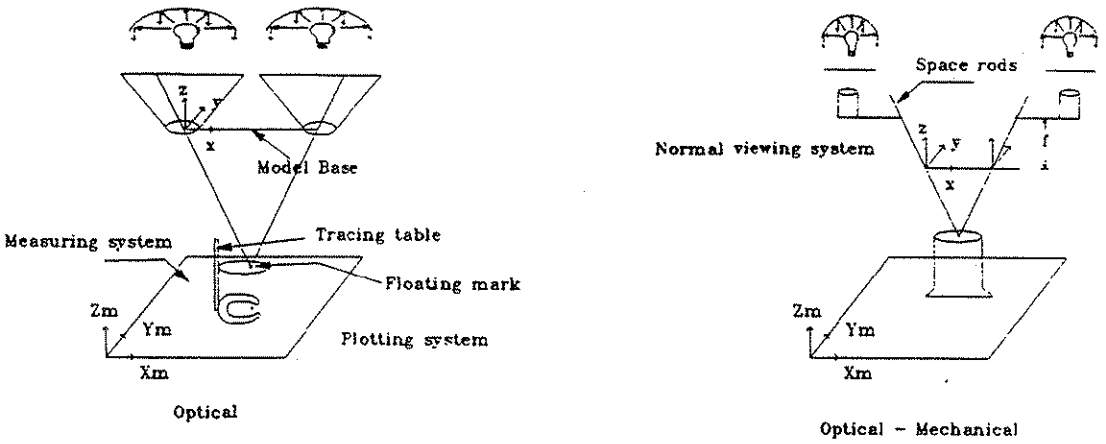

Fig. 3.11 Analog stereo plotter.

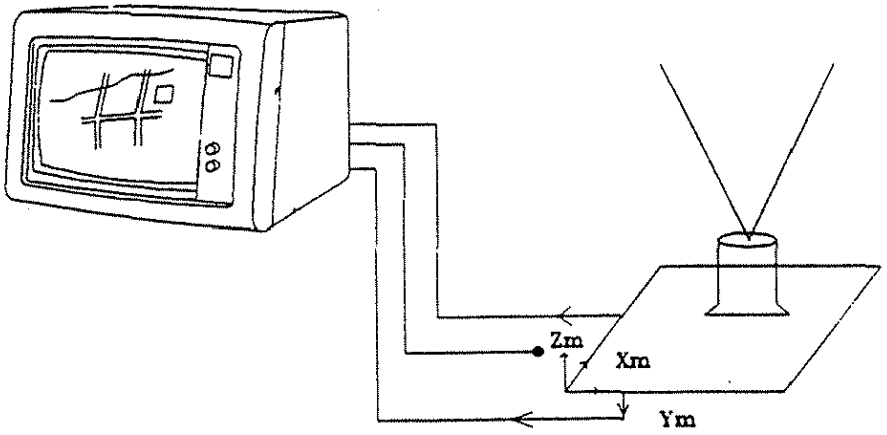

Fig. 3.12 Digital photogrammetry.

and the plate holder to eliminate the Y parallax, enabling the viewer to see a continuous stereo model as the plate is scanned. In some analytical plotters the plate holder or scanner can be moved relative to each other so that the viewer could eliminate the X-parallax and determine the elevation. However, in the more expensive analytical plotters the scanner has the ability to collect the radiometric values for point images in the viewing area and pass this information to the computer to perform the matching process, known as autocorrelation, in which X-parallax necessary to match identical point images are determined. The computed X-parallax is fed back to the plate or scanner to determine the elevation. The autocorrelation technique is used in producing orthophotos automatically without human intervention.

Knowing exterior orientation elements and plate coordinates of conjugate points, the computer can figure out the ground coordinates. These ground coordinates are then used as vectors to plot and display the earth system features and contours.

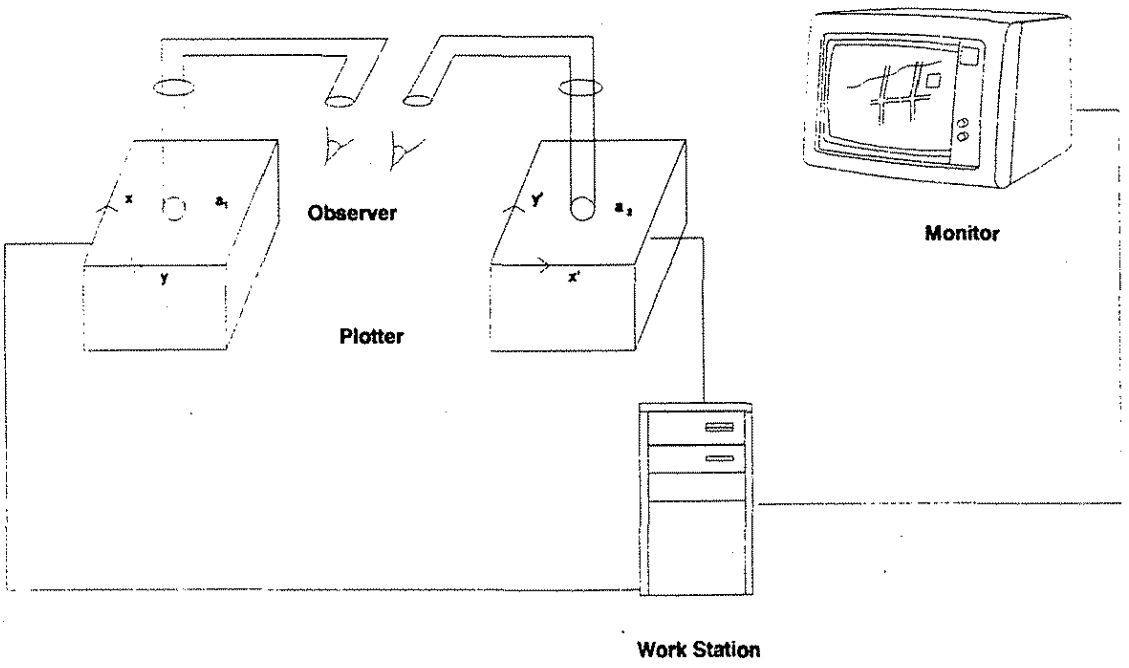

Fig. 3.13 Analytical plotter.

4.0 Aerial Triangulation

The objective of aerial triangulation is to provide control for plotting maps from aerial photography. Every stereo model used for plotting requires twelve exterior orientation elements or three control points.Until now, it was not possible to determine exterior orientation elements of aerial photograph with accuracy required in mapping projects. This research project showed that it is possible to determine six of the twelve exterior orientation elements accurately, and further research is needed to determine the other six. Presently, the method of providing three control points per stereo model is either by conventional ground survey or by aerial triangulation. The aerial triangulation method is more cost effective than ground survey. The cost effectiveness improves as the number of photographs in the project increases. However, the aerial triangulation requires five absolute orientation elements. In the past, this was provided by ground control established by conventional ground survey methods. This research showed that airborne GPS can be used to determine the five absolute orientation elements.

Aerial triangulation can be performed using either the independent model approach or the simultaneous adjustment approach. A strip of photographs requires two ground control at the beginning, two ground control at the end, one elevation control every 5th photograph and three common points (known as pass points) between three adjacent photographs. A block of photographs consisting of a number of strips needs four controls, one at each corner of the block, three pass points common to three adjacent photographs, and three tie points common to two adjacent strips. The accuracy and success of the aerial triangulation depends on careful planning of the flight, selection of pass, tie and control points.

4.1 Independent Model Aerial Triangulation

In independent model triangulation, the model is formed with by analogue or analytical methods. The models are joined to form a strip (see fig 4.1) using the equation

$$\begin{pmatrix} s_x \\ s_y \\ s_z \end{pmatrix} = S\,R \begin{pmatrix} x'-x'_n \\ y'-y'_n \\ z'-z'_n \end{pmatrix} + \begin{pmatrix} x_n \\ y_n \\ z_n \end{pmatrix}$$

where

$\begin{pmatrix} s_x \\ s_y \\ s_z \end{pmatrix}$ *are strip coordinates of a point*

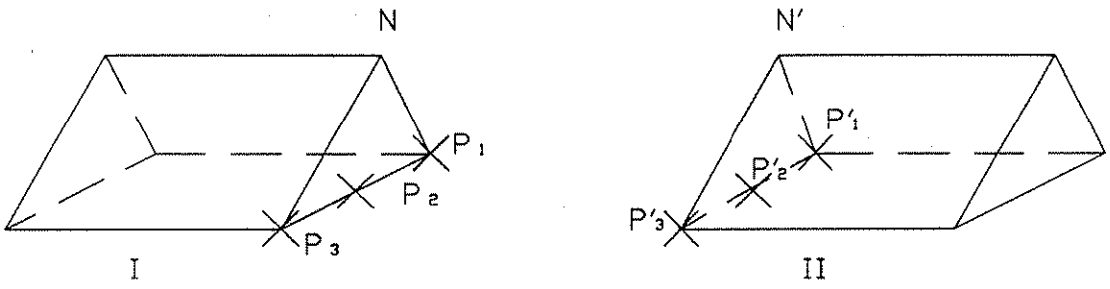

Fig. 4.1 Independent model.

$\begin{pmatrix} x_n \\ y_n \\ z_n \end{pmatrix}$ *are left nodal point coordinates of the* n^{th} *model*

$\begin{pmatrix} x'_n \\ y'_n \\ z'_n \end{pmatrix}$ *right nodal point coordinates of the* $n+1^{th}$ *model*

$\begin{pmatrix} x' \\ y' \\ z' \end{pmatrix}$ *model coordinates of a point in the* $(n+1)^{th}$ *model*

S - Scale factor between the $(n+1)^{th}$ model and the strip

R - Rotation between the $(n+1)^{th}$ model and the strip

The nodal points are determined either by calibrating the stereo plotters or in the process of forming model coordinates by analytical photogrammetry. The rotation matrix R and the scale factor S are determined using the common pass points P_1, P_2, P_3 and the nodal point n.

The strip coordinates are then formed into block coordinates (see fig.4.2) using the equation

$$\begin{pmatrix} B_x \\ B_y \\ B_z \end{pmatrix} = S_B \, R_B \begin{pmatrix} s_x - x'_T \\ s_x - y'_T \\ s_z - z'_T \end{pmatrix} + \begin{pmatrix} x_T \\ y_T \\ z_T \end{pmatrix}$$

where (B_x, B_y, B_z) - are the block coordinates
(x_T, y_T, z_T) - are the block coordinates of a tie point between adjoining strips
(x_T', y_T', z_T') - are the strip coordinates of a tie point
S_B - is the scale factor between adjoining strips
R_B - is the rotation matrix between adjoining strips

The rotation matrix R_B, and the scale factor S_B are determined using the common tie points T_1, T_2, T_3 etc.

The block coordinates are then transformed to ground

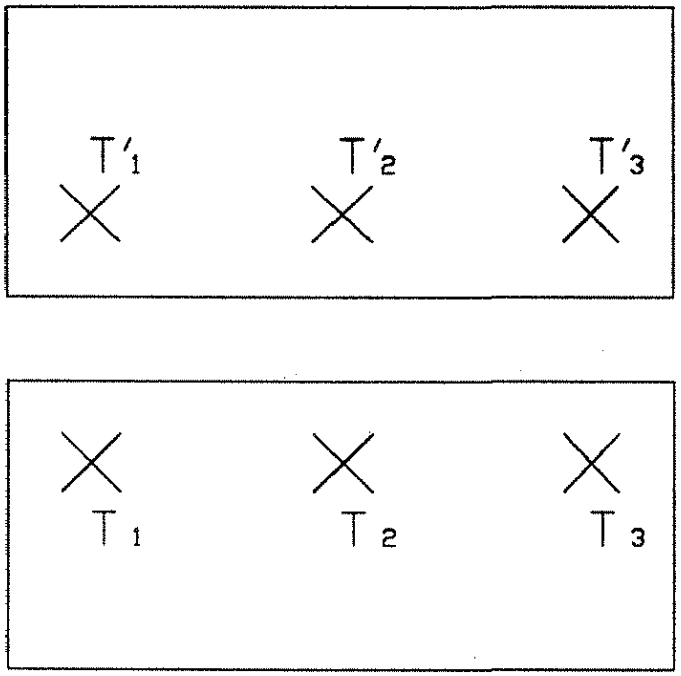

Fig. 4.2 Tie for block.

coordinates using the equation

$$\begin{pmatrix} G_x \\ G_y \\ G_z \end{pmatrix} = S_G\, R_G \begin{pmatrix} B_x - x_c' \\ B_y - y_c' \\ B_z - z_c' \end{pmatrix} + \begin{pmatrix} x_c \\ y_c \\ z_c \end{pmatrix}$$

where (G_x, G_y, G_z) - are the ground coordinates
(x_c', y_c', z_c) - are the block coordinates of ground control point
(x_c, y_c, z_c) - are the ground coordinates of a control point
S_G - is the scale factor between block and ground system
R_G - is the rotation matrix between block and ground system

The scale factor S_G and rotation matrix R_G are determined using three or more control points G_1, G_2, G_3, and G_4 .(see fig 4.3)

4.2 Simultaneous adjustment method

Simultaneous adjustment method uses the collinearity equation (4.2.1)

$$x = \frac{a_{11}(Gx - Gx_0) + a_{12}(Gy - Gy_0) + a_{13}(Gz - Gz_0)}{a_{31}(Gx - Gx_0) + a_{32}(Gy - Gy_0) + a_{33}(Gz - Gz_0)}$$

$$y = \frac{a_{21}(Gx - Gx_0) + a_{22}(Gy - Gy_0) + a_{23}(Gz - Gz_0)}{a_{31}(Gx - Gx_0) + a_{32}(Gy - Gy_0) + a_{33}(Gz - Gz_0)}$$

where (x,y) are photo coordinates of a point in the photo system
(Gx, Gy, Gz) are the ground coordinates of a point in the ground system
(Gx_0, Gy_0, Gz_0) are the camera's nodal point coordinate in the ground system. (see fig 4.4)

$\begin{pmatrix} a_{11} & a_{12} & a_{13} \\ a_{21} & a_{22} & a_{23} \\ a_{31} & a_{32} & a_{33} \end{pmatrix}$ *is the rotation elements* (κ, ϕ, ω) *and scale matrix between the ground and photo system*

Assuming all the photo coordinates and some of the parameters are

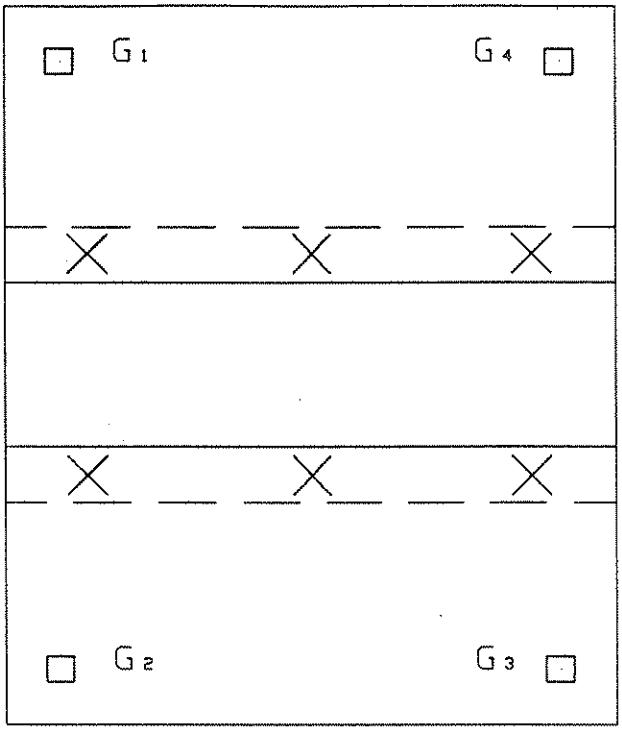

Fig. 4.3 Control for block.

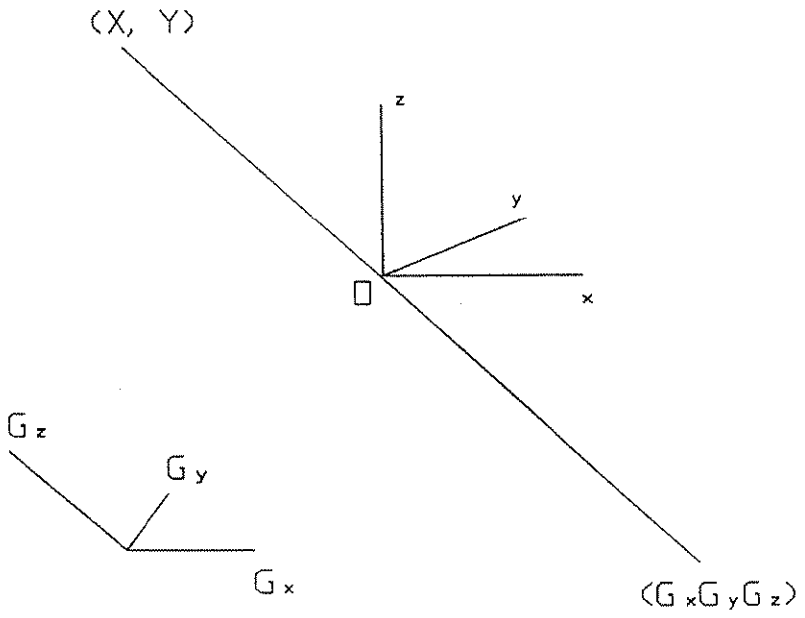

Fig. 4.4 Collinearity.

observed, the observation equation in the least squares method with weight matrix P is

$$Ax = l + v \qquad (4.2.2)$$

where l is the vector of observations with residuals v, x is the vector of parameters and A is the Jacobian matrix of equation (4.2.1). By the least squares principle the vector x is given by

$$x = (A^T PA)^{-1} A^T Pl.$$

By assigning a weight of zero for unknown parameters and proper weight between zero and infinity for the known parameters and the photo coordinates, the unknown parameters are determined. The method depends on assigning weights and ensuring that the rank of matrix A is greater than the unknown parameters. Unlike the independent model, this method is flexible for various combinations of parameters.

4.3 Strip triangulation

An aerial triangulation performed using a strip of photographs is known as strip triangulation. In order to form a model between two adjacent photos there should be five common points. To form a strip there should be three common points between two adjacent models (see fig.4.5). As the models are formed and added to the strip, errors due to observations and other factors propagate rapidly. For a short strip, less than five models, the propagation of errors is given by equation (4.3.1).

$$\text{error} = Ax^2 + Bxy + Cy^2 + Dx + E \qquad (4.3.1)$$

where A, B, C, D, and E are constants
x - coordinates along the strip
y - coordinates orthogonal to x

For longer strips, the error takes higher polynomials. The error propagation is contained by having frequent ground control along the strip. In engineering projects accurate elevations are required. The propagation of error in elevation is large in strip triangulation; therefore elevation controls are required more frequently than the horizontal control.

4.0 Block Triangulation

An aerial triangulation performed using strips of photographs is known as block triangulation (see fig.4.3). In a block, two adjacent strips should have at least three common points. Unlike in the strip error propagations in the block do not propagate rapidly because they are contained by the adjacent strips. Thus in a block only three to four control are required at each corner. However, every model should have at least three points common to all the adjacent models both in the forward and lateral directions, which means at least a 20-30 % lateral overlap between strips. The

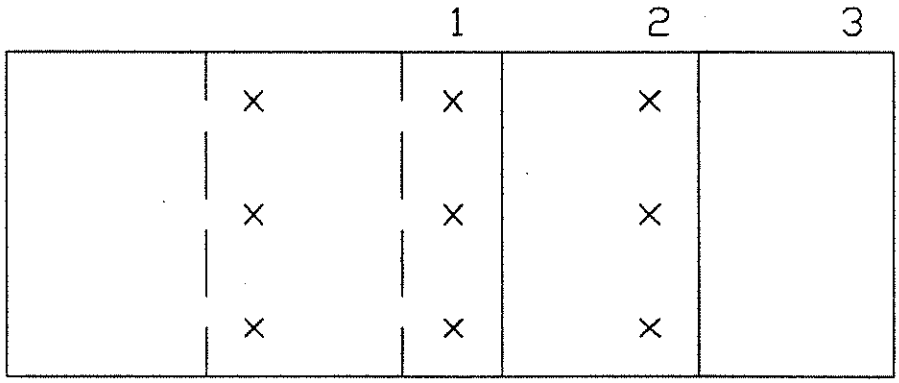

Fig 4.5 Model Strip.

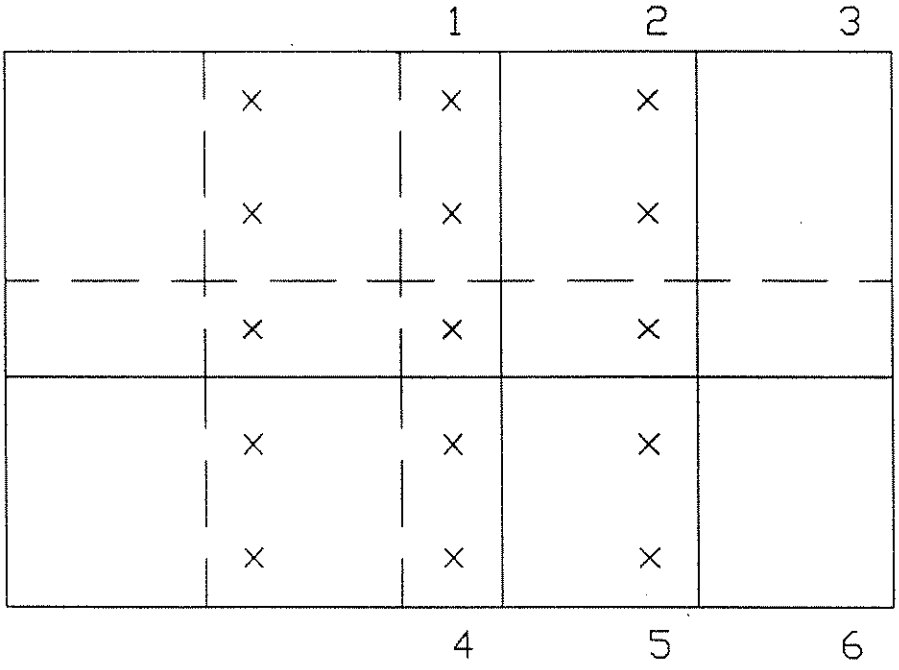

Fig 4.6 Block.

best results are obtained if every photograph has five points common to all adjacent photographs, both in the forward and lateral directions, which means a 50-60% forward and lateral overlap.

Flight Planning

An important aspect of aerial triangulation is flight planning which ensures that the area for mapping has stereo coverage. Flight planning is normally prepared on an existing topo map on which the area for mapping is outlined.

Prior to flight planning, information such as flying height H, focal length of camera f, decimal portion of forward overlap, FO, decimal portion of lateral overlap, LO, are determined according to the accuracy reqired in the final map. The objective of the flight planning is to determine the optimum number of photographs and flight lines. For a project of length L, and width W the number of strips, NS, required is given by

$$NS=\frac{(W-F)}{(1-LO)\,F}+1$$

where F = (H/f) * D
D = dimensions of the photograph

The number of photograph/strip, NP, is given by

$$NP=\frac{L}{(1-FO)\,F}+1$$

Using modern software such as AutoCAD, a graphic software, it is possible to optimize the number of strips and photographs. The location of the center of photographs are then plotted on the topo map, which is then used by the navigator of the aircraft to take the aerial photographs.Fig (6.2) shows the overlap of flight plan on a topographic map. Presently, navigation for aerial photographs are done using visual points on the ground. Because of visual navigation, some flights lack sufficient lateral and forward overlaps. However, airborne GPS can be used to navigate the aircraft and take photographs precisely over predetermined locations and lines.

4.6 Control Planning

Control planning depends on whether a strip or a block of photographs is used in the mapping project .(see fig.4.6) In a strip, the requirements based on practical experience are

1) 6 points common to two adjacent photos
2) 3 pass points common to 3 adjacent photos
3) 2 ground controls at the beginning of the strip and two at the end
4) 2 ground controls in every fifth photo in the strip
5) Elevation control along the center of the strip in every other photo.

The first two requirements for a strip are the same as for a block . Additionally a block requires

a) 4 ground controls at the four corners of the block
b) 3 common tie points between 2 adjacent models in 2 adjacent strips or 6 pass points between adjacent photographs in the forward and lateral directions.

4.7 Location of Control

Once the flight and control planning are done, the ground control points have to be selected in the field and their ground coordinates determined. The points should be natural, easily photo identifiable points, or targeted points. To eliminate misidentification and to obtain the most accurate photo coordinates, targeting is preferred. The size and color of the target depends on the scale of the photograph and the location. A cross with 5' × 3" seemed satisfactory for 1:3000 scale photography,see fig.4.7 . Ten micron fiducial marks should fit a 25 micron square within one micron. A GPS observation scheme using three or more national geodetic control points can then be prepared and observed using static mode. See fig 4.8. The observations can then be adjusted by network adjustment program such as Geolab.

The pass and tie points can either be pre-selected and targeted before flight or selected after flight. Targeted pass and tie points ensures high accuracy, but need precise navigation. After the flight, photo identifiable pass and tie points can be selected, but this is time consuming. Alternatively, these points can be marked or pugged on the plate by special marking devices. Pugging is cost-effective but less accurate.

4.8 Determination of Photo coordinates

The photo coordinates are determined using comparators. Usually comparators can measure (x',y') in plate coordinates to an accuracy of ± 0.001mm. On every plate, the plate coordinates of pass, tie and control points and four or more fiducial points are measured using the comparator see fig. 4.9. The coordinates of the fiducial points are determined by calibrating the camera. The plate coordinates are then transformed to photo coordinates using the equation

$$\begin{pmatrix} x \\ y \end{pmatrix} = \begin{pmatrix} a & b \\ c & d \end{pmatrix} \begin{pmatrix} x' \\ y' \end{pmatrix} + \begin{pmatrix} x_0 \\ y_0 \end{pmatrix}$$

The parameters a, b, c, d, x_0, y_0 are determined using the plate coordinates and calibrated coordinates of the fiducial points.

The photo coordinates are then refined for lens distortion and refraction.

4.9 Determination of Pass and Tie Point Coordinates

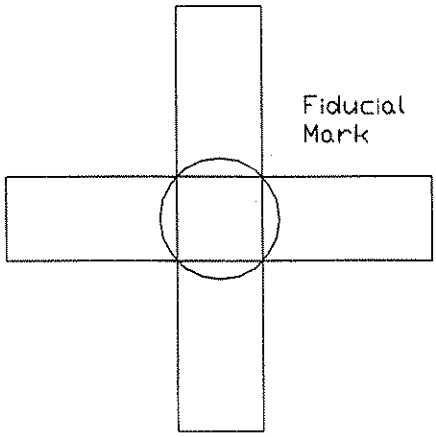

Fig. 4.7 Target.

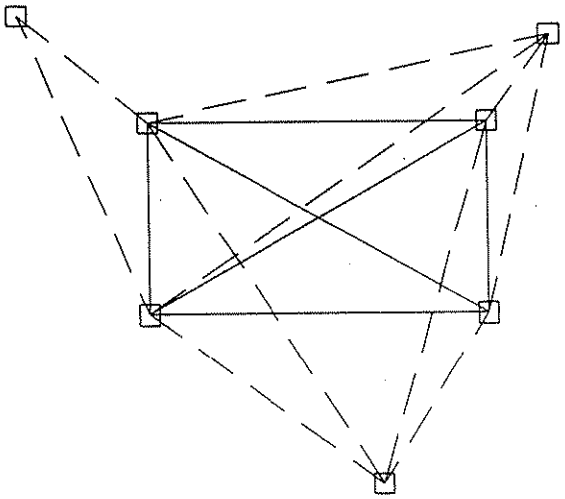

Fig. 4.8 Control network.

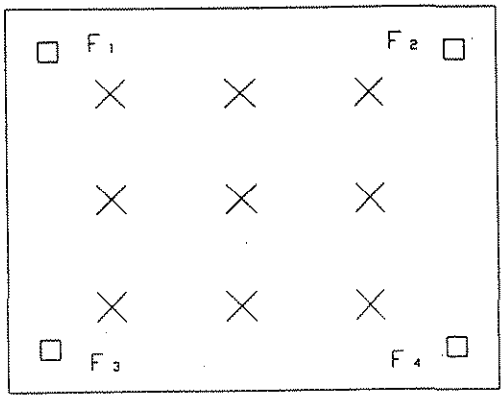

Fig 4.9 Fiducial point.

Using the photo coordinates, ground coordinates, and exterior orientation elements, a standard software such as "Albany" can either do a strip or simultaneous adjustment. In most cases, it is better to eliminate any large errors or inconsistencies before simultaneous adjustment. A relative orientation software can be used to eliminate errors in pass points between two photos. A strip adjustment software can be used to eliminate errors in pass points between models. A block adjustment software can be used to eliminate errors in tie and ground control points. Once the errors in the various coordinates are eliminated, the simultaneous adjustment software can be used to determine precisely the coordinates of pass and tie points as well as the exterior orientation elements. These values can then be used in stereoplotting or in digital photogrammetry.

5.0 Airborne GPS

The objective of airborne GPS is to determine the camera location at the instant of the film exposure using GPS. This is determined using precise kinematic GPS mode. The GPS antenna is firmly fixed above the camera in the aircraft. The offset of the camera nodal point from the antenna is determined either by calibration or by conventional survey methods. In order to perform kinematic GPS, two base stations are required (See fig.5.1). Using kinematic survey, the location of the antenna at every second or half second can be determined. Knowing the time of exposure the camera location can be interpolated.

5.1 Camera offset from Antenna

The camera offset from the antenna fixed to the aircraft can be determined in a number of ways (see Fig.5.2). One simple method is to determine the difference in coordinates between the taxi point and the base station precisely using static mode. The aircraft is then taxied over the taxi point. The difference in coordinates between aircraft antenna and base point is determined precisely by static method. The difference in coordinates between the nodal point of the camera and the taxi point can be determined precisely by conventional survey methods. From this information, the camera offset from the aircraft antenna can be determined precisely. As long as the aircraft is level during exposure, which is normally the case, this offset will be a constant.

5.2 Base Station Coordinates

In order to ensure that the camera location and the ground control points in the aerial triangulation project are in the same system, it is important that the base station used for kinematic survey be a part of the network.

By including the base station in the GPS network for ground control locations and adjusting them, the camera location determined from the base station will be in the same system as the ground control. See fig 5.3.

5.3 Camera Location

The aircraft is initially taxied over the taxi station and GPS data are collected from all the available satellites (a minimum of four). Knowing the coordinate differences between the base station and the taxi station from the static mode observation, the integer ambiguity can be fixed fairly rapidly for each satellite. After a few minutes of observations, the aircraft takes off on its flight mission, while the GPS receiver continuously tracks the satellites; thus, ensuring the continuity in the integer ambiguity. At every epoch, the receiver collects the phase differences to all available satellites. Using the phase differences and the integer ambiguity, the locations of the antenna can be determined at every epoch.See fig 5.4.

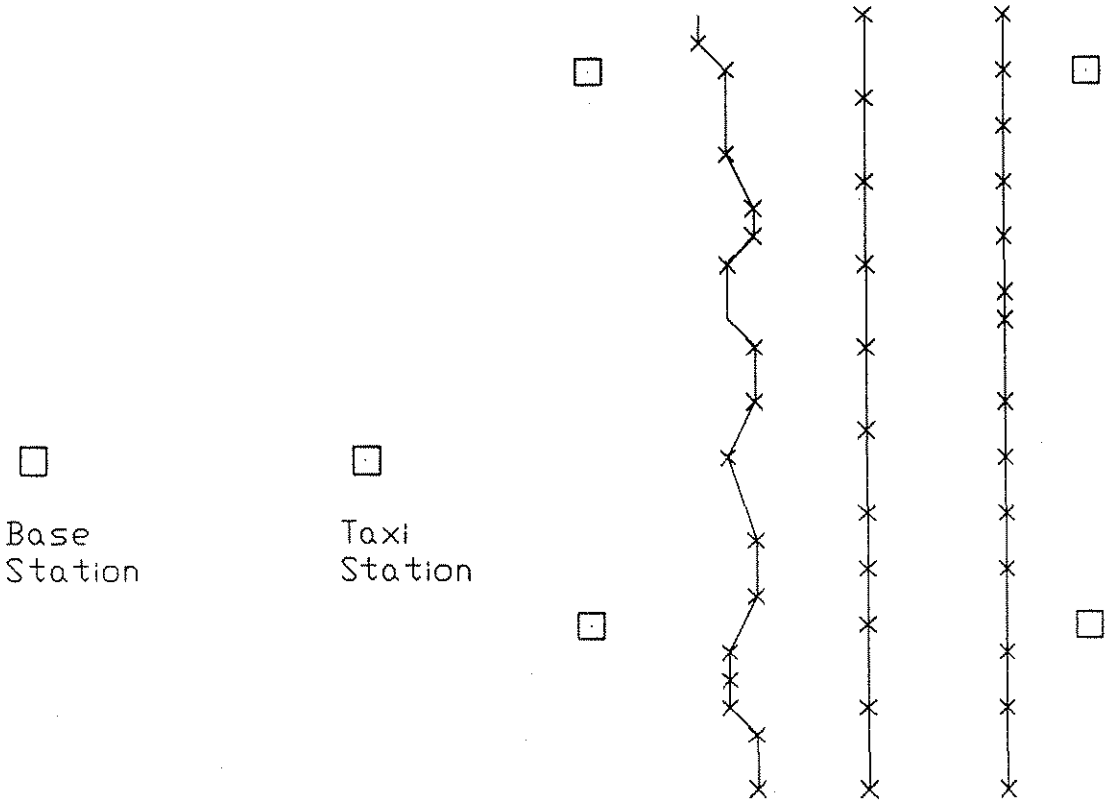

Fig. 5.1 Control and base station.

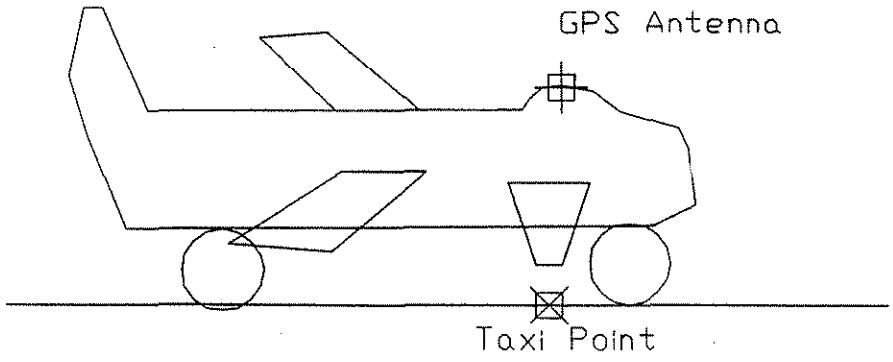

Fig 5.2 Taxi point.

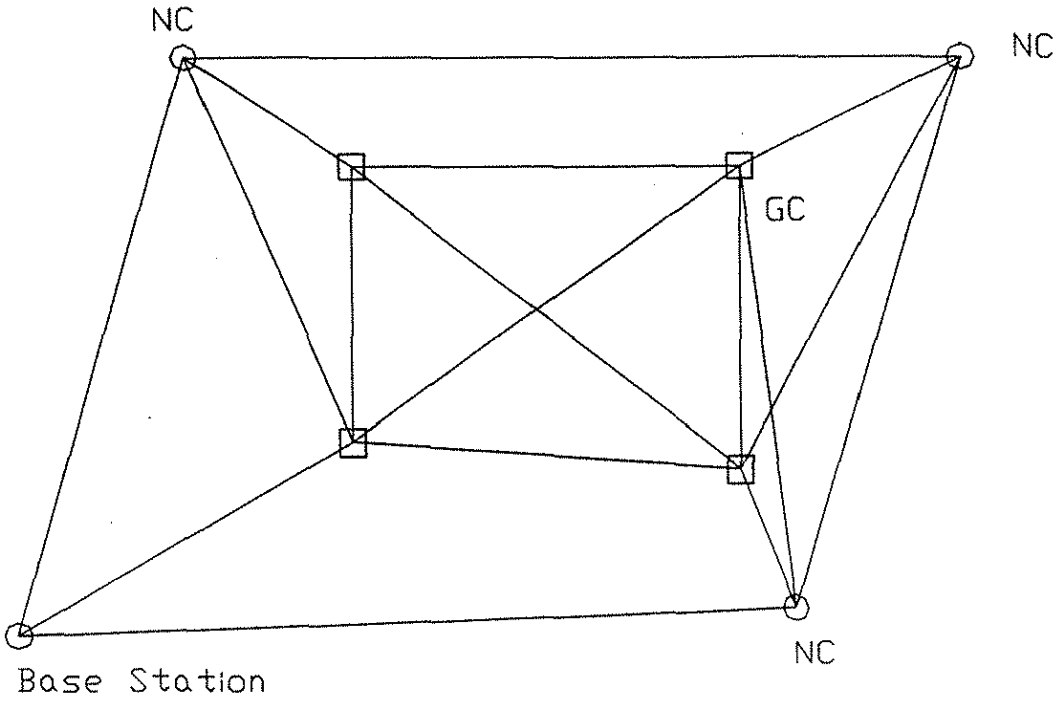

Fig 5.3 Control network.

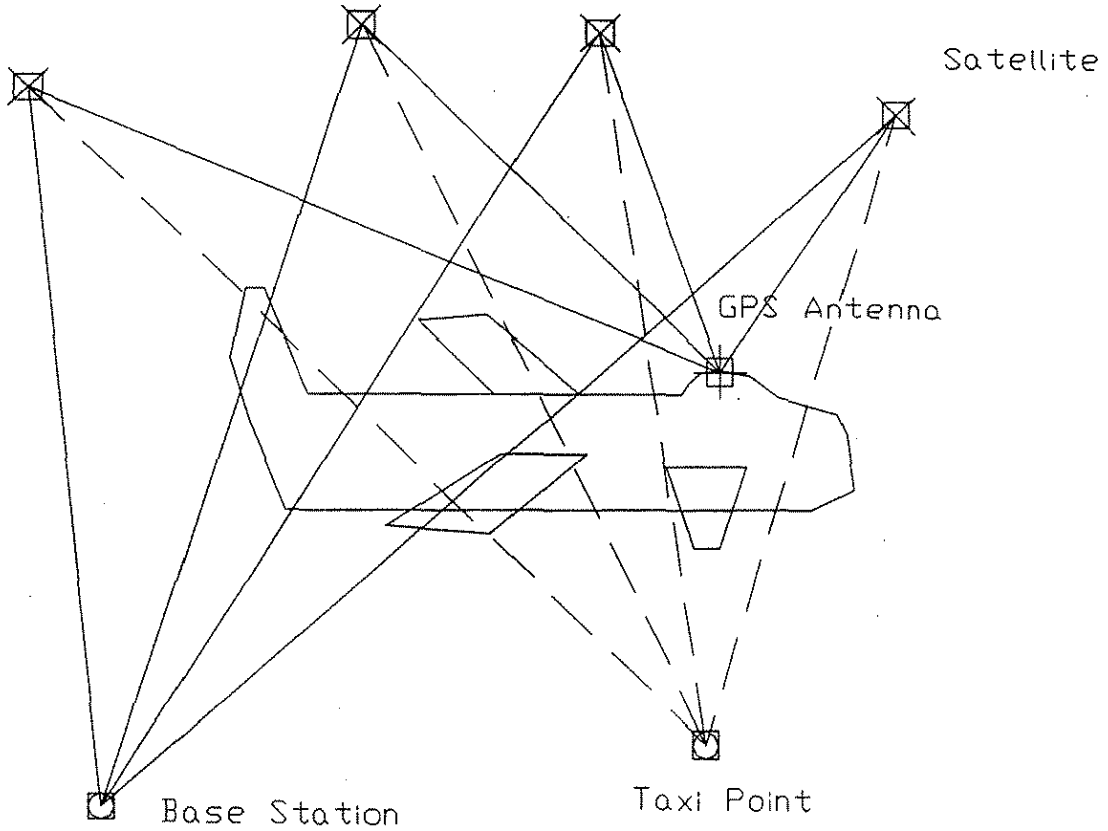

Fig 5.4 GPS camera Location.

The exposure time of the camera can either be controlled by the GPS receiver, or the time of the exposure can be marked as an event in the GPS receiver together with the GPS data.. Suppose x_i is the location of the aircraft at the i^{th} second a, x_{i+1} and x_{i+2} at the subsequent seconds, then, the first difference will give the velocity $v_{i+.5}$ at (i+.5)th second, and the second difference the acceleration, f_{i+1} at the (i+1)th second. Thus, if T is the exposure time between i and i+1, then the location of the aircraft at T is given by

$$x = x_i + v_{i+.5}(T-i) + 0.5*f_{i+1}(T-i)^2.$$

Assuming the aircraft is traveling with steady speed during photography, the camera location can be determined precisely.

6.0 Test Flights and Results

In photogrammetric mapping every stereo model requires four controls or camera locations and orientations. By using GPS and aerial triangulation the number of ground controls can be minimized. Iowa Department of Transportation (IA DOT) uses an analytical plotter and a strip triangulation software. Simultaneous block adjustment software capable of processing three strips of 100 or more photos covering six miles with about 100 control points is required for this project. Various private commercial software for processing a large number of photos on a personal computer (PC) were examined. The software "Albany" was selected mainly because the vendor is willing to provide this software at half price for our research work, and work with the Iowa State University (ISU) research team to modify the software for GPS application at no extra cost. If, at the end of this research, the IA DOT would like to use this software, then they could do so by paying the vendor the initial discount.
In addition, special bundle adjustment softwares AGPS, FORTBLK, and GAPP are used in this research. The AGPS software runs on Project Vincent (a unix based computer system) at ISU; it has the capability of correcting for systematic error between ground control and camera location by GPS. The FORTBLK software runs on Wylber (a main frame computer system) at ISU; it has the capability to constraint camera orientation parameters. The GAPP software is used by National Geodetic Survey (NGS) and is similar to the Albany.

6.1 Mustang 90 flight

In order to evaluate the use of GPS for photogrammetric controls, a strip consisting of 33 photos flown in 1990 at 1500 feet flying height were used. See fig. (6.1). The coordinates of Point of Intersections (PIs) and other controls were obtained by traversing between the six GPS points. The coordinates were computed on a surface state plane coordinate system. The PIs along the center line were painted and the GPS points were targeted prior to flight. Table (6.1) gives the standard errors in x, y, z between coordinates obtained by using different softwares and different control distributions. GPS and centerline controls provides a minimum acceptable control for strip triangulation. This will be cost effective for IA DOT both in field surveys and photogrammetric mapping. The results obtained from the IA DOT software do not agree completely with those from Albany software, mainly because of the degree of polynomial used in the strip adjustment. The photo coordinates were observed using both the IA DOT's analytical plotter and ISU's stereocomparater. Initially the agreement was misleading. After several attempts, a method of obtaining proper photo coordinates from analytical plotter was determined. Appendix (1) gives the documentation for running the Albany software. Appendix (2) gives the observation procedure in aerial triangulation.

Table 6.1 Standard deviation of differences of coordinates comparing various adjustments.

ALBANY	X (m)	Y (m)	Z (m)
DOT(m)- Albany using DOT control	0.755	1.295	0.534
Albany GPS control -DOT(m)	0.731	0.796	1.880
Albany GPS control -Albany GPS and Centerline	0.253	0.104	1.407
MAPP(STRIP)			
DOT(m)- Strip using DOT control	0.277	0.550	1.140
All metric control- GPS control	0.296	0.242	0.647
All metric control- GPS and Centerline	0.304	0.315	0.477
DOT(m)- All metric control	0.534	0.212	0.746
All metric control- Strip using DOT control	0.445	0.606	0.933
GPS control- GPS and Centerline	0.029	0.123	0.424

NEVADA - COLO FLIGHT STRIP

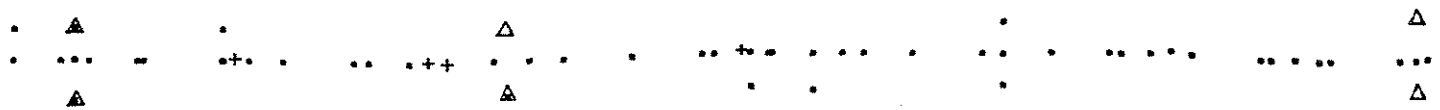

△ GPS Control Point

\+ 1990 X,Y Control

· 1990 X,Y,Z Control

Fig. 6.1 90 - Strip and control.

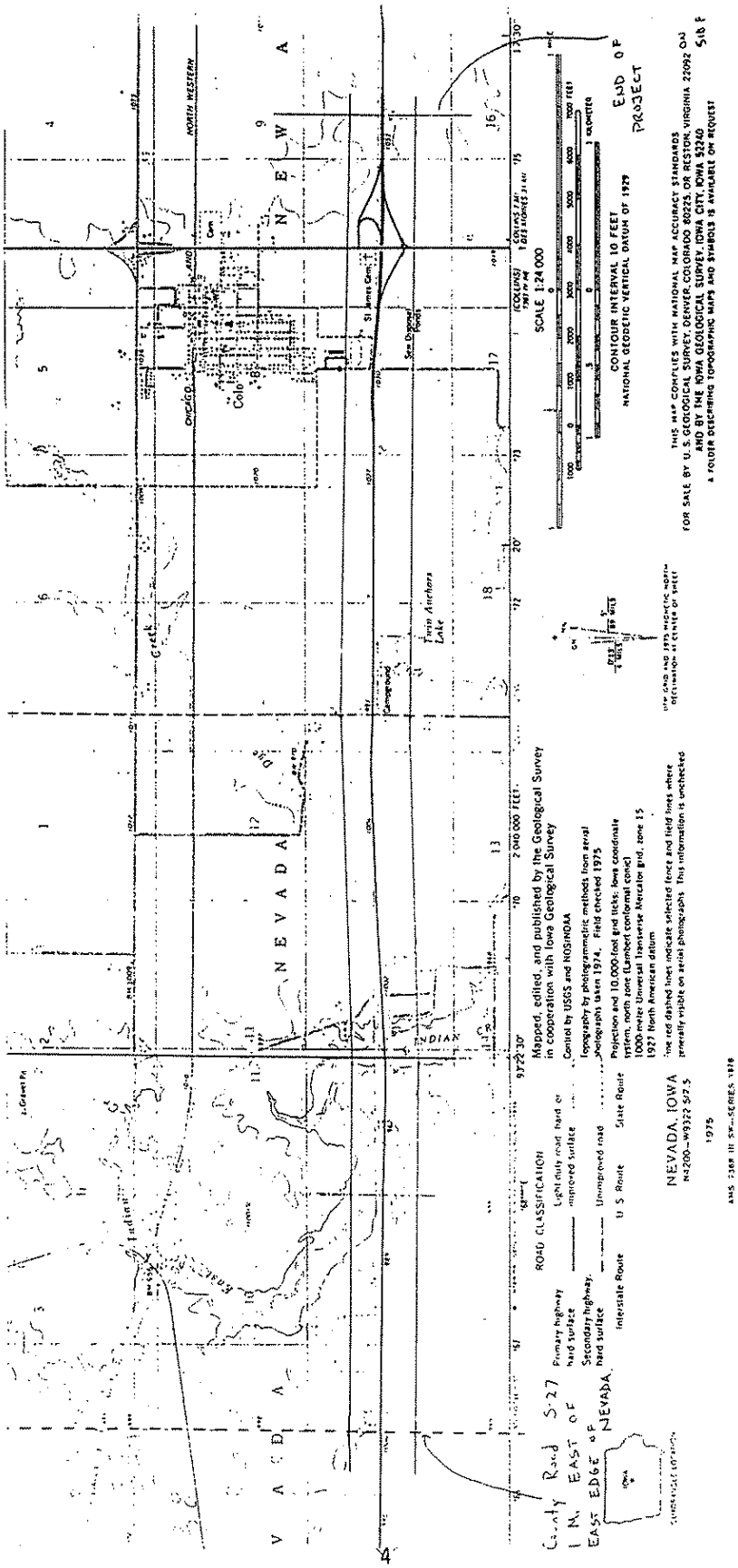

Fig. 6.2 Flight plan for 91.

6.2 NOAA 91 flight

A study was done to identify public and private agencies engaged in using GPS for camera location. Many are in the early stages of development. We identified four agencies, two private and two public agencies, who are willing to work with ISU research team. Of these, the National Oceanographic and Atmospheric Administration (N.O.A.A.) in Washington, D.C. is more advanced in this field than the other agencies. Agreement was reached between NOAA and ISU research teams to cooperate in this research project. In order to get maximum accuracy and dynamic calibration of the camera, it was decided to take aerial photos over the six mile Mustang project at 1500 feet and 3000 feet flying heights. Also, it was decided to take three strips of photos at the lower flying height with 60% forward overlap and 30% lateral overlap. Only one strip of photos at 3000 feet flying height was taken along the center line. See fig. (6.2). To minimize observation and identification error, it was decided to pretarget as many pass points as possible. The coordinates of these points were then determined from the GPS and PI points, established for 90 photos, using total station and geolab software. In all, about 90 targeted pass points were established. See fig. (6.3). Other required pass points were marked (pugged) on the plates prior to observation.

To determine the camera locations along the strip using GPS, the aircraft is equipped with an antenna fixed to the aircraft. See fig. (6.4). By prior calibration, the offset of the camera's nodal point from the antenna was determined. See fig. (6.5). The antenna's position during the flight was determined by kinematic GPS processing. For kinematic processing, three stations were established at the Ames Airport. See fig. (6.6). These stations were tied to the control in the Mustang Project by GPS. For about 15 minutes prior to take off, the aircraft taxied over the taxi station and collected GPS data from four or more satellites using the receiver on board. The GPS receivers at Base #1 and Base #2 continuously collected data from the same four or five satellites. At the end of the mission, the aircraft taxied over the taxi station and continued to collect the data for another 15 minutes. The offset from the nodal point to the taxi station was precisely determined in both instances. See fig. (6.7). The data was then post-processed using the OMNI software. The antenna's position was determined every second and the camera location was then interpolated. See fig. (6.8) and fig. (6.9). The photo coordinate of the high flight were observed at ISU and processed with Albany software. Tables (6.2) and (6.3) shows the results of strip and simultaneous adjustment using the Albany software. The difference of about 23 m between GPS elevation and aerial triangulation is due to geoid undulation. The standard errors of the difference between camera locations determined by GPS and that by aerial triangulation of 0.28 m in x, 0.08 m in y and 0.08 m in z, are

NEVADA - COLO FLIGHT STRIP

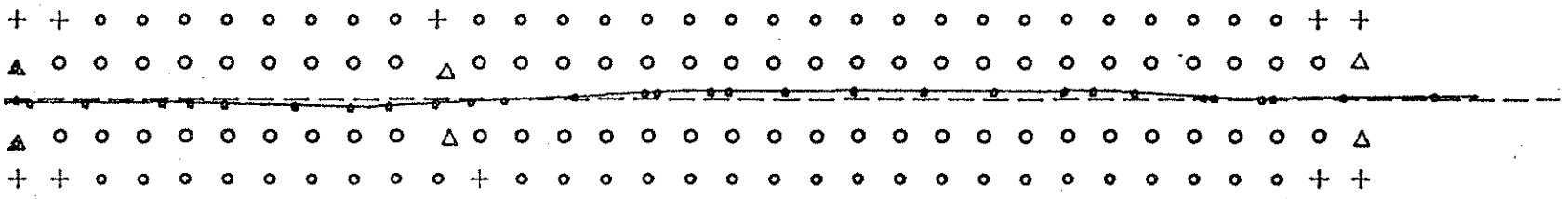

△ GPS POINTS
⬠ PAINTED CONTROL ON HIGHWAY
\+ NEW CONTROL POINTS
○ TARGETED PASS POINTS (WHERE POSSIBLE)
——— CENTER LINE
– – – FLIGHT LINE

Fig. 6.3 91 Control.

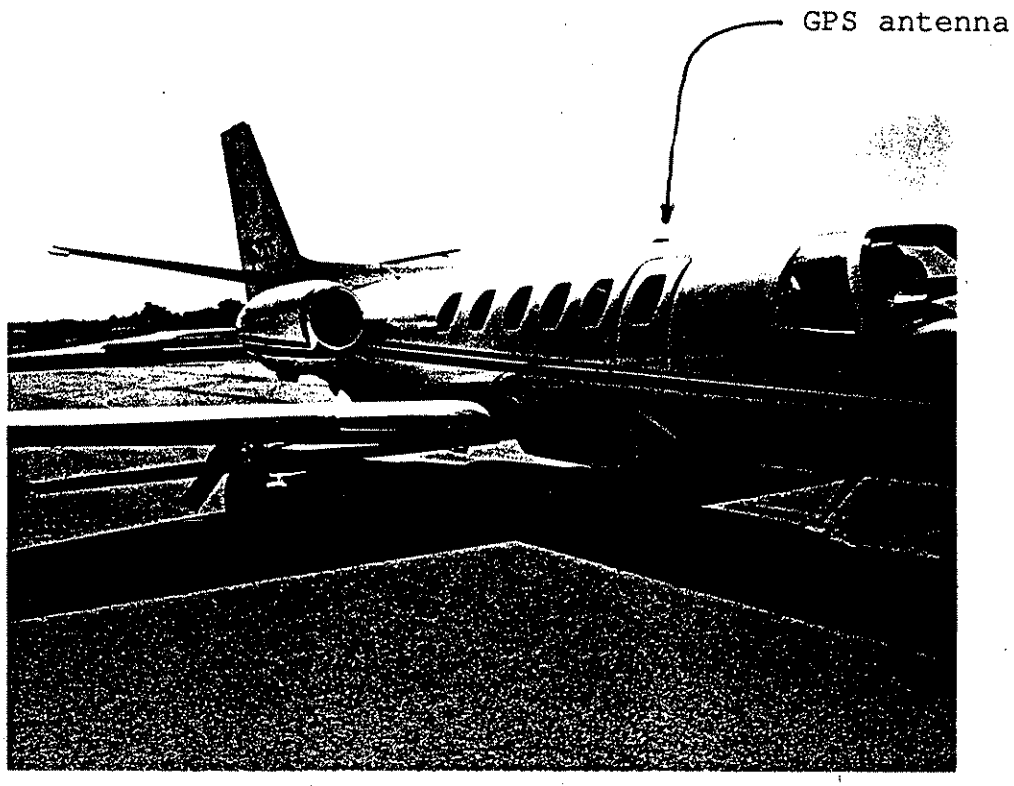

Fig. 6.4 Aircraft with GPS antenna.

GPS	dx	dy	dz	sx	sy	sz	s-omega	s-phi	s-kappa

dx, dy, dz are the offsets from the front nodal point of the camera lens to the gps antenna in ground units.

sx, sy, sz are the standard errors for the camera centers in ground units.

s-omega, s-phi, s-kappa are the standard errors for the camera rotations in radians.

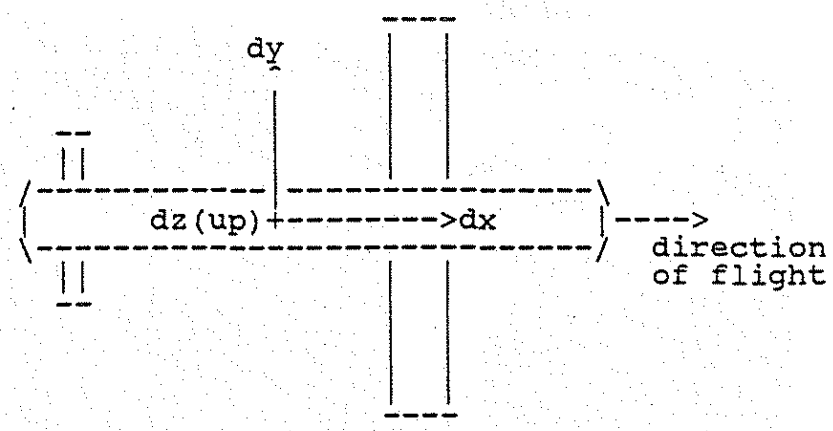

Fig. 6.5 Offset of camera.

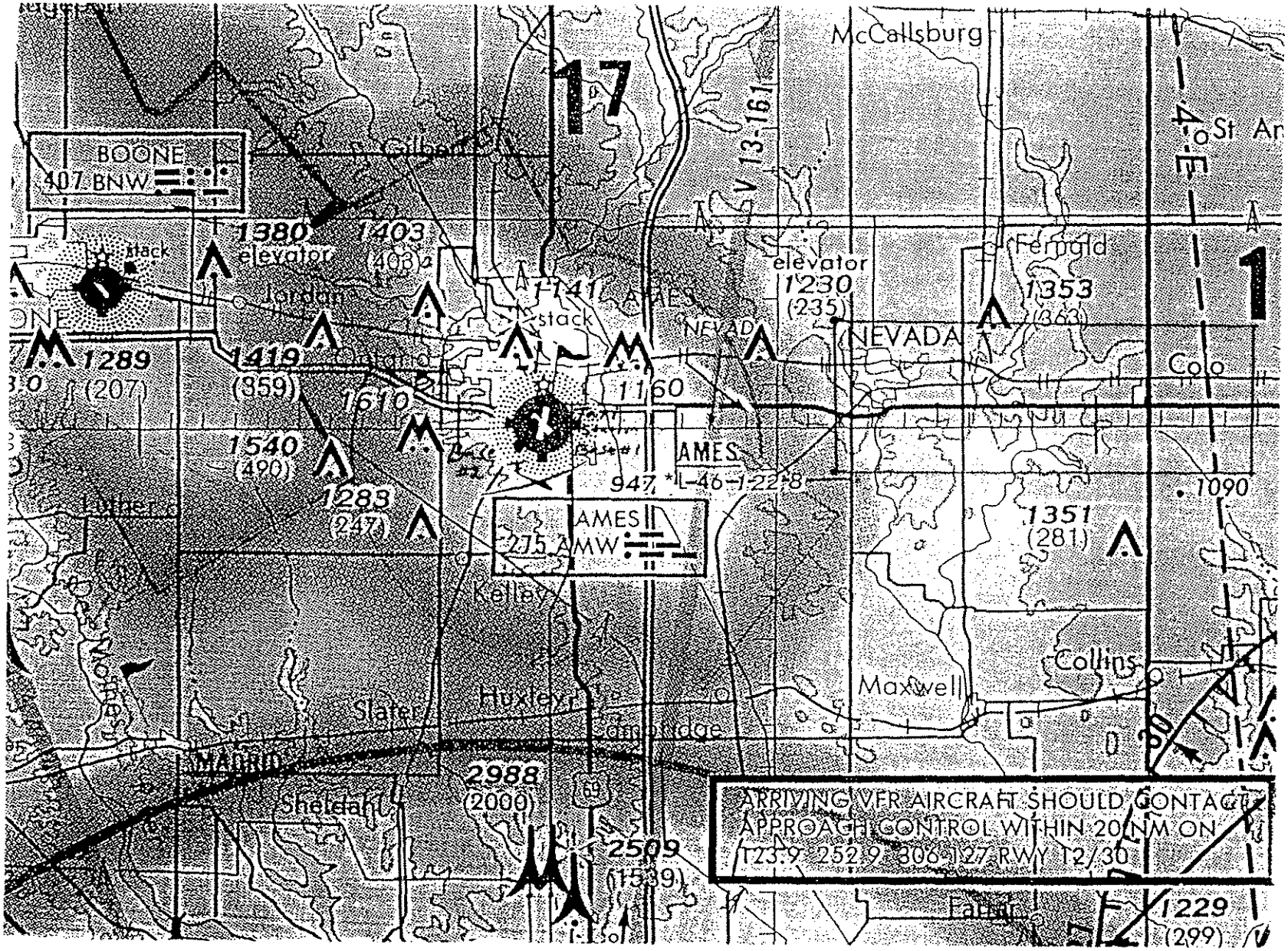

Fig. 6.6 Ames airport stations.

Fig. 6.7 Location of camera from taxi station.

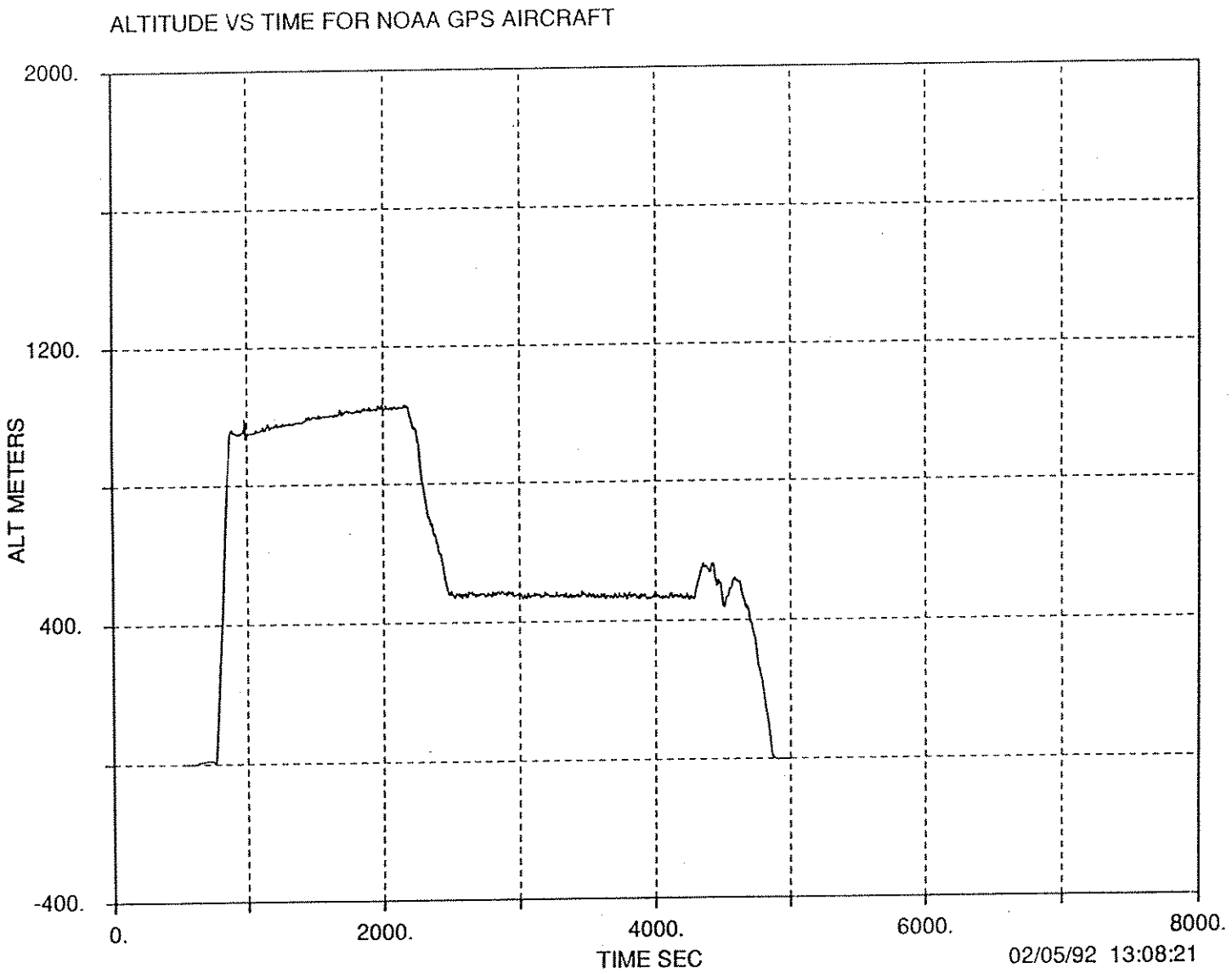

Fig. 6.8 Elevation vs. Time by GPS tracking of aircraft.

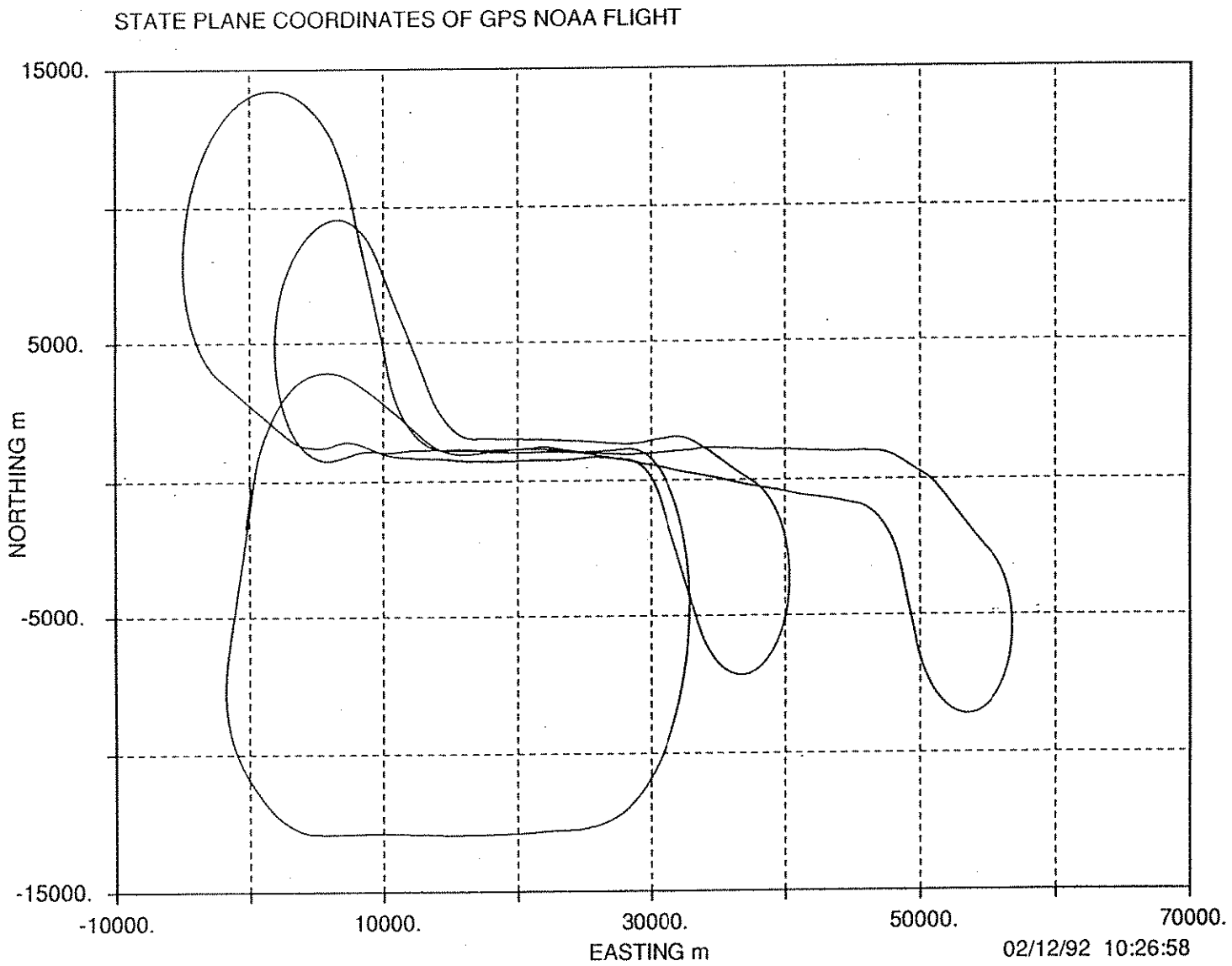

Fig. 6.9 Northing vs. Easting from GPS tracking by aircraft.

-11033	1507408.190	1056463.948	1303.800	-0.643	-0.976	0.584	-0.389	23.746	-0.057
-11031	1507977.506	1056475.946	1298.744	-0.408	-0.740	0.908	-0.065	23.848	0.044
-11029	1508551.951	1056487.167	1297.677	0.037	-0.296	1.152	0.179	23.795	-0.008
-11027	1509132.392	1056492.404	1298.474	0.243	-0.090	1.038	0.065	23.724	-0.080
-11025	1509699.917	1056499.279	1299.787	0.586	0.253	0.924	-0.049	23.811	0.007
-11023	1510263.337	1056506.823	1299.904	0.270	-0.062	1.253	0.280	23.699	-0.105
-11021	1510829.851	1056503.007	1297.110	0.039	-0.293	0.628	-0.345	23.718	-0.085
-11019	1511399.840	1056500.704	1296.368	0.379	0.047	0.861	-0.112	23.777	-0.027
-11017	1511972.017	1056489.160	1298.974	0.671	0.338	1.217	0.244	23.707	-0.097
-11015	1512527.757	1056463.545	1301.605	0.310	-0.023	0.994	0.021	23.577	-0.227
-11013	1513074.472	1056435.430	1300.020	0.105	-0.227	1.123	0.150	23.594	-0.210
-11011	1513613.874	1056409.211	1297.198	-0.215	-0.547	1.305	0.332	23.803	-0.001
-11009	1514166.019	1056382.794	1295.043	-0.289	-0.621	1.089	0.116	23.993	0.189
-11007	1514715.971	1056364.810	1299.127	0.473	0.140	1.312	0.339	24.123	0.319
-11005	1515271.333	1056351.395	1298.855	0.523	0.191	0.642	-0.331	24.198	0.394
-11003	1515821.574	1056347.652	1294.779	0.664	0.332	0.973	0.000	24.110	0.306
-11001	1516384.660	1056342.956	1295.661	1.543	1.210	0.945	-0.028	23.803	-0.001
-11099	1516942.155	1056332.148	1295.468	1.697	1.365	0.570	-0.403	23.442	-0.361
			AVG	0.333		0.973		23.804	
			VAN		0.339		0.055		0.036

Table 6.2 Camera data from strip.

33	1507408.042	1056463.906	1303.050	152.280	-0.791	-1.041	0.542	-0.245	22.996	-0.729
31	1507977.262	1056475.872	1298.214	152.280	-0.652	-0.902	0.834	0.047	23.318	-0.407
29	1508551.696	1056486.925	1297.382	152.280	-0.218	-0.468	0.910	0.123	23.500	-0.225
27	1509132.368	1056492.181	1298.295	152.280	0.219	-0.031	0.815	0.028	23.545	-0.180
25	1509699.734	1056499.231	1299.474	152.280	0.403	0.153	0.876	0.089	23.498	-0.227
23	1510263.198	1056506.881	1299.632	152.280	0.131	-0.119	1.311	0.524	23.427	-0.298
21	1510829.264	1056503.157	1297.014	152.280	-0.548	-0.798	0.778	-0.009	23.622	-0.103
19	1511399.385	1056501.021	1296.443	152.280	-0.076	-0.326	1.178	0.391	23.852	0.127
17	1511971.710	1056489.176	1299.260	152.280	0.364	0.114	1.233	0.446	23.993	0.268
15	1512527.929	1056463.496	1301.997	152.280	0.482	0.232	0.945	0.158	23.969	0.244
13	1513074.805	1056435.036	1300.323	152.280	0.438	0.188	0.729	-0.058	23.897	0.172
11	1513614.301	1056408.682	1297.361	152.280	0.212	-0.038	0.776	-0.011	23.966	0.241
9	1514166.574	1056382.014	1295.088	152.280	0.266	0.016	0.309	-0.478	24.038	0.313
7	1514716.249	1056364.146	1299.040	152.280	0.751	0.501	0.648	-0.139	24.036	0.311
5	1515271.494	1056350.882	1298.667	152.280	0.684	0.434	0.129	-0.658	24.010	0.285
3	1515821.514	1056347.275	1294.606	152.280	0.604	0.354	0.596	-0.191	23.937	0.212
1	1516384.083	1056342.859	1295.704	152.280	0.966	0.716	0.848	0.061	23.846	0.121
99	1516941.726	1056332.280	1295.630	152.280	1.268	1.018	0.702	-0.085	23.604	-0.121
				AVG	0.250		0.787		23.725	
				VAR		0.284		0.082		0.084

Table 6.3 Camera date from Albany.

satisfactory for highway applications.They are also within the accuracy that is achievable by aerial triangulation.

Table 6.4

Block adjustment using different control

Method	Block using only ground control			Block using camera and 6 GPS as control			Block using camera & 6 GPS height control		
	σ_x (m)	σ_y (m)	σ_z (m)	σ_x (m)	σ_y (m)	σ_z (m)	σ_x (m)	σ_y (m)	σ_z (m)
Std error in control	.31	.17	.27	.16	.07	.18	.34	.08	.12
Std error in check points	.17	.14	.37	.19	.10	.55	.6	1.21	.43

Table (6.4) shows the results after GPS elevations were adjusted for Geoid undulation, and the Albany software was run as an independent model with and without ground control. Satisfactory results were obtained by using six ground controls and GPS coordinates of the camera location.

The diagram fig 6.10,H191.WQ1, shows the differences between camera locations obtained by GPS and by aerial triangulation for a strip of 18 photos. The larger differences are due to the fact that in strip aerial triangulation the error propagates as the square of the distance for a short strip (less than 5 photos) and for a long strip it takes higher order polynomials. The graph clearly shows a 3^{rd} or higher order systematic error between camera location by GPS and by aerial triangulation, therefore the error is largely due to aerial triangulation. The graph also shows that the difference is large at the beginning and the end of the strip, but it is small at the center, which is typical of strip aerial triangulation. Thus it can be concluded that the accuracy of camera location by GPS is better than 10, cms and the determination of camera location by aerial triangulation is weak.

HI 91- Difference in Camera Location

Airborne GPS vs Aerial Triangulation

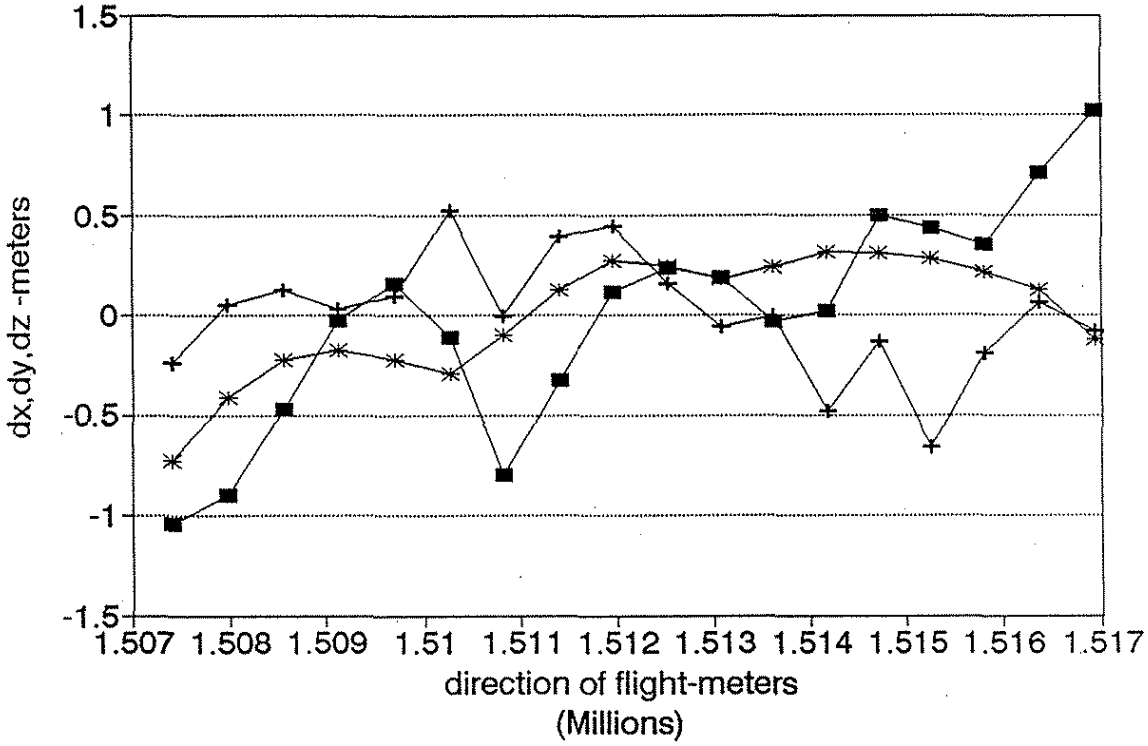

x	dx	dy	dz
1507408	-1.041	-0.245	-0.729
1507977	-0.902	0.047	-0.407
1508551	-0.468	0.123	-0.225
1509132	-0.031	0.028	-0.18
1509699	0.153	0.089	-0.227
1510263	-0.119	0.524	-0.298
1510829	-0.798	-0.009	-0.103
1511399	-0.326	0.391	0.127
1511971	0.114	0.446	0.268
1512527	0.232	0.158	0.244
1513074	0.188	-0.058	0.172
1513614	-0.038	-0.011	0.241
1514166	0.016	-0.478	0.313
1514716	0.501	-0.139	0.311
1515271	0.434	-0.658	0.285
1515821	0.354	-0.191	0.212
1516384	0.716	0.061	0.121
1516941	1.018	-0.085	-0.121

Fig. 6.10

Table 6.5

A1. Flight 91. AGPS vs. Albany in NOAA flight

pt	Δx	Δy	Δz	Res x	Res y
2004	-0.296	-0.220	-0.100	0.002	0.005
2006	-0.393	-0.235	-0.830	0.005	0.006
2016	-0.003	0.172	-0.150	0.001	0.001
2018	-0.001	0.104	0.187	0.003	0.005
2040	-0.107	0.006	0.296	0.001	0.002
2042	-0.081	0.070	0.369	0.001	0.000
std error	0.147	0.156	0.407		

In order to evaluate the Airborne GPS (AGPS), which is an aerial triangulation program, that compensates for small systematic errors in GPS locations of camera, the NOAA high flight was run with weights of 1000 on photo coordinates, 10,000 on the location of camera , and 0.01 on ground points along the center line. Light weights on some points are required to run a strip only with GPS location of camera . Table 6.5 compares the AGPS coordinates of six points(GPS) with those obtained using the Albany software.The Albany software was run with six GPS points and points along center line as control. The standard errors shown in table 6.5 compares well with those of check points by Albany shown in table (6.4). Thus, AGPS using camera locations by GPS will yield satisfactory results. The table 6.5 also shows photo coordinate residuals in the AGPS run. They show that if photo coordinates are error free, then AGPS using camera locations by GPS can yield excellent results .

Table 6.6

Standard error at control

Method Albany	Control σ_x m	Control σ_y m	Control σ_z m	Check σ_x m	Check σ_y m	Check σ_z m
4×3 with ground control	0.05	0.07	0.23			
3×3 with camera control	0.10	0.10	0.04	1.67	0.26	0.38
3×3 with camera and ground	1.05	0.46	0.11			
4×3 with camera control	0.62	2.77	0.09			
4×3 with camera and ground	0.47	1.93	0.20			

The table 6.6 shows the Albany run using 3 strips at a low flying height and one strip at an high flying height (4x3). From these results it can be seen that using only camera location for low flight (3x3) gives the best results ($\sigma_x = \sigma_y$ =0.1 and σ_z = 0.04) indicating the GPS locations of camera are consistent with each other . However, the residuals on the check points (1.67, .26, .38) are large, mainly because the

Albany program does not compensate for systematic error in the camera location. The table also shows that the program gives satisfactory results (σ_x = 0.05, σ_y = 0.07 and σ_z = 0.23)when using ground control only. Therefore the program and the coordinates are satisfactory. The table also shows that when flights of different height are included in the bundle adjustment, the program does not compensate well in x, y resulting in errors of 0.62 in x and 2.27 in y. Also, when we mix camera location and ground control the errors are large σ_x = 1.03, σ_y = 0.46 and σ_z = 0.11 indicating the existence of systematic error in between the coordinates. One of the important results shown in this table , that it is possible to do aerial triangulation without any ground control, and it gives the best results ($\sigma_x = \sigma_y$ = 0.1 and σ_z = 0.04). However, the check on ground control is poor because of the systematic error between camera location and ground.

Table 6.7
Standard error of unit weight by AGPS

Method AGPS	Std. error of unit weight
4×3 with ground control	σ_0 = 0.81
4×3 with camera & ground control	σ_0 = 1.10

The table 6.7 gives the results of AGPS run using the 4×3 photos. The adjustment was done with weights of 1000 on photo coordinates and of 10,000 on camera locations. Using the ground control only, the program yields σ_0 =0.81, where as using camera location and ground control, it yields σ_0 = 1.10 . Therefore the improvement is not significant. Thus, the AGPS program compensates for the systematic error in camera location ; and there is a systematic error between camera location by GPS and ground control. The camera location is obtained by kinematic GPS mode within 1 hour of observation, while ground control is obtained by static mode and adjusted by simultaneous adjustment program.

Table 6.8
Standard error of unit weight by Fortblk

	Method		Std. error of unit weight
1.	3 high 91 photo with weight on $_{photo}$ weight on $_{ground}$	= 1 = 10,000	0.012
2.	weight on $_{photo}$ weight on $_{ground}$ weight on $_{camera}$	= 1 = 10,000 = 1	0.018
3.	weight on $_{photo}$	= 1	∞
	weight on $_{camera}$	= 1	no solution
4.	weight on $_{photo}$ weight on $_{camera}$ = 1 wt on one elevation control = 10000	= 1	0.016

Three photos from NOAA high flight were adjusted using a FORTBLK simultaneous adjustment program to evaluate the use of camera location for a strip. The table 6.8 gives the results under four conditions. The best result $\sigma = 0.012$ is obtained by using ground control only. There is no solution with camera location only. $\sigma = 0.018$ for the camera and ground control is a satisfactory solution. However there is systematic error between camera and ground due to the large difference in that were used . $\sigma = 0.016$ using camera and one ground elevation control is a satisfactory solution that is not significantly different from $\sigma_0 = 0.012$ obtained using only ground control.

These experimental results show that by using camera location by GPS, a block of photos consisting of 2 or more strips with 60% forward and 30% lateral overlap can be used to do aerial triangulation without any ground control.A systematic error exists between ground control and camera location, which can be eliminated using the AGPS software with block of photos from high and low flights. Another significant finding is that aerial triangulation of a strip using camera location only is not possible; however, with at least one elevation control and camera locations, a satisfactory adjustment is possible. These results also show that camera location is best determined by GPS than by aerial triangulation. Aerial triangulation determines camera location by resection; thus a small error in pass or control point data will adversely affect the error in the camera location.

Table 6.9

The SAS System 1
11:10 Thursday, August 13, 1992

OBS	X1	Y1	Z1	X2	Y2
1	1510750.50	1056395.30	1227.75	1510750.79	1056395.97
2	1510189.74	1056410.33	1227.00	1510190.27	1056410.89
3	1509630.99	1056412.15	1224.24	1509631.44	1056412.53
4	1509066.92	1056412.69	1226.26	1509067.10	1056413.13
5	1508520.93	1056414.72	1226.66	1508520.58	1056415.47
6	1507977.19	1056414.59	1224.76	1507977.69	1056414.99
7	1507434.51	1056412.63	1224.88	1507435.16	1056413.19

OBS	Z2	DX	DY	DZ
1	1227.94	-0.28690	-0.6725	-0.18160
2	1227.22	-0.53090	-0.5678	-0.21345
3	1224.72	-0.45680	-0.3815	-0.47659
4	1226.99	-0.18180	-0.4464	-0.73012
5	1227.22	0.35080	-0.7503	-0.56012
6	1225.37	-0.50150	-0.4046	-0.60321
7	1225.66	-0.64900	-0.5687	-0.78661

The SAS System 2
11:10 Thursday, August 13, 1992

Variable	Mean	Std Error
DX	-0.3223000	0.1267268
DY	-0.5416857	0.0524575
DZ	-0.5073855	0.0890465

6.2 St.Louis 92 Flight

In order to ensure the success of the 91 flight and to use a different GPS receiver and aircraft the 92 flight over the Mustang project area was undertaken. A Twin Engine Cessna airplane owned by a private firm in St. Louis was used for this flight. The GPS data were collected using Ashtech receivers capable of collecting data every 1/2 second. Three low flights at 1500 ft. with 60% forward and 60% lateral overlaps were and a high flight at 3000 ft. with 60% forward overlap were done. Almost all pass points and six GPS points were targeted. Also all PIs along the Highway 30 were painted (see figure 6.11).

The photo coordinates were observed by Wild Stereo comparator. Because the flight lines were not exactly as planned, the targeted pass points were not at the right location. As a result, few natural points had to be used. The camera location were interpolated from GPS data collected every 1/2 second (see appendix 3). These data were then adjusted by Albany and AGPS. The table 6.9 (SAS system) shows the difference between camera location by GPS and by aerial triangulation using Albany software and ground control for the high flight. After eliminating the systematic difference between ground control and camera location the two agreed with $\sigma_x = 0.12$, $\sigma_y = 0.05$ and $\sigma_z = 0.02$. The graph in fig 6.12 (Strip23.wq1) shows the agreement for the central low flight. It can be concluded that the accuracy of camera location by GPS is better than 10 cms, allowing for errors in strip adjustment.

Table 6.10
Standard error by Albany

Data	Method	Std error in output		
		σ_x	σ_y	σ_z
High 92	Albany	0.063	0.083	0.103
3 Low 92	Albany	0.033	0.034	0.107
Hi Low 92	Albany	0.063	0.088	0.090

Table 6.10 shows the results of the adjustment using Albany software. The improvement in the std error, $\sigma_x = 0.05$ for 91 flight and $\sigma_x = 0.03$ for 92 flight, is due to the fact that we had no pug points; and mostly targeted points as control and pass points. The improvement in std error, $\sigma_z = 0.23$ from 91 flight and $\sigma_z = 0.107$ for 92 flight, is due to the 60% side overlap. The table "A" also indicates that the accuracy in z, in the high flight is about the same as in the low flight. A combination of high and low photos improves the standard error, σ_z, in elevation. Even though σ_x, σ_y in the high flight is twice as much as in the low flight, this is to be expected because the flying height is 1500 ft for low flight and 3000 ft for high flight; still the std error in the high flight is less than 10 cms which is acceptable for highway earthwork computations. At present, the Ia DOT uses the low

1992 Flight

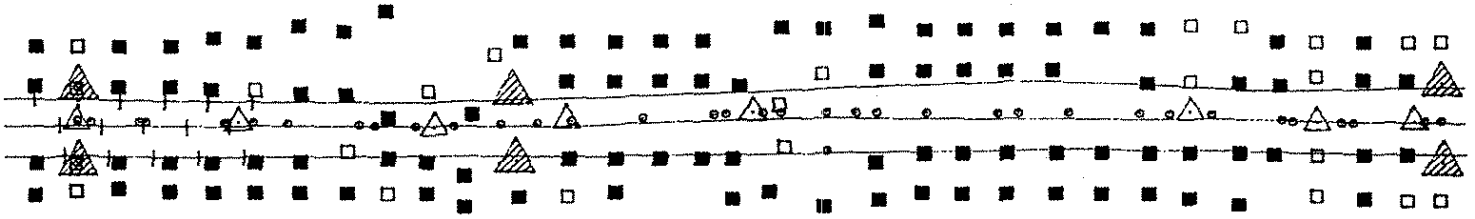

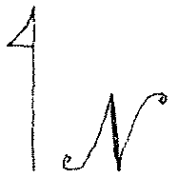

GPS Control Points

PI's Established by DOT traverse

Points retargeted from '91 flight

Approximate locations of '92 targeted poss points

DOT points established on highway

GPS camera location point

Low flight lines

Fig. 6.11 1992 flight.

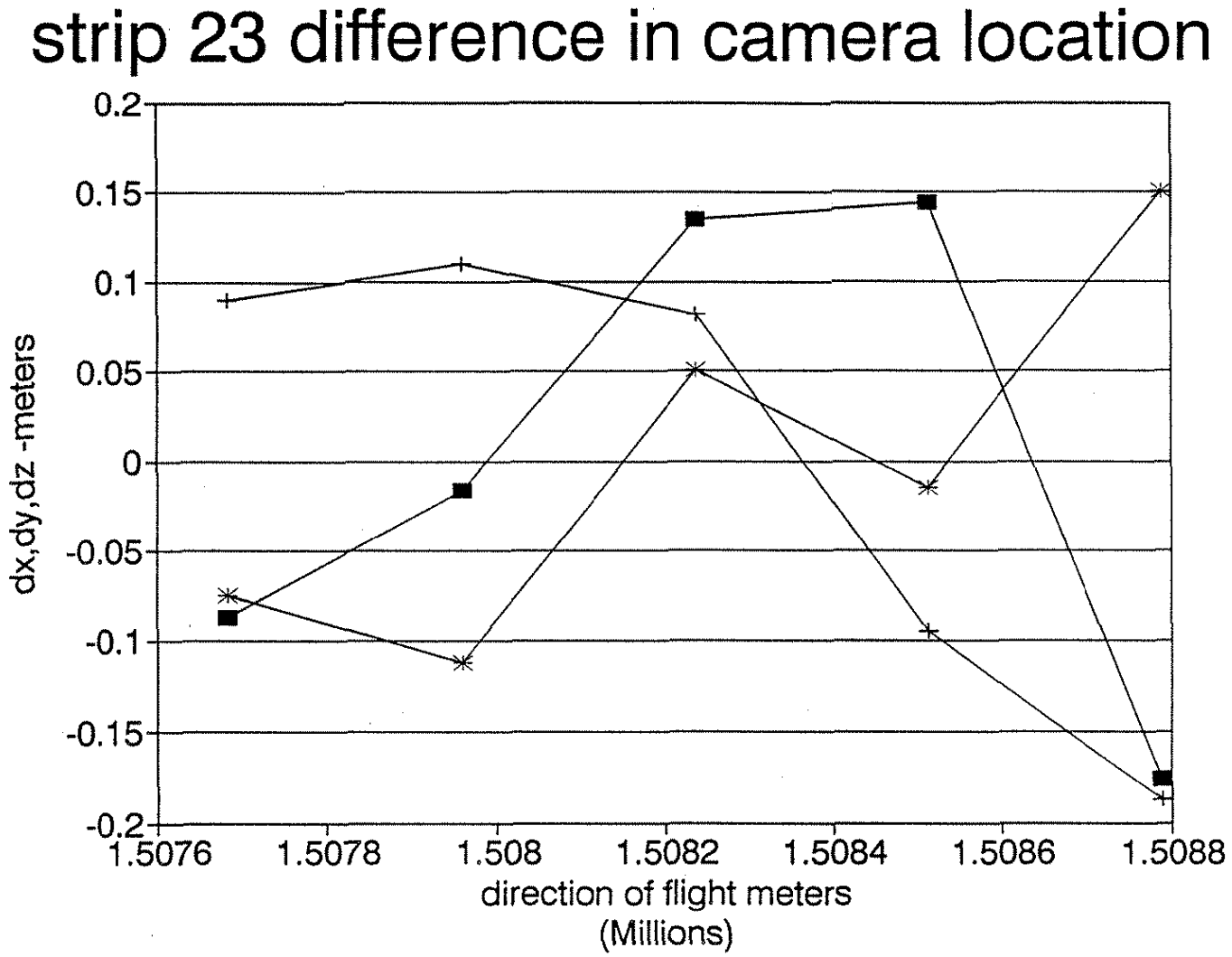

photo#	x	dx	dy	dz	dx'	dy'	dz'
119	1056384.28	-0.489	-0.1386	-29.787	-0.087	0.0897	-0.075
118	1056382.39	-0.5595	-0.1584	-29.75	-0.016	0.1095	-0.112
117	1056379.77	-0.7099	-0.1306	-29.913	0.1342	0.0817	0.051
116	1056377.18	-0.7195	0.0454	-29.848	0.1438	-0.094	-0.014
115	1056377.08	-0.4005	0.1378	-30.0122	-0.175	-0.187	0.1502
	mean	-0.5757	-0.04888	-29.86204	0	0	-7E-16
	std.error	0.12423	0.1187102	0.0933017			

Fig. 6.12

Table 6.11a Standard deviation of difference in x by ground control and camera location.

SD of difference of X-coordinates between HILO92.CNT and HILO92.CAM

POINT NO.	X1 (cnt)	X2 (cam)	(X1-X2)	(X1-X2)**2
20004	1507811.252	1507811.161	0.091	0.0082810000
5004	1508383.102	1508382.922	0.180	0.0324000000
20006	1507810.753	1507810.656	0.097	0.0094090000
2050	1507713.666	1507713.648	0.018	0.0003240000
2051	1507805.165	1507805.114	0.051	0.0026010000
2052	1507896.566	1507896.471	0.095	0.0090250000
2011	1508780.061	1508779.825	0.236	0.0556960000
2004	1507806.134	1507806.045	0.089	0.0079210000
8113	1510075.814	1510075.594	0.220	0.0484000000
9026	1509818.621	1509818.392	0.229	0.0524410000
9029	1509557.788	1509557.508	0.280	0.0784000000
8017	1508964.947	1508964.701	0.246	0.0605160000
2103	1510541.434	1510541.320	0.114	0.0129960000
2017	1510775.418	1510775.332	0.086	0.0073960000
20016	1510612.643	1510612.520	0.123	0.0151290000
20018	1510629.855	1510629.751	0.104	0.0108160000
2013	1509726.356	1509726.081	0.275	0.0756249999
2056	1509989.558	1509989.346	0.212	0.0449440000
2055	1508947.742	1508947.487	0.255	0.0650250001
2101	1509169.701	1509169.442	0.259	0.0670809999
2008	1508211.382	1508211.180	0.202	0.0408040000
2100	1508255.613	1508255.404	0.209	0.0436809999
2053	1508765.155	1508764.916	0.239	0.0571210000
2002	1507403.333	1507403.361	-0.028	0.0007840000
			3.882	0.[illegible]160000

MEAN = 0.1617500000

SD = 0.[illegible]83381192

Table 6.11b Standard deviation of difference in y by ground control and camera location.

SD of difference of Y-coordinates between HILO92.CNT and HILO92.CAM

POINT NO.	Y1 (cnt)	Y2 (cam)	(Y1-Y2)	(Y1-Y2)**2
20004	1056144.597	1056144.032	0.565	0.3192250002
5004	1056878.944	1056878.159	0.785	0.6162249999
20006	1056629.359	1056628.536	0.823	0.6773289998
2050	1056405.954	1056405.294	0.660	0.4355999999
2051	1056416.663	1056415.930	0.733	0.5372890000
2052	1056405.148	1056404.452	0.696	0.4844160000
2011	1056402.580	1056401.866	0.714	0.5097960002
2004	1056144.592	1056144.028	0.564	0.3180960000
8113	1056612.292	1056611.629	0.663	0.4395689999
9026	1055951.772	1055950.962	0.810	0.6561000001
9029	1056221.110	1056220.377	0.733	0.5372890000
8017	1056615.744	1056615.007	0.737	0.5431689998
2103	1056392.134	1056391.431	0.703	0.4942090000
2017	1056403.222	1056402.530	0.692	0.4788640001
20016	1056597.959	1056597.278	0.681	0.4637610001
20018	1056164.290	1056163.573	0.717	0.5140869999
2013	1056381.274	1056380.557	0.717	0.5140889999
2056	1056375.037	1056374.330	0.707	0.4998489999
2055	1056400.161	1056399.455	0.706	0.4984360000
2101	1056394.869	1056394.168	0.701	0.4914009996
2008	1056404.233	1056403.522	0.711	0.5055209998
2100	1056404.133	1056403.425	0.708	0.5012639998
2053	1056402.612	1056401.897	0.715	0.5112249998
2002	1056407.846	1056407.173	0.673	0.4529289999
			16.914	11.9997399991

MEAN = 0.7047500000

SD = 0.0575899658

Table 6.11c Standard deviation of difference in z by ground control and camera location.

SD of difference of Z-coordinates between HILO92.CNT and HILO92.CAM

POINT NO.	Z1 (cnt)	Z2 (cam)	(Z1-Z2)	(Z1-Z2)**2
20004	302.879	303.497	-0.618	0.3819240000
5004	298.193	298.556	-0.363	0.1317690000
20006	304.347	304.672	-0.325	0.1056250000
2050	303.975	304.441	-0.466	0.2171560000
2051	304.668	305.010	-0.342	0.1169640000
2052	305.272	305.641	-0.369	0.1361610000
2011	301.373	301.602	-0.229	0.0524410000
2004	303.174	303.787	-0.613	0.3757690000
8113	294.196	294.297	-0.101	0.0102010000
9026	302.451	302.788	-0.337	0.1135690000
9029	290.717	290.998	-0.281	0.0789610000
8017	298.313	298.380	-0.067	0.0044890000
2103	299.414	299.818	-0.404	0.1632160000
2017	305.574	305.969	-0.395	0.1560250000
20016	307.623	307.959	-0.336	0.1128960000
20018	307.127	307.607	-0.480	0.2304000000
2013	292.862	293.017	-0.155	0.0240250000
2056	293.544	293.717	-0.173	0.0299290000
2055	301.826	301.968	-0.142	0.0201640000
2101	299.000	299.221	-0.221	0.0488410000
2008	302.467	302.814	-0.347	0.1204090000
2100	301.927	302.263	-0.336	0.1128960000
2053	301.239	301.470	-0.231	0.0533610000
2002	302.556	302.883	-0.327	0.1069290000
			-7.658	2.9041200000

MEAN = -0.3190833333

SD = 0.1385309582

Table 6.11d Standard deviation of difference in x photo coodinates residual by ground control and camera location.

SD of difference of X - residuals between HILO92.CNT and HILO92.CAM

POINT NO.	DX1 (cnt)	DX2 (cam)	(DX1-DX2)	(DX1-DX2)**2
20004	0.013	0.009	0.004	0.0000147379
5004	0.000	-0.022	0.022	0.0004934174
20006	0.001	-0.005	0.006	0.0000343279
2050	0.000	-0.015	0.015	0.0002306146
2051	-0.008	-0.004	-0.004	0.0000167854
2052	-0.010	-0.008	-0.002	0.0000054336
2011	0.001	-0.002	0.003	0.0000078905
2004	-0.009	-0.012	0.003	0.0000094495
8113	0.000	-0.002	0.002	0.0000049640
9026	0.000	0.000	0.000	0.0000002162
9029	-0.001	-0.002	0.002	0.0000027192
8017	0.003	-0.002	0.005	0.0000206479
2103	0.000	0.000	0.000	0.0000000204
2017	-0.001	0.000	-0.001	0.0000006708
20016	0.001	0.000	0.001	0.0000010754
20018	0.000	0.000	0.000	0.0000000640
2013	-0.011	-0.009	-0.002	0.0000050400
2056	-0.001	0.000	-0.001	0.0000012365
2055	0.002	-0.006	0.009	0.0000748744
2101	0.002	0.000	0.002	0.0000046699
2008	0.002	0.003	-0.001	0.0000009801
2100	0.000	-0.002	0.002	0.0000037018
2053	0.005	0.005	0.001	0.0000002735
2002	0.001	0.000	0.001	0.0000002540
			0.064	0.0009340649

MEAN = 0.0026772500

SD = 0.0056348652

Table 6.11e Standard deviation of difference in y photo coordinates residual by ground control and camera location.

SD of difference of Y - residuals between HILO92.CNT and HILO92.CAM

POINT NO.	DY1 (cnt)	DY2 (cam)	(DY1-DY2)	(DY1-DY2)**2
20004	0.007	0.011	-0.004	0.0000130682
5004	0.007	-0.008	0.016	0.0002449225
20006	0.003	0.017	-0.014	0.0002081960
2050	-0.004	0.015	-0.019	0.0003674122
2051	0.003	-0.012	0.015	0.0002310704
2052	-0.003	-0.013	0.010	0.0001087432
2011	0.003	0.003	0.000	0.0000002070
2004	-0.005	-0.001	-0.003	0.0000110889
8113	0.006	0.007	0.000	0.0000000605
9026	0.000	0.001	-0.001	0.0000004886
9029	-0.005	-0.002	-0.002	0.0000050355
8017	-0.003	-0.002	-0.001	0.0000012343
2103	-0.002	-0.001	-0.001	0.0000008263
2017	-0.002	-0.001	-0.001	0.0000006162
20016	0.003	0.004	-0.001	0.0000013995
20018	0.003	0.004	0.000	0.0000001232
2013	0.001	0.005	-0.004	0.0000170321
2056	-0.010	-0.007	-0.003	0.0000063706
2055	-0.005	-0.007	0.001	0.0000014884
2101	0.006	-0.009	0.014	0.0002060373
2008	0.000	-0.010	0.009	0.0000838323
2100	0.000	-0.013	0.013	0.0001704852
2053	0.008	0.008	0.000	0.0000000339
2002	-0.002	-0.004	0.003	0.0000063908
			0.020	0.0016861633

MEAN 0.0010930833

SD 0.0083103534

flight photo for earthwork computations. The use of high flight photo with GPS control will cut down the cost by almost 50 %.

Table 6.11
92 flight by AGPS

Data	Method	wt on ground	wt on camera	wt on photo	σ_0
Hi Lo 92	AGPS	1.0	0.0	1000	4.7
Hi Lo 92	AGPS	0.0	100.0	1000	0.35
Lo 92	AGPS	1.0	0.0	1000	0.05
Hi 92	AGPS	1.0	0.0	1000	0.01

Table 6.11 gives the results using AGPS software. Since, σ_0 = 0.35 with camera location and σ_0 = 4.7 with ground control, camera location is relatively more accurate than ground control. The table also indicates that satisfactory results can be obtained with hilo photo and 60% forward and lateral overlap with weight on camera locations and without any ground control .Also, the accuracy of camera location is comparable to photo coordinate, indicating a relative accuracy of 1 cms or better in the camera location. The low or high photographs with weights on ground control give an accuracy of 1cm or better on ground coordinates.Even though this adjustment is satisfactory , the values of the camera locations and parameters thus obtained may not as is indicated by the high standard error when high and low flight photograph are combined.

Table 6.11 (a,b,c,d,e) gives the difference between adjustment using ground control and camera control with AGPS software. The results indicate a systematic error between ground control and camera location. After eliminating the systematic errors the two agree within 10 cms, showing that camera control and AGPS software give satisfactory results.

Table 6.12
Weights used in Fortblk

Data	Method	wt on ground	wt on camera	wt on photo	σ_0
HiLo 92	FortBlock	0.0	100.0	1000	5.8
HiLo 92	FortBlock	0.0	100.0	1000	2.2
Hi 92	FortBlock	0.04	100.0	1000	0.9

Table 6.12 gives the results of adjustment using FORTBlK. When the weight on photo coordinates is made equal to that of camera location σ_0 changes from 5.8 to 2.2, showing that the accuracy of camera location is equal to that of photo coordinates and that photo coordinates of points have to be determined precisely using targets. Introducing a small weight on ground control improves the standard error from 2.2 to 0.9, suggesting that few ground control points of even low accuracy will enhance adjustment when combined with camera location. Thus, in a typical highway project, the PIs established during

preliminary survey can be targeted and used as ground control. The PIs together with camera location will give satisfactory results by triangulation adjustment.

6.4 California Project

This project was conducted by U.S. Forest Department under the direction of Kent Whitaker. This was a NS flight with flying height of about 20,000 ft. A Trimble GPS receiver able to collect pseudo range and kinematic data was used. There were 4 strips with 5 points each, with 60% forward and lateral overlap of about 40%. The project area covers over 2US quad sheets. There were 12 control points which are natural points whose coordinates were obtained by Static GPS method and least squares network adjustment (see fig 6.13). The base station for Airborne GPS was included in the same network as the control points. The pass and tie points were pugged using Wild Pug-4 and the coordinates were observed with mono and stereo comparators.

Table 6.13

Difference between kinematic camera control and ground control bundle adjustment

	Δx_m	Δy_m	Δz
Min	-5.381	-4.170	-3.180
Max	1.412	2.857	3.847
Mean	-1.534	-0.116	-0.489
Std error	1.353	1.228	0.970

Table 6.13 summarizes the results of the block adjustment using GAPP software (this software is developed by the National Geodetic Survey). The table shows the difference in x, y, z coordinates of the tie and pass points obtained using camera location by kinematic method and by ground control only. These results show a systematic error between ground control and camera location. The error is large because of the small scale photography, where a small error in photo coordinates of pass points and tie points will affect the quality of the bundle adjustment; thus, emphasizing the importance of targeting the pass, tie and control points. Also, the error could have been improved if there was 60% lateral overlap.

Table 6.14

Difference between pseudorange camera control and ground control bundle adjustment

	Δx_m	Δy_m	Δz
Min	-6.429	-7.007	2.063
Max	0.000	0.703	9.582
Mean	-2.985	-2.135	0.831
Std error	1.031	1.094	1.362

APPENDIX 1

California Flight Layout Diagram

By Jiyong Wang Sept.15, 1992

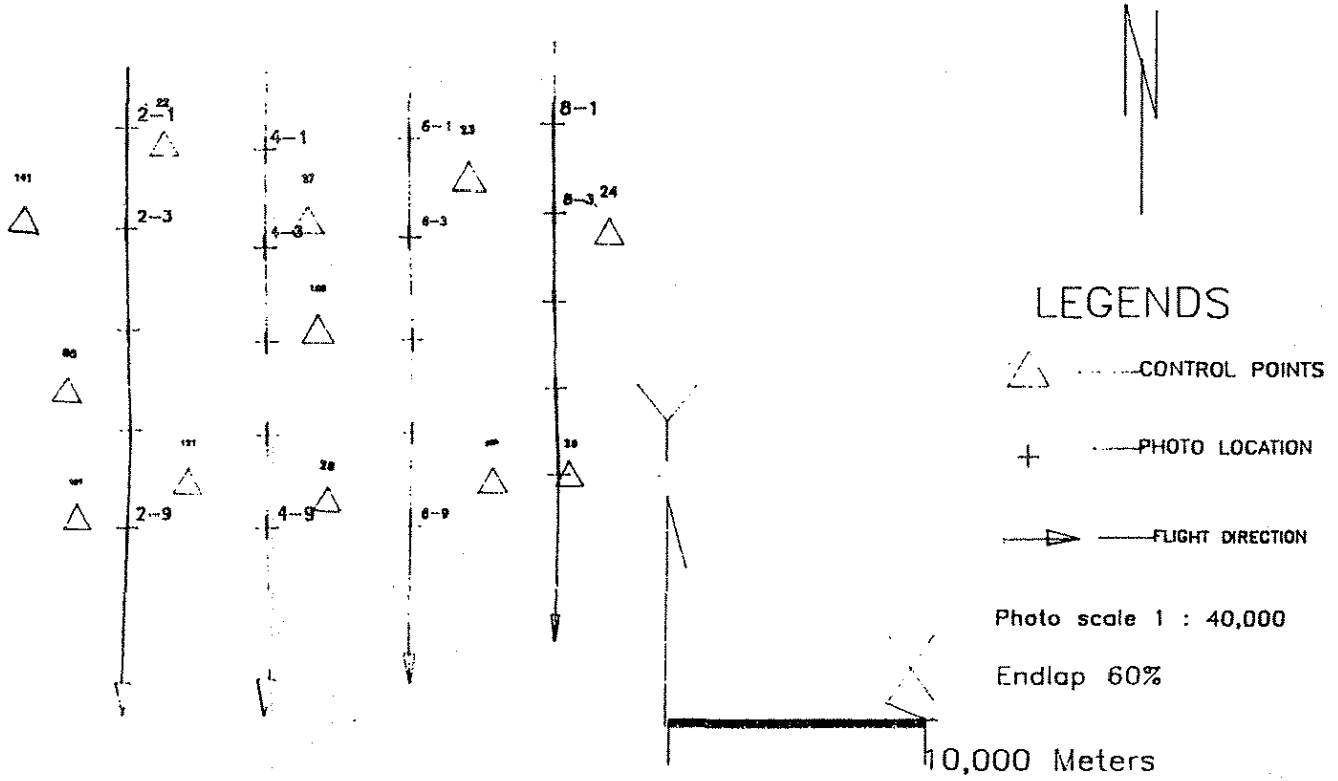

Fig. 6.13

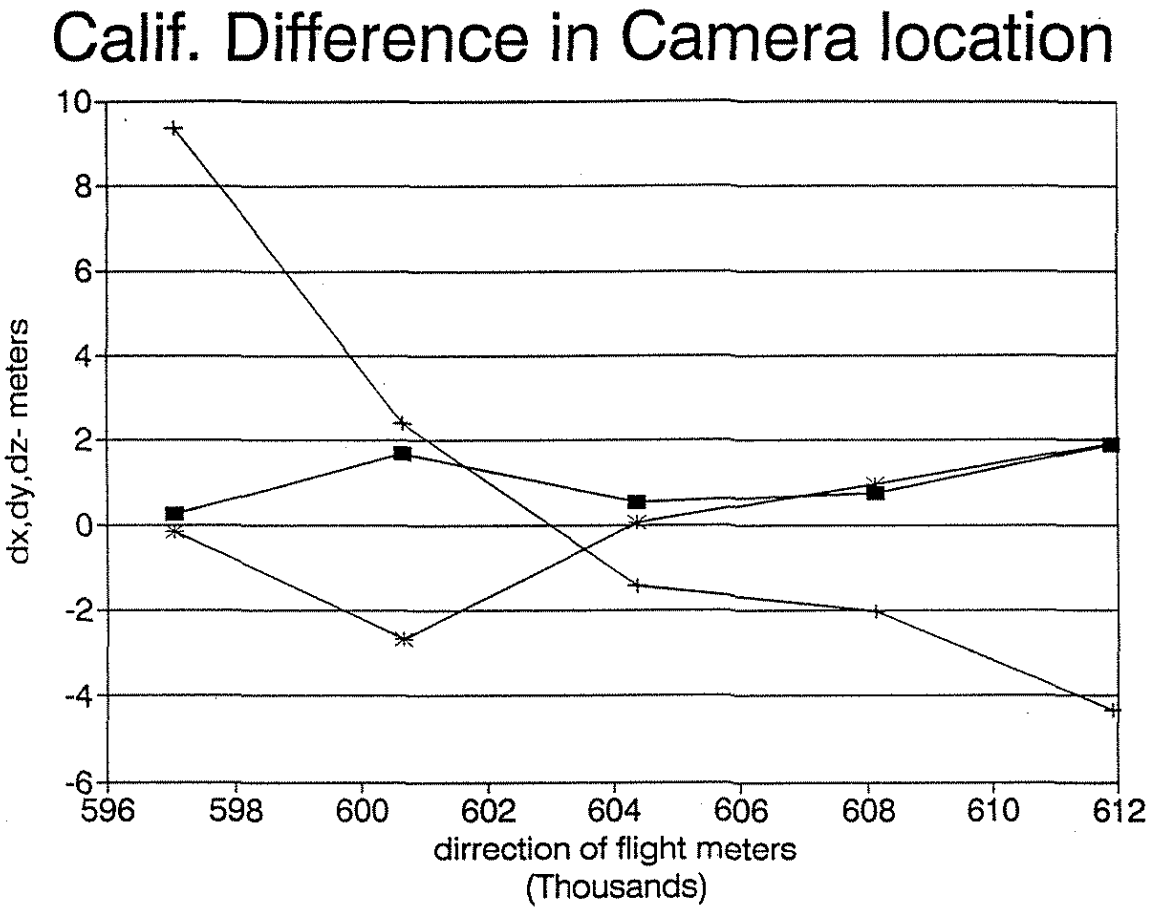

x	dx	dy	dz
4693.103	0.278	9.35	-0.147
4703.619	1.699	2.403	-2.658
4621.752	0.534	-1.416	0.057
4578.54	0.77	-2.035	0.957
4589.656	1.88	-4.325	1.898
mean	1.0322	0.7954	0.0214
std	0.640180724	4.793443631	1.523534391

Fig. 6.14

Table 6.14 gives the difference in x, y, z of the tie and pass points obtained using pseudo-range camera control and ground control in the bundle adjustment. Comparing the means in the tables 6.13 and 6.14 it can be concluded that the kinematic method of determining camera location is twice as good as that by pseudo-range.

Table in fig. 6.14 ,Calif.wq1, shows the results obtained using Albany software. Specifically it shows the difference between camera location determined by Albany using ground control and that by kinematic GPS. The mean is less than a meter (see the graph in fig 6.14) indicating the error is in the aerial triangulation than in the camera location by GPS. It can be concluded that camera location by GPS is satisfactory for high altitude photography and that there is a systematic error between camera location by GPS and by aerial triangulation.

Table 6.15

Residuals in control and images

	σ_x	σ_y	σ_z
control	0.906m	0.478m	0.824m
images	0.025mm	0.0305mm	0.091mm

The Albany software gives a std error on the control as σ_x = 0.906m, σ_y = 0.478m, σ_z = 0.824m (see table 6.15), thus the accuracy of the adjusted coordinates are less than 1m. The Albany also gave standard error in the image residuals as σ_x = 0.0255mm, σ_y = 0.0305mm, σ_z = 0.0919mm all errors in the image coordinates as less than 0.05mm. These image tie and pass points are not identical due to pugging.

The California data were also adjusted using AGPS software with weight on control = 0.01, weight on camera = 10,000 and weight on photo = 1000. The std error of unit weight = 1.7, an excellent adjustment compensating for systematic errors between control and camera location. This also shows that camera location is about 3 times better than photo coordinates. Thus the accuracy of camera location by GPS is 0.003m or 3mm, assuming photo coordinate accuracy to be about 0.001mm. Also, the results indicate that camera locations are comparable to photo coordinates as opposed to the ground control. This is to be expected since the kinematic GPS determine camera location within an hour. Therefore, the relative accuracy between camera locations is much better than that of ground control. Also ground control is determined at a different plane, 20,000 ft below the camera location and photo coordinates.

6.5 Texas Project

This project was done by the Texas DOT. It consists of 3

Appendix 1

TEXAS FLIGHT LAYOUT DIAGRAM

by Jiyong Wang Sept. 11,1992

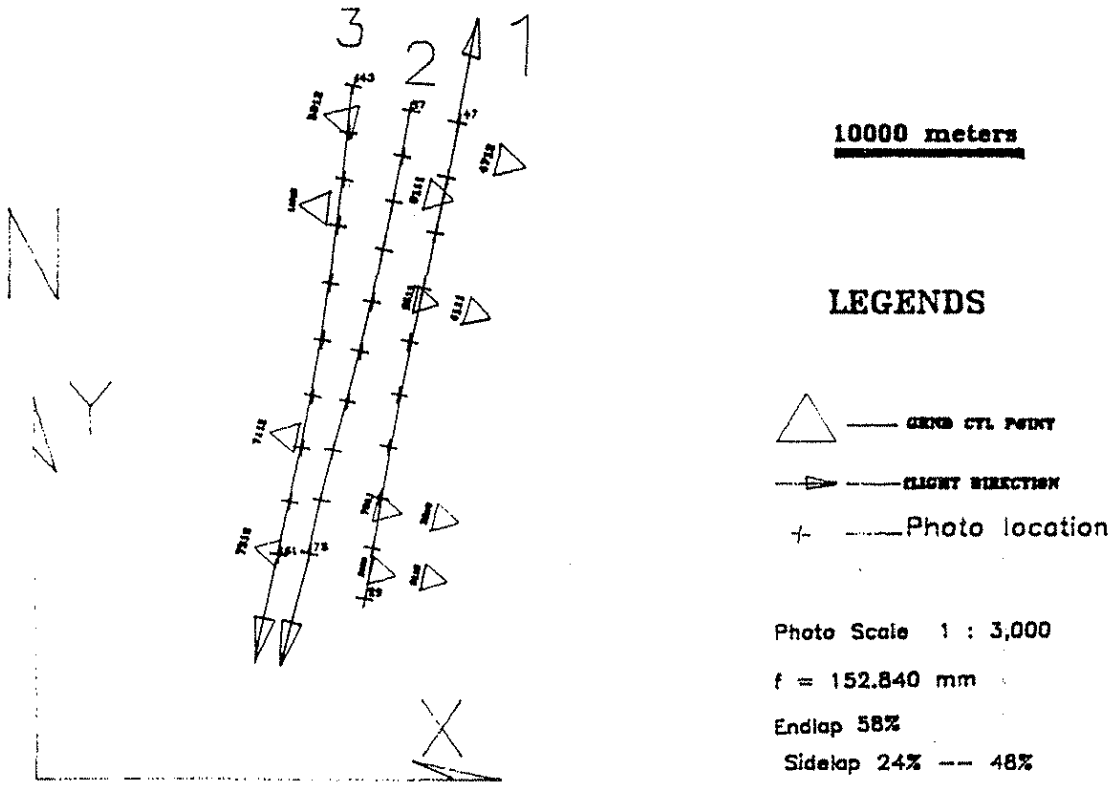

Fig.6.15

strips in a North Easterly direction at 1500 ft flying height with 60% forward and side overlap, and 12 control points (see figure 6.15). The aircraft belongs to Texas DOT; and a Trimble GPS receiver was used to determine the camera location. The GAPP software was used by Texas DOT to adjust the data. The Albany and AGPS software were used by ISU.

The middle strip was adjusted using Albany software and 12 ground control points. Table in fig. 6.16 ,texas.wq1, shows the difference between camera location by GPS and by aerial triangulation. The graph (in fig 6.16) shows that the accuracy of camera location by GPS is better than 10 cms. The large errors at the beginning and the end are due to propagation of errors in aerial triangulation and the systematic error between ground control and camera location by GPS.

Table 6.16

Std error in control by Albany

Data	σ_x	σ_y	σ_z
middle strip	0.041	0.032	0.035
block of strip	0.643	0.317	0.643

The table 6.16 shows the standard error in the control by Albany software. The small error, less than 10 cms, when the middle strip is adjusted, is consistent with the Mustang project. The large error, is more than 50 cms, when all 3 strips are simultaneously adjusted and is mainly due to the fact that the tie points were not targeted, but pugged.

Table 6.17
Weight for AGPS

Method	wt on photo	wt on ground control	wt on camera	σ_0
camera	1000	0.0	1.0	8.4
control	1000	100.0	0.0	4.2
cam & control	1000	0.04	1.0	3.3

Table 6.17 shows the adjustment results of the 3 strips using AGPS software. It is obvious that a light weight on control and camera gives the best result. The results using camera location only are poor when compared to others because the tie and pass points are pugged and because of the lack of good geometry in the selection of these points. The lack of geometry may also be due to the inability to maintain side overlap of 40 to 50% as planned due to visual navigation. Using GPS for navigation may eliminate this problem. The improvement of camera and control method over the control method shows that AGPS compensates for the systematic error between ground control data and camera location by GPS. It also shows that photo coordinates are slightly better than camera

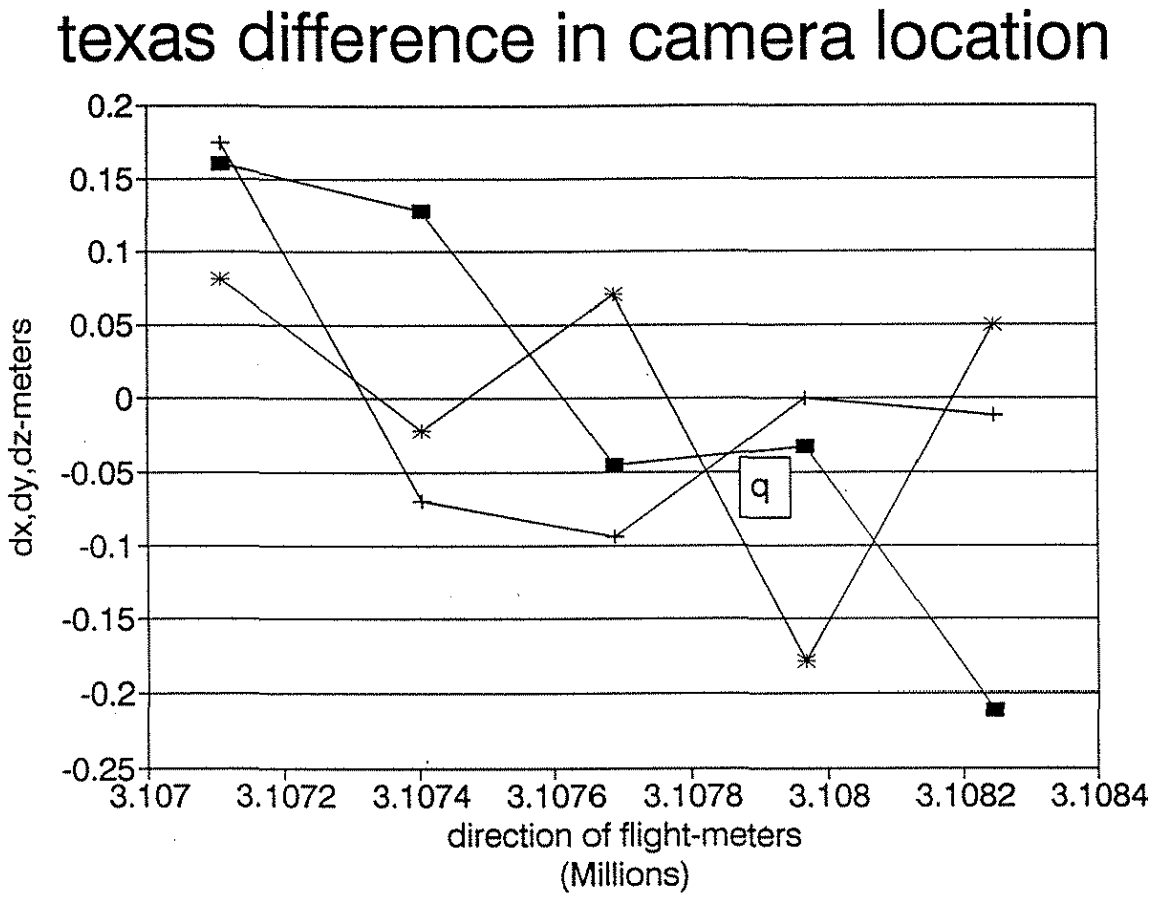

photo #	x	dx	dy	dz	dx'	dy'	dz'
75	692186.469	0.131	0.279	-1.149	0.161	0.1746	0.0802
73	692251.826	0.164	0.523	-1.047	0.128	-0.069	-0.0218
71	692323.676	0.336	0.547	-1.139	-0.04	-0.093	0.0702
69	692398.414	0.324	0.454	-0.89	-0.03	-0.000	-0.1788
67	692470.896	0.503	0.465	-1.119	-0.21	-0.011	0.0502
	mean	0.292	0.454	-1.069	0	1.1E-17	0
	std.error	0.134	0.094	0.0963			

Fig. 6.16

location. Assuming that the accuracy of the photo coordinates is about ± 0.001 mm, the accuracy of the camera location can be estimated to be about ± 0.03 m or ± 3 cms.

6.6 Study on Multi-antenna Airborne GPS

The figure 6.17 shows the concept of the multi-antenna. The objective of Multi-antenna GPS is to determine the (x,y,z) and (κ,ϕ,ω) of the camera at the time, where as the single antenna can only determine the location of the camera (x,y,z).

Table 6.18

Exterior orientation Elements

	x m	y m	z m	κ (rad)	ϕ	ω
Photo 1						
	1507798.042	105649.885	787.040	-0.03328	0.002919	-0.011726
σ_0	0.055	0.054	0.046	0.00014	0.00016	0.00019
weight	100.00	100.00	100.0	0.0	0.0	0.0
Photo 2						
	1508081.416	1056541.879	786.283	-0.038609	0.001711	-0.0085
σ_0	0.051	0.051	0.034	0.000108	0.000113	0.00017

weight on photo = 1000, σ_0 = 0.35

Table 6.18 shows the exterior orientation elements of two photo in the HILO92 project using AGPS software. This table shows the absolute accuracy of x, y, z is about 5 cms and the relative accuracy is about (0.001×$\sqrt{3}$) mm in photo scale or about 0.001×3$\sqrt{3}$ m = 5 mm or better on ground scale . The table also shows that the accuracy required on κ,ϕ,ω is about ± 0.0001 (rad) ~ 20". Thus, if we locate the multiple antenna, as shown in figure 6.17, the required separation, L, between antenna in the x or y direction is .005/.0001 = 50m when the relative accuracy is 5 mm or if the relative accuracy is 0.001 m, then x = 10m.

Recently Ashtech GPS receivers have designed a 3DF GPS receiver. This receiver can simultaneously receive data from 4 multi-antenna receivers and determine the κ,ϕ,ω of an aircraft on dynamic mode with an accuracy of 3 minutes when L=2 m giving a relative accuracy of ± 0.00045 m on the antenna locations. Thus, if the relative accuracy desired is 20", the required L = 5 m. From a study of the different aircraft used, it is found that a distance L = 12 m is normally possible. Thus, using x = 10 m and 3DF GPS receiver it is possible to get an accuracy of better than 10" in κ,ϕ,ω.

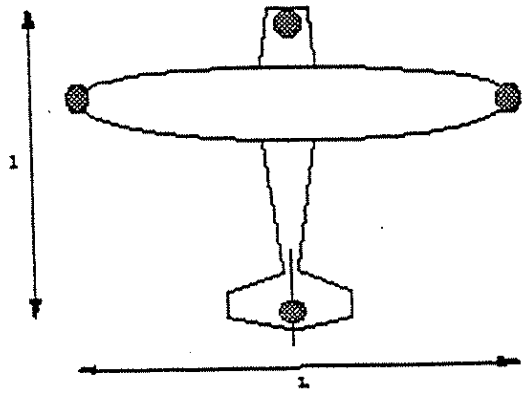

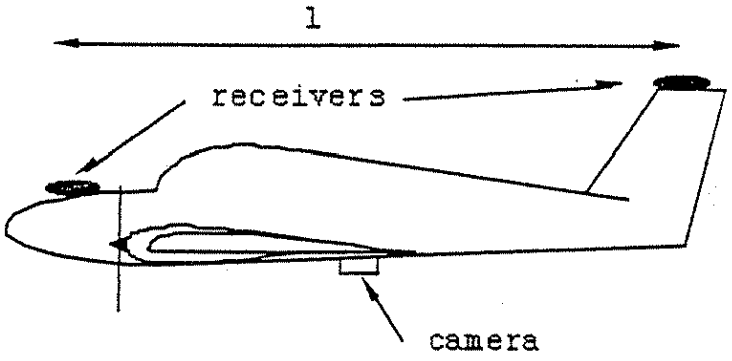

Fig. 6.17 Multi-antenna concept.

It is recommended that we do further research. Based upon its success, we will be able to do direct plotting using airborne GPS without aerial triangulation of a block of photos or ground control.

7.0 CONCLUSIONS AND RECOMMENDATIONS

Results of the five test flights showed that the camera locations determined by GPS agree with those obtained by analytical photogrammetry. Agreement using the 3000 scale photography were less than five centimeters and agreement using the 40,000 scale photography was less than a meter. Thus, it can be concluded that the error in camera locations by analytical photogrammetry depends on the scale of the photography used and that the accuracy of camera locations by GPS is better than five centimeters.

Method of constraints used in analytical triangulation showed that the relative accuracy of the camera location by GPS is equivalent to that of the photo coordinates. Thus assuming that the photo coordinates have an accuracy of .001 mm the relative accuracy of the camera location by GPS is one millimeter or better.

Strip triangulation using camera locations by GPS needs at least one ground height control. It is recommended that the elevation of Point of Intersections established during the preliminary survey be used as height control in the simultaneous adjustment of a strip of photographs using software such as Albany.

Block triangulation using camera locations by GPS only, without any ground control, is possible. The best results are obtained when using sixty percent forward and lateral overlap.

In both strip and block triangulation, pretargeting of pass and tie points is preferred to pugging and selecting natural points. Pretargeting requires precise navigation. It is recommended that GPS be used in navigating the aircraft and taking photographs at predetermined locations.

In both strip and block triangulation GPS can be used cost effectively to establish ground control. There exists a systematic error between ground control and camera location by GPS. Special software such as AGPS can be used to eliminate the systematic errors. It is recommended that the base station for camera location by GPS and the ground control be part of the same GPS network. It is also recommended that six GPS ground control points be used for block triangulation, and additional elevation control be used along the center line for strip triangulation.

Airborne GPS has the capability of determining exterior orientation elements including tip and tilt of the camera with sufficient accuracy for plotting topographic maps from a stereo pair without ground control or aerial triangulation. It is highly recommended that research be conducted to exploit this unique possibility.

ACKNOWLEDGMENT

The authors wish to thank the Iowa Highway Research Board for supporting this research project. The authors appreciate the confidence shown by Mr. George Sisson and Mr. Mel Nutt of the Iowa Department of Transportation. Thanks are due Mr. Vernon Marks of the Iowa DOT for his assistance in getting this project completed in time. Thanks also are due to members of the Photogrammetric Section of the Iowa Department of Transportation, especially Marlee Walton, Alice Walsh, Roland Popelka, Dennis O'Brien, John Rainey, Jeff Danielson, Mel Holmberg and others for their unselfish support and assistance during this research period.
Our thanks also go to Lt. Commanders Lewis Lapine , Peter Connors and others of the National Oceanic and Atmospheric Administration for their assistance in obtaining aerial photographs and airborne GPS data for the NOAA project. We also wish to thank Mr. George Erio of Erio Technologies Inc. for supplying the MAPP\PAL\ALBANY software and training our researchers to use it. Rick Hoffman and others from MAPS Inc. obtained aerial photographs for the St. Louis Project. Mr. Bill Martin of Ashtech Inc. obtained airborne GPS data for the St. Louis Project. Mr. Kent Whittaker of the United States Forestry Department supplied the information for the California Project and Dr.Bains of the Texas Department of Transportation for supplied the information for the Texas Project. We thank them all for their support.

Finally, we also wish to thank Dr. Lowell Griemann, Chairman, and the staff of the Civil and Construction Engineering Department; Dr. lord, and staff of the Engineering Research Institute, and to Iowa State University for their assistance in getting this project completed on time.

BIBLIOGRAPHY

1. ACSM-NGS. Coordinate Transformation Workshop (Unpublished Xeroxed paper), ACSM, Falls Church, Virginia, 1987.
2. Ashjaee, J. New Results on the Accuracy of the C/A Code GPS Receiver: Proceedings of the First International Symposium on Precise Positioning with the Global Positioning System, U.S. Department of Commerce, Rockville, Maryland, Vol. 1, pp. 207-214, 1985.
3. Ashtech Inc. Ashtech XII Receiver Operations Manual, Sunnyvale, California, 1990.
4. Ashtech Inc. Ashtech XII Model L Operating and Processing Manual, Sunnyvale, California, 1989.
5. Ashtech Inc. Documentation for Ashtech GPPS Software, Sunnyvale, California, 1989.
6. Baker, P. J. Global Positioning System (GPS) policy: Proceedings of the Fourth International Geodetic Symposium on Satellite Positioning, Sponsored by the Defense Mapping Agency and the the National Geodetic Survey at Austin, Texas, Vol. 1, pp.51-64, 1986.
7. Bitwise Ideas Inc. Geolab Documentation, Ottawa, Ontario, Canada, 1988.
8. Bitwise Ideas Inc. The GPS Environment for Geolab Manual, Ottawa, Ontario, Canada, 1987.
9. Bodnar, A. N. Jr. User's Guide for the Establishment of Tidal Bench Marks and Leveling Requirements for Tide Stations, National Geodetic Survey Charting and Geodetic Services National Ocean Service, NOAA, Rockville, Maryland, p. 11, 1975.
10. Bomford, G. Geodesy, 4th ed., Claredon Press, Oxford, pp. 736-739, 1980.
11. Bouchard, R. H. Optimized Observation Periods Required to Achieve Geodetic Accuracies Using the Global Positioning System, M. S. Thesis, Naval Postgraduate School, Monterey, California, 1988.
12. Brown, R. G. and Hwang, P. Y. C. "GPS Geodesy: A Kalman Filter Solution to the Wavelength Ambiguity Problem," Proc. of the 39th Annual Meeting of the Institute of Navigation, pp. 87-92, June 20-23, 1983.
13. Brown, R. G. and Hwang, P. Y. C. "A Kalman Filter Approach to GPS Geodesy," Global Positioning System, Vol. II, Institute of Navigation, Washington, D.C., pp. 155-166, 1984.
14. Brown, R. G. and Hwang, P. Y. C. "GPS Geodesy: Real-Time Processing Possibilities with Karman Filter Approach," Institute of Navigation, January, 1987.
15. Brown, R. G., Jeyapalan, K., et al, "Use of Global Positioning System for Precise Relative Positioning and Land Surveying," Final Report, Iowa High Technology Council, July, 1985.
16. Counselman, C. C. and Shapiro, I. I. "Miniature Interferometric Terminals for Earth Surveying," Bulletin Geodesic, 53(2), 1979.
17. Davis, R. E., Foote, F. S., Anderson, J. M. and Mikhail, E. M. Surveying: Theory and Practice, 6th ed., McGraw-Hill, New York, pp. 160-168, 1986.

18. Defense Mapping Agency Department of Defense World Geodetic System, DMA Technical Report 8350.2, Washington, D.C., pp. 3-10, 3-11, 1987.
19. Defense Mapping Agency Geodesy for the Layman, DMA Technical Report, 80-003, pp. 24, 39, 64, 1983.
20. Denker, H. and Wenzel, G. "Local Geoid Determination and Comparison with GPS Result," Bulletin Geodesique, 61(4), pp. 349-366, 1987.
21. Erck, E.S. "Orthometric Height Difference Recovery Tests from GPS Observations and Gravimetry," M.S. Thesis, Iowa State University, 1989.
22. Ewing C. E. and Mitchell, M. M. Introduction to Geodesy, New York: Elsevier, 1979.
23. Fell, P. J. "The Use of Standard Values and Refraction Bias Parameters in Orbit Determination," The Canadian Surveyor, 29(3), pp. 301-305, 1975.
24. Fell, P. J. "Geodetic Positioning Using a Global Positioning System of Satellites," Report No. 289, Dept. of Geodetic Science, Ohio State University, 1980.
25. Fury, R. J. "Prediction of the Deflections of the Vertical by Gravimetric Methods," NOAA Technical Report NOS NGS 28, 1984.
26. Fury, R. J. National Geodetic Survey, U. S. Dept. of Commerce, Rockville, Maryland, Personal communication, 1988.
27. Gigierano, J. D. Geological Survey Bureau, Iowa City, Iowa, Personal communication, 1988.
28. Heiskanan, W. A. and Moritz, H. Physical Geodesy, Graaz, Austria: Institute of Physical Geodesy, Technical University, Reprint, 1984.
29. Howell, T.F. "Surveying and Mapping in Texas - A Case Study Using Automation for Transportation Application", Surveying and Land Information Systems, Vol. 50, No. 2, 1990.
30. Jeyapalan, K. "Photogrammetry", Encyclopedia of the Earth System Science, Volume 3, Academic Press, Inc., 1992.
31. Jeyapalan, K. "Feasibility Study of the Triangulation of Tanzania," California State University, Fresno, California, 1979.
32. Jeyapalan, K. et al. "Use of GPS for Precise Prediction of Local Geoid Undulation," ASCM-ASPRS Annual Convention (pp. 78-83), Denver, Colorado, 1990.
33. Jeyapalan, K. et al. "Maximized Utility of the Global Positioning System", Iowa State University, Ames, Iowa 1991.
34. Jeyapalan, K. "Data Snooping Using Observations and Parameters With Constraints," International Archives of Photogrammetry, Vol. XXXV, 1984
35. Jeyapalan, K. "Evaluation of a Prototype Global Positioning System (GPS) Satellite Receiver," ACSM-ASPRS Annual Convention, Vol. 2, 1986.
36. Jeyapalan, K. and Mohamed, M. "The Accuracy Obtainable Using Global Positioning Satellite System," ACSM-ASP Annual Convention, Washington, D.C., 1984.
37. Jeyapalan, K. "Calibration of Comparators by the Method of Collocation," Unpublished Report, Topographic Division, U.S. Geological Survey, Reston, Virgina, pp. 2-7, 1977.

38. Kaula, W. M. "The Need for Vertical Control," Surveying and Mapping, 47(1), pp. 57-64, 1987.
39. Kearsley, A. H. W. "Tests on the Recovery of Precise Geoid Height Differences from Gravimetry," Journal of Geophysical Research, 93, no. B6, pp. 6559-6570, June, 1988.
40. King, R. W., Masters, E. G., Rizos, C. and Collins, J. Surveying with GPS, School of Surveying. The University of New South Wales, Kensington N.S.W., Australia, p. 128, 1985.
41. Lapine, L.A. "NOAA Tests Kinematic GPS", ACSM Bulletin pp. 12-14, August 1990.
42. Ma, Wei-ming. Local Geoid Determination Using the Global Positioning System, M. S. Thesis, Naval Postgraduate School, Monterey, California, 1988.
43. Mikhail, E. M. Observations and Least Squares, IEP-Dun-Donnelley, New York, pp. 418-426, 1976.
44. Milliken, R. J. and Zoller, C. J. "Principle of Operation of NAVSTAR and System Characteristics," Global Positioning System, Institute of Navigation, Washington, D.C., Vol. 1, pp. 3-14, 1980.
45. Moritz, H. "Geodetic Reference System 1980," Bulletin Geodesique, 54(3), pp. 395-405, 1980.
46. NASA. Directory of Station Locations, 4th ed., Godard Space Flight Center, Greenbelt, Maryland, pp. 1-11, 1978.
47. National Geodetic Survey. Geodetic Glossary, Rockville, Maryland: U.S. Government Printing Office, 1986.
48. Rapp, R. H. and Cruz J. Y. "Spherical Harmonic Expansions of the Earth's Gravitational Potential to Degree 360 Using 30' Mean Anomalies," Report no. 376. Department of Geodetic Science and Surveying. The Ohio State University, Columbus, Ohio, December, 1986.
49. Rapp, R. H. Department of Geodetic Science and Surveying, The Ohio State University, Columbus, Ohio, Personal communication, 1988.
50. Reilly, J. Surveying with GPS (Unpublished Xeroxed paper), Presented at ASCE/ICEA Surveying Conference, Ames, Iowa, ASCE/ICEA, 1988.
51. Remondi, B. W. "Global Positioning System Carrier Phase: Description and Use," Bulletin Geodesique, 59(4), pp. 361-377, 1985.
52. Remondi, B. W. Using the Global Positioning System (GPS) Phase Observable for Relative Geodesy: Modeling, Processing and Results, Ph.D. Dissertation, The University of Texas at Austin, 1984.
53. Rockwell International. Instruction Manual Collins Navcore I GPS C/A Receiver, Cedar Rapids, Iowa, August 1986.
54. Strange, W. E., Vincent, S.F,, Berry, R. H., and Marsh, J.G. "Detailed Gravimetric Geoid for the United States," The Use of Artificial Satellites for Geodesy, Geophysical monograph 15. Eds. S. W. Henriksen, A. Mancicni, B. H. Chovitz. Washington: American Geophysical Union, pp. 169-176, 1972.
55. Tetley, L. and Calcutt, D. Electronic Aids to Navigation, London, Edward Arnold Ltd., pp. 225-232, 1986.
56. Torge, W. Geodesy, Berlin: DeGruyter, 1980.

57. Trimble Navigation. Trimble Model 4000SX GPS Surveyor-Preliminary-Installation and Operation Manual, Sunnyvale, California, p. 96, 1987.
58. Van Dierendonck, A. J., Russell, S. S., Kopitzke, E. R., and Birnbaum, M. "The GPS Navigation Message," Global Positioning System, Institute of Navigation, Washington, D.C., 1980.
59. Wells, David G. et al. Guide to GPS Positioning, Fredericton, New Brunswick, Canada: University of New Brunswick Graphic Services, 1987.

APPENDIX 1

Summary of Mapp/Pal/Albany

In this section the Mapp/Pal/Albany programs for analytical aerotriangulation will be described using the independent model coordinate method and also the refined photo coordinate method. Some preliminary procedures must first be completed. A job directory name must be given to the project and a job.dat file completed concerning the project. This directory is a subdirectory of the C:\JOBS directory. Various parameters concerning the project are set in the job.dat file such as description of project, feet or meters, number of strips, flight altitude, average terrain elevation, type of coordinates, camera code or focal length, and so on. The camera information usually is contained in the camera.dat file which also needs to be completed.

Using Refined Photo Coordinates

After completing the camera and job files, a ground control and the measurement files must be copied into the job directory. For each strip there must be a STRIPnn.MEA file which are the refined photo coordinates (we arrived at these by using the SAT9 program after making the measurements on the WILD STK-1 Stereocomparator). The nn is the number of the specified strip. There also should be a jobname.CTL file in the job directory which is a collection of the control points for the project. As mentioned earlier the CAMERA.DAT file is also in this directory. For each of these files it is imperative that they are in the

correct format as described in the manual in order for the programs to run correctly.

A command file is now built for each of the strips in the project. This is done by running the "X" program, choosing the B option for building command files, S for strip command file and entering various information about the strip. The tpa command file can now be built followed by the block command file, the resect command file, the pal command file and the albany command file. Each strip is then run one at a time until each processes without error. This is done by choosing the run applications option under the main menu and picking each particular strip. If there is only one strip, the run MAPP option is chosen (R in the main menu and M for MAPP). The tie point analysis is run next by choosing this option (R in the main menu, and then T for TPA). If there is only one strip, the tie point analysis can be skipped. The block adjustment runs next (R in the main menu and B for BLOCK) followed by executing the space resection (R in the main menu and R for RESECT). The PAL command file is then run which prepares the input files so that the ALBANY command file can be executed which performs a simultaneous least squares adjustment of photos and/or independent models in the block.

Using Independent Model Coordinates

In this section, using the MAPP/PAL/ALBANY series for independent model coordinates will be described. Again, a job directory for a project is created under the C:\JOBS directory and

the job.dat file created. The independent model coordinate option is chosen when creating this file. The CAMERA.DAT file is created or copied to this directory. The control file jobname.CTL is also copied into this directory along with the IMA (independent model assembly) file from the refined coordinate process. This file is renamed jobname.IMA. It is important that the standard deviation values in the control file are in place. The output from the relative orientation using the refined coordinates will yield STRIPnn.TWO files which are copied into this new directory and are renamed STRIPnn.IMC. These files contain the independent model coordinates for each of the strips.

After all these files are in the project directory, the strip command files can be created and edited. The strip command file is built in the same fashion as it was when using the refined coordinates. This time, however, the independent model coordinates option is chosen instead of refined coordinates. The strip command file must also be edited. These two lines in the command file are deleted, 1) OPEN 15 ... .MEA r and 2)DATA .... . A negative sign is also added infront of the strip number in the IMA command line. After making these changes the individual strips may be run. After each strip runs successfully, the TPA and BLOCK command files are built using the "X" program as described earlier. The TPA and BLOCK commands are then run by choosing the R run an application option. A MAPP command file is then built or copied and edited in the current job directory. The final MAPP command file should look like the following one which is displayed.

```
ECHO
MAPP
JOB jobname
OPEN 13 jobname.IMC R
OPEN  9 jobname.CTL R
MAPP  **
OPEN 16 jobname.GPS
OPEN  7 jobname.OPS
IMSR -sn .030 1
END
```

The sn in the second to the last line represents the strip number. If there are a number of strips an IMSR command for each strip is included. The parameters in the IMSR command line can also be changed if deemed necessary. The MAPP option is next chosen after choosing to run an application. The final steps when using independent model coordinates in the MAPP\PAL\ALBANY series is to build the PAL and ALBANY command files and then to run these. This is done in the same manner as was done when using the refined photo coordinates.

This discussion was intended to be a brief overview of the steps involved when using the MAPP\PAL\ALBANY software in the phototriangulation process. A phototriangulation flowchart summarizing this process will be included on the next page. For more detailed information on the specifics of the software programs, the MAPP\PAL\ALBANY manual should be consulted.

PHOTOTRIANGULATION FLOWCHART

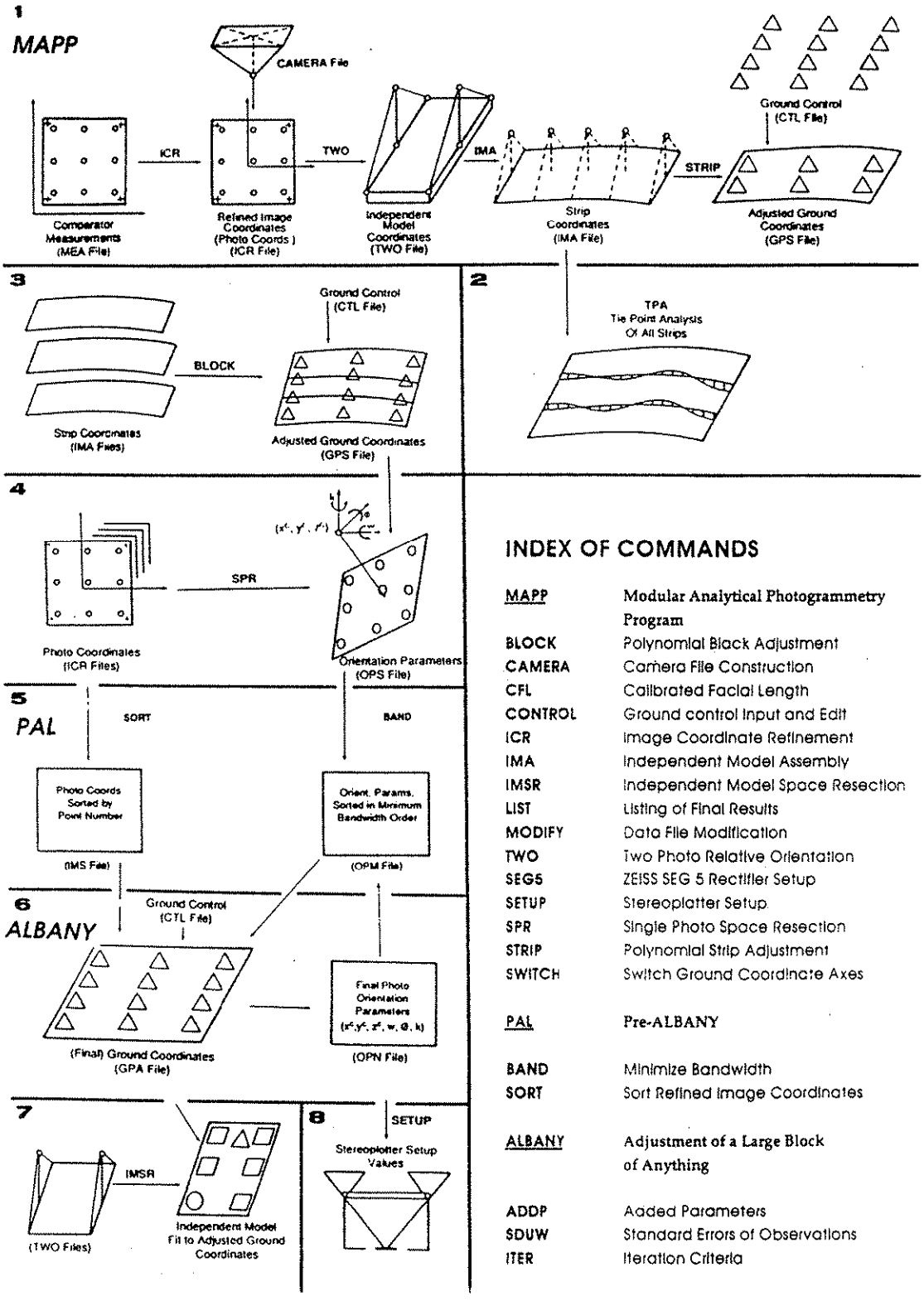

INDEX OF COMMANDS

MAPP	Modular Analytical Photogrammetry Program
BLOCK	Polynomial Block Adjustment
CAMERA	Camera File Construction
CFL	Calibrated Facial Length
CONTROL	Ground control Input and Edit
ICR	Image Coordinate Refinement
IMA	Independent Model Assembly
IMSR	Independent Model Space Resection
LIST	Listing of Final Results
MODIFY	Data File Modification
TWO	Two Photo Relative Orientation
SEG5	ZEISS SEG 5 Rectifier Setup
SETUP	Stereoplatter Setup
SPR	Single Photo Space Resection
STRIP	Polynomial Strip Adjustment
SWITCH	Switch Ground Coordinate Axes
PAL	Pre-ALBANY
BAND	Minimize Bandwidth
SORT	Sort Refined Image Coordinates
ALBANY	Adjustment of a Large Block of Anything
ADDP	Added Parameters
SDUW	Standard Errors of Observations
ITER	Iteration Criteria

APPENDIX 2

OBSERVATION PROCEDURES USING THE WILD STK-1112 STEREOCOMPARATOR AND SEQUENMCE OF STEPS IN RUNNING THE RELATIVE ORIENTATION PROGRAM

Introduction:

In using photogrammetric methods to determine the coordinates of points, the desire to attain the best results of photo coordinates free from errors is the ultimate goal. This goal can only be achieved by going through a series of processes involving good observational procedures and also running through a series of programs to eliminate most of the errors including a final least square solution.

Using the WILD STK-1112 stereocompator as the observing instrument and going through a series of computer programs to eliminate some errors is the subject here.

The procedure of measurement is explained later in the paper but one most important thing to note is that, since the human eye is not absolutely perfect and also coupled with the fact that data entry can be mistakenly erroneous, it is always a laudable idea to realize the need to render an input data file free from measuring errors and blunders. This part of the problem is handled by running the SAT9 program. A look at the output file from this program will suggest blunders and errors. One can always tell from the values of residuals if the data is satisfactory or not. Blunders are usually distinct as they deviate largely from the expected range of values. The next stage is to ascertain the fact that the same point on two different photos are oriented relatively satisfactorily. This brings in the concept of relative orientation. Running the Ro program also explained later in this piece is the method of solving this problem.

series of photographs on a particular flight line (a strip). Quite naturally, relative orientation for two photograph cannot suffice for the entire strip and hence a relative orientation of one photo to another in the entire strip is necessary. This is necessary to eliminate error between models and it is done by running the Strip program in the MAPP/ALBANY software.

Similarly, a block program is run to eliminate errors between strips by properly orienting one strip to another.

These processes will remove some of the errors inherent in the measurement and hence help produce a better results in the subsequent programs; MAP

P and ALBANY.

Using the Wild stereocomparator model stk-1112 for model observation involves a number of steps.

STEP 1. Put the diapositives in the instrument's plate holder and perform inner orientation. Do this by aligning the 4th and 8th fiducial marks to the horizontal line on the glass plate and the 2nd and 6th to the vertical line.

NOTE: Make sure the lines on the glass plate do not lie directly on the fiducials otherwise putting the floating mark on the center of the fiducial marks is quite difficult.

STEP 2. Turn the instrument lights on.

STEP 2. After step 2 put the plate holder back to the instrument and illuminate the plates to suit your eyes so you can see the little black floating marks clearly. (caution: there are a couple of other black spots on the lens and probably the glass plate, be careful not to use any of them. The main dots are quite distinct- a prefect round black dot. You may also change the magnification. 20× seems to be the best for observation though.

STEP 3: To check on the attainment of the correct overlap, put the right light on a distinct point on the left plate using the x and y gears. Do the same for the corresponding point on the right plate using the px and the py gears. Note that you do all these while looking through the eye piece. Once satisfied that the proper

(The proper overlap may not be obtained if the diapositives are improperly oriented in the plate. Try to avoid this. Once the first model is correctly done , follow the positions of the writings on the photos to continue in the strip)

STEP 4. OBSERVATION.

Using the x and y gears, put the left dot on fiducial number 1 (top left corner mark). Now, do the same for the right plate using the px and the py gears. The same procedure is used for all the other points by moving clockwise from point 1 until the last point 8 is read which is right below point 1. For every point the x, y, px, and the py scale readings are entered into the computer in that same order. The entry procedure is explained below.

STEP 5 DATA ENTRY.

The data entry procedure is just editing a pre-existing file of a previously observed model. Copy the file of the old model to the file you wand to observe.

Example:Suppose you have on the disk an old file with the name P12.in which apparently signifies the model of photo one and two and your new model is that of two and three then you do this

B>copy p12.in p23.in

Entering data for model 2-3 is therefore an editing of the file p23.in using edlin.

The first data goes to line 26 which is the x value of point 1.

57. Line 58 is the number of points to be observed in the model. Line 59 therefore takes the x value of the first non-fiducial point read. Note y and py values are negatives and be sure to put at line 58 the correct number of points to be observed.

After observing all the points needed on the model, the file is saved and the SAT9 program is run to check on the residuals of the points which is usually kept under 30microns. The Sat9 program needs be run after the 8 fiducials are read.

STEP 6 RUNNING SAT9

In your data directory do the following.

B>a:basic (make sure the disk in drive a has the ms-basic and the SAT9 programs on it)

ok

F8 (to load)

load"a:sat9

ok

F2 (to run)

name of input file(type p23.in)

After a few scrolling of values you will be prompted to put the output file name

output file name (type p23.out)

Using the pause key, you can check on the residuals. Try to keep residuals below 30microns by reobserving points with large residuals. Once satisfied with the residuals, the next step is to run the Relative orientation program RO.

STEP 7 RUNNING THE RO.

To run RO, the output file from SAT9 need to be formatted in a particular format. The format should include the following;

a. photo number (PN)

b. strip number (SN)

c. point number (PtN)

d. a column of zeroes (O)

e. x and y values

Follow the format below;

```
01234567890123456789012345678901234567890123456789012345
    SN  PN    PtN    O  X--- .--            Y---- .------
```

EXPLANATION:

COLUMN	WHAT?
4-5	strip number
8-9	photo number
15-19	point number
21	a column of zeroes
29	decimal point of x value.
41	decimal point of y value.

After formatting, rename the file as filename.mea, in this case it will be p23.mea.(mea - measurement)

Running the RO also involves the editing of the RO command file in the Ro directory. type edlin ro.cmd

Then edit the filename to the current filename, edit the data filename to the current one and edit the strip number. Thus three things are edited here, the mea filename, the dat filename and the strip number. Before running the Ro you need to copy the new mea

file to the RO directory.

After the editing type RO to run the program. All points with bad residuals are flagged depending on the precision you set.

SAMPLE INPUT FILE FOR RUNNING THE SAT9 PROGRAM

```
8
1
-109.983
-110.015
2
0.017
-112.024
3
110.015
-110.015
4
112.024
-0.018
5
110.014
109.978
6
0.013
111.982
7
-109.986
109.986
8
-111.984
-0.013
890.778
-1111.987
1000.623
-998.493
1000.843
-1114.212
1000.637
-998.611
1110.885
-1112.399
1000.669
-998.729
1113.090
-1002.407
1000.781
-998.737
1111.297
-892.389
1000.903
-998.727
1001.271
-890.169
1000.911
-998.591
891.199
-891.943
1000.873
-998.480
888.981
-1001.955
1000.735
-998.488
28
1001
933.903
-1008.650
918.888
-999.529
1002
937.272
-1079.055
920.444
-999.387
4900
996.616
-1079.332
920.3525
-998.657
2002
1027.349
-1077.517
```

SAMPLE OUTPUT FILE FROM THE SAT9 PROGRAM

THE TRANSFORMATION PARAMETERS FOR THE LEFT PLATE ARE:
AL= .9996911
BL= 1.931105E-03
CL= 1.625061E-02
DL=-1.737779E-02

THE TRANSFORMATION PARAMETERS FOR THE RIGHT PLATE ARE:
AR= .9998128
BR= 8.096933E-04
CR= 1.625061E-02
DR=-1.737779E-02

THE LEFT PLATE SCALE IS .9996931
THE RIGHT PLATE SCALE IS .9998131

THE ADJUSTED VALUES AND RESIDUALS FOR THE LEFT PLATE ARE:

1	-110.003	-110.001
	0.020	-0.014
2	0.033	-112.013
	-0.016	-0.011
3	110.037	-109.988
	-0.022	-0.027
4	112.029	-0.025
	-0.005	0.007
5	110.024	109.955
	-0.010	0.023
6	0.028	111.962
	-0.015	0.020
7	-110.007	109.976
	0.021	0.010
8	-112.012	-0.006
	0.028	-0.007

THE ADJUSTED VALUES AND RESIDUALS FOR THE RIGHT PLATE ARE:

1	-109.996	-110.004
	0.013	-0.011
2	0.036	-112.022
	-0.019	-0.002
3	110.024	-110.002
	-0.009	-0.013
4	112.028	-0.021
	-0.004	0.003
5	110.024	109.965
	-0.010	0.013
6	0.009	111.959
	0.004	0.023
7	-110.003	109.986
	0.017	0.000
8	-111.993	0.000
	0.009	-0.013

THE PHOTO COORDINATES FOR THE LEFT PLATE ARE :

1001	-67.0905	-6.6124
1002	-63.5867	-76.9892
4900	-4.2604	-77.1515
2002	26.4596	-75.2777
470	22.5182	-34.0719
440	20.3461	-11.4315
2001	20.1954	-7.4600
24	2.2851	2.0250
19	-6.9277	12.9579
20	-7.7193	10.2671
22	-9.4515	9.6110
21	-11.7768	7.0103
500	-25.0994	58.0689
600	-24.7045	59.1254

700	-18.7507	59.8197
2000	18.6452	58.0895
800	-19.3138	48.6060
900	-10.7919	44.6907
13	-11.9433	43.0570
14	-13.5253	40.7026
15	-10.8097	31.7006
162	1.0362	30.8918
16	1.3580	30.9234
10	17.3449	35.6919
400	-6.2324	23.5270
18	-8.2285	22.9123
17	-9.7811	22.9168
300	-13.1589	21.3093

THE PHOTO COORDINATES FOR THE RIGHT PLATE ARE :

1001	14.7565	-5.5498
1002	16.6263	-76.0821
4900	76.0515	-77.0408
2002	106.2921	-75.5675
470	103.1362	-34.2428
440	101.4231	-11.5110
2001	101.2810	-7.5418
24	83.6249	2.1736
19	74.6501	13.2292
20	73.8004	10.5411
22	72.0893	9.9428
21	69.7397	7.3668
500	57.6036	58.5500
600	57.9847	59.5761
700	63.7291	60.1916
2000	101.1129	58.0034
800	63.0833	49.0132
900	71.3740	44.9977
13	70.2380	43.3930
14	68.6102	41.0521
15	71.1416	32.0259
162	82.8231	31.0616
16	83.1591	31.0748
10	99.2743	35.6475
400	75.5294	23.7955
18	73.5302	23.2095
17	71.9965	23.2317
300	68.6444	21.6713

SAMPLE OUTPUT FILE OF THE RO PROGRAM

```
 OPEN FILE 12   r p12.mea
 OPEN FILE 13     p12.dat

 TWO PHOTO RELATIVE ORIENTATION
 ------------------------------
 STRIP NUMBER                      1
                                   ---
 IMAGE PARALLAX LIMIT           .020
 FOCAL LENGTH                152.212
 FIXED    BX                  90.000
 FULL  PRINTOUT

-MODEL    1   2/  1,  CFL  152.212, 28 POINTS  4 ITER, SDUW     .0072
 --------------
      OMEGA        PHI        KAPPA         BX          BY          BZ
      .1739       .0476       .8301    90.0000      1.8434       .0085
      .0078       .0137       .0045       .0000       .0240       .0178

      POINT          X           Y           Z          VX          VY
       1001       73.815       7.275     167.468       .000       -.003
       1002       70.596      85.476     168.992       .000       -.001
       4900        4.730      85.662     169.002       .000        .000
       2002      -29.585      84.170     170.193       .000        .011
        470      -25.075      37.940     169.494       .000       -.025     *
        440      -22.598      12.697     169.060       .000        .007
       2001      -22.441       8.289     169.135       .000        .000
         24       -2.534      -2.246     168.797       .000       -.009
         19        7.672     -14.349     168.555       .000       -.007
         20        8.551     -11.373     168.610       .000       -.015
         22       10.466     -10.643     168.549       .000        .020
         21       13.040      -7.762     168.533       .000        .014
        500       27.594     -63.841     167.342       .000        .010
        600       27.169     -65.023     167.395       .000       -.013
        700       20.675     -65.960     167.835       .000       -.013
       2000      -20.554     -64.037     167.795       .000        .002
        800       21.283     -53.562     167.732       .000       -.004
        900       11.919     -49.358     168.108       .000        .001
         13       13.185     -47.534     168.037       .000        .012
         14       14.935     -44.944     168.075       .000        .003
         15       11.948     -35.038     168.236       .000        .005
        162       -1.147     -34.210     168.560       .000        .002
         16       -1.504     -34.239     168.531       .000       -.012
         10      -19.188     -39.484     168.386       .000        .001
        400        6.896     -26.034     168.431       .000        .002
         18        9.105     -25.352     168.422       .000        .005
         17       10.820     -25.351     168.382       .000        .002
        300       14.549     -23.560     168.288       .000        .004

*POSITIVE Z MAY INDICATE PSEUDO STEREO FOR    1   2/  1*
```

SAMPLE MEA FILE

1	2	1001	0	-67.0905	-6.6124
1	2	1002	0	-63.5867	-76.9892
1	2	4900	0	-4.2604	-77.1515
1	2	2002	0	26.4596	-75.2777
1	2	470	0	22.5182	-34.0719
1	2	440	0	20.3461	-11.4315
1	2	2001	0	20.1954	-7.46
1	2	24	0	2.2851	2.025
1	2	19	0	-6.9277	12.9579
1	2	20	0	-7.7193	10.2671
1	2	22	0	-9.4515	9.611
1	2	21	0	-11.7768	7.0103
1	2	500	0	-25.0994	58.0689
1	2	600	0	-24.7045	59.1254
1	2	700	0	-18.7507	59.8197
1	2	2000	0	18.6452	58.0895
1	2	800	0	-19.3138	48.606
1	2	900	0	-10.7919	44.6907
1	2	13	0	-11.9433	43.057
1	2	14	0	-13.5253	40.7026
1	2	15	0	-10.8097	31.7006
1	2	162	0	1.0362	30.8918
1	2	16	0	1.358	30.9234
1	2	10	0	17.3449	35.6919
1	2	400	0	-6.2324	23.527
1	2	18	0	-8.2285	22.9123
1	2	17	0	-9.7811	22.9168
1	2	300	0	-13.1589	21.3093
1	1	1001	0	14.7565	-5.5498
1	1	1002	0	16.6263	-76.0821
1	1	4900	0	76.0515	-77.0408
1	1	2002	0	106.2921	-75.5675
1	1	470	0	103.1362	-34.2428
1	1	440	0	101.4231	-11.511
1	1	2001	0	101.281	-7.5418
1	1	24	0	83.6249	2.1736
1	1	19	0	74.6501	13.2292
1	1	20	0	73.8004	10.5411
1	1	22	0	72.0893	9.9428
1	1	21	0	69.7397	7.3668
1	1	500	0	57.6036	58.55
1	1	600	0	57.9847	59.5761
1	1	700	0	63.7291	60.1916
1	1	2000	0	101.1129	58.0034
1	1	800	0	63.0833	49.0132
1	1	900	0	71.374	44.9977
1	1	13	0	70.238	43.393
1	1	14	0	68.6102	41.0521
1	1	15	0	71.1416	32.0259
1	1	162	0	82.8231	31.0616
1	1	16	0	83.1591	31.0748
1	1	10	0	99.2743	35.6475
1	1	400	0	75.5294	23.7955
1	1	18	0	73.5302	23.2095
1	1	17	0	71.9965	23.2317
1	1	300	0	68.6444	21.6713

****** NOTE*** The position of each column should conform to the format exlained above.

APPENDIX 3

DETERMINATION OF CAMERA LOCATION

DETERMINATION OF CAMERA LOCATIONS.

Introduction:

In aerial photography, photographs are taken at specific time intervals usually 0.5second or 1.0 second interval. The actual position of the camera may be determine by interpolating between these time intervals.

Method:

In this particular case, interpolation was done by using the principles of Newtonian mechanics. The following formulas were used.

$$a = (V - U)/t$$

$$X = UT + .5at^2$$

a = acceleration

U = initial velocity between two distance intervals

V = final velocity between two distance intervals.

X = coordinate needed (x, y, and the z coordinates)

A systematic approach of how the whole work was done is summarized in the table below.

time	X	dX	V	a	X
3.5	m				
4.0	b	b-m	V1=(b-m)/.5		
4.3333	u			(V2-V1)/.5	u

4.5 c c-b V2=(c-b)/.5

Thus knowing all the necessary parameters, we compute the value of u which is the X coordinate of the camera location at time t=4.222 as

$$u = b + V2 * 0.222 + .5 * a * (0.222)^2.$$

*Note here that the velocity V2 is used since we are only interested in the velocity between times 4 and 4.5

A similar method of interpolation is used to determine the Y and Z coordinates at time 4.222 (see attached sample sheet). One should note however that the change in X or Y per time may be significantly big depending on the direction of motion of the airplane. One should expect a larger change in X and not in Y or Z if the direction of photography is in the X direction. The sample data below extracted from the 1992 flight clarifies the point above.

Time	X	Y	Z
18:37:53	476159.32977	4650886.771263	751.052
18:37:53.5	476118.76877	4650887.414900	751.249

One can see from the above data that, the plane is moving in the X direction.

For this particular work, since the final coordinates were needed

in the state plane coordinates system (Iowa North), the computed UTM coordinates were transformed to the corresponding State plane using a coordinate transformation program.

The procedure of transformation involves the creation of an input file in accordance with the data format given.

The UTM coordinates are then transformed to Longitude and Latitude and then to the state plane coordinate system.

TIME	DT	X	DX
18:30:19.5		475556.39847	
20	0.5	475513.42596	-42.972504
20.30488863	0.30488863		
20.5	0.5	475470.42316	-43.002803
26		474995.93525	
26.5	0.5	474952.45703	-43.478225
26.72269878	0.22269878		
27		474909.17262	-43.284403
32.5		474431.68682	
33	0.5	474388.31321	-43.373614
33.14371181	0.14371181		
33.5	0.5	474344.9736	-43.339606
39		473869.20833	
39.5		473826.04582	-43.162514
39.56446616	0.0646616		
40		473782.91455	-43.131271

velocity	acceleration	X
-85.945008		
	-0.1211959999	475487.21688
-86.005606		
-86.95645		
	0.7752879998	474932.73895
-86.568806		
-86.747228		
	0.1360319997	474375.84747
-86.679212		
-86.325028		
	0.1249719998	473820.46416
-86.262542		